Journal of Medicinal Chemistry

Article

Synthesis and Biological Investigation of Phenothiazine-Based Benzhydroxamic Acids as Selective Histone Deacetylase 6 (HDAC6) Inhibitors

Katharina Vögerl, Nghia Ong, Johanna Senger, Daniel Herp, Karin Schmidtkunz, Martin Marek, Martin Müller, Karin Bartel, Tajith Baba Shaik, Nicholas J. Porter, Dina Robaa, David W. Christianson, Christophe Romier, Wolfgang Sippl, Manfred Jung, and Franz Bracher

J. Med. Chem., **Just Accepted Manuscript** • DOI: 10.1021/acs.jmedchem.8b01090 • Publication Date (Web): 15 Jan 2019

ACS Publications

is published by the American Chemical Society. 1155 Sixteenth Street N.W., Washington, DC 20036

Synthesis and Biological Investigation of Phenothiazine-Based Benzhydroxamic Acids as Selective Histone Deacetylase 6 (HDAC6) Inhibitors

Katharina Vögerl[1], Nghia Ong[1], Johanna Senger[2], Daniel Herp[2], Karin Schmidtkunz[2], Martin Marek[3], Martin Müller[1], Karin Bartel[1], Tajith B. Shaik[3], Nicholas J. Porter[4], Dina Robaa[5] , David W. Christianson[4], Christophe Romier[3], Wolfgang Sippl[5], Manfred Jung[2], Franz Bracher[1*]

[1]Department of Pharmacy - Center for Drug Research, Ludwig-Maximilians University Munich, Butenandtstr. 5-13, 81377 Munich, Germany

[2]Institute of Pharmaceutical Sciences, University of Freiburg, Albertstraße 25, 79104 Freiburg, Germany

[3]Département de Biologie Structurale Intégrative, Institut de Génétique et Biologie Moléculaire et Cellulaire (IGBMC), Université de Strasbourg (UDS), CNRS, INSERM, 67404 Illkirch Cedex, France

[4]Department of Chemistry, University of Pennsylvania, 231 South 34th Street, Philadelphia, PA 19104-6323, USA

[5] Institute of Pharmacy, Martin-Luther University of Halle-Wittenberg, 06120 Halle/Saale, Germany

*Corresponding author. Tel.: +49-89-2180-77301, E-Mail: franz.bracher@cup.uni-muenchen.de

ABSTRACT

The phenothiazine system was identified as a favorable cap group for potent and selective histone deacetylase 6 (HDAC6) inhibitors. Here we report the preparation and systematic variation of phenothiazines and analogues containing a benzhydroxamic acid moiety as zinc-binding group. We evaluated their ability to inhibit selectively HDAC6 by a recombinant HDAC enzyme assay, by determining the protein acetylation levels in cells by Western blotting (tubulin vs histone acetylation), and by assessing their effects on various cancer cell lines. Structure-activity relationship studies revealed that incorporation of a nitrogen atom into the phenothiazine framework results in increased potency and selectivity for HDAC6 (more than 500-fold selectivity relative to the inhibition of HDAC1, HDAC4, and HDAC8), as rationalized by molecular modeling and docking studies. The binding mode was confirmed by co-crystallization of the potent azaphenothiazine inhibitor with catalytic domain 2 from *Danio rerio* HDAC6.

INTRODUCTION

Lysine acetylation is a major, reversible posttranslational modification on proteins that is regulated by two families of enzymes with opposing activity, the histone acetyltransferases (HATs) and the histone deacetylases (HDACs)[1]. Whereas the substrates of most zinc-dependent HDACs are histones, the HDAC6 isozyme is unique in that it is predominantly localized in the cytoplasm and as a result mainly deacetylates non-histone proteins as α-tubulin in microtubules[2], the HSP90 chaperone[3], and cortactin[4], among others. A structural peculiarity of HDAC6 is its tandem catalytic domains termed CD1 and CD2, an inter-domain linker, and an ubiquitin-binding domain[5, 6]. Through this ubiquitin-binding domain HDAC6 recruits misfolded polyubiquitinated protein aggregates to the dynein motors and promotes subsequent transport to the aggresomes where they are processed[7]. Both catalytic domains are active and structurally highly conserved, although CD1 has much more stringent substrate selectivity, whereas CD2 exhibits broad substrate specifity[5, 6]. The inter-domain linker has a significant impact on optimal activity of HDAC6[8] and is reportedly involved in binding dynein motor proteins[9]. Besides a nuclear localization signal (NLS), HDAC6 possesses a nuclear export signal (NES) and serine-glutamate tetradecapeptide repeat (SE14) ensuring stable anchorage of the enzyme in the cytoplasm[10]. By formation of complexes with its partner proteins HDAC6 regulates many important cellular processes such as cell motility, cell spreading, misfolded protein degradation,

transcription, cell proliferation and death, and stress or immune response[11]. In consequence, misregulation of HDAC6 activity is associated with a variety of human diseases, which highlights it as a potential therapeutic target. HDAC6 is implicated in various neurodegenerative disorders, including Alzheimer´s, Parkinson´s, and Huntington´s diseases[12] as well as autoimmune and inflammatory disorders[13]. Moreover high expression levels of HDAC6 seem to play a crucial role in the pathogenesis of cancer, for instance, as found in acute myeloid leukemia, myeoblastic, breast, and ovarian cancer[14]. Until now, all approved HDAC inhibitors for cancer treatment target multiple HDACs. Their poor selectivity, however, can dose-dependently cause serious side effects[15, 16], which might limit their clinical use in oncology and beyond. Therefore the development of inhibitors for the particular isoform of interest is of great relevance, and selective inhibition of HDAC6 may lead to fewer severe side effects[17].

Various selective HDAC6 inhibitors have emerged over the years, mainly containing a hydroxamic acid as a zinc-binding group[18] (Chart 1). Some of them mimic N-acetyl-lysine structurally through an alkyl chain. Tubacin was identified by combinatorial chemistry methods and was found to decrease cell motility[19]. As a consequence of its nondrug-like properties, high lipophilicity and tedious synthesis it is more useful as a research tool than a drug candidate[20]. Ricolinostat, another potent but less selective inhibitor with at least 10-fold selectivity for HDAC6 relative to class I HDACs, possesses more favorable characteristics for drug development. In preclinical studies, Ricolinostat showed synergistic anti-multiple myeloma activity in combination with the proteasome inhibitor Bortezomib and Dexamethasone[21]. Other clinical trials in combinatory treatments, e.g. with next-generation analogue Citarinostat[22], are still in course[23]. Tubastatin A, a γ-carboline-based hydroxamic acid with a benzylic linker, was developed utilizing structure-based drug design combined with homology modelling and

displays high potency on HDAC6 with an IC_{50} of 15 nM and over 1000-fold selectivity over HDAC1[24]. Tubastatin A showed neuroprotective effects without adverse toxicity and in recent preclinical testing in animal models it reduced stroke-induced brain infarction and functional deficits[25] as well as reverted cognitive impairment in Alzheimer's disease transgenic mice[26].

Second-generation Tubastatin A analogues, a series of β- and γ-carboline-based hydroxamic acids, displayed subnanomolar IC_{50} values for inhibition of HDAC6 with an enormous increase of selectivity against HDAC1[27]. Tubastatin A and its analogues were found to enhance the immunosuppressive effects of Foxp3+ T-regulatory cells[27]. ACY-775, a novel HDAC6 inhibitor with improved brain bioavailability compared to Tubastatin A, showed low nanomolar potency and high selectivity over class I HDAC enzymes, linked to an antidepressant activity[28]. Marbostat 100, a tetrahydro-β-carboline derived from Tubastatin A with anti-inflammatory activity, was published as a very potent and selective HDAC6 inhibitor during the completion of this manuscript[29]. Nexturastat A which inhibits the growth of B16 melanoma cells, bears a benzylic substituted urea linker. It shows low nanomolar potency against HDAC6 as well and a selectivity of ~600-fold over HDAC1 making it the first HDAC6-selective inhibitor with antiproliferative effects[30]. A new Nexturastat A analogue demonstrated improved capability to inhibit tumor growth in melanoma models through the regulation of inflammatory and immune responses[31]. Like Nexturastat A, HPOB is also HDAC6 specific, albeit with lower selectivity (~50-fold over HDAC1) and features similarly a benzylic linker. This inhibitor was shown to cause growth inhibition without inducing cell death and in combination therapy it may enhance the efficacy of other anticancer drugs[32]. Further, inhibitors bearing five-membered heteroaromatic linkers such as oxazoles have been reported to exhibit good HDAC6 selectivity[33]. Diverse novel hydroxamate-based HDAC6 inhibitors have been published very recently[34-38].

A large number of HDAC inhibitors share common structural features, including the zinc-binding group (ZBG), the linker, and the cap group[39]. Until recently, the crystal structure of human HDAC6 was not available and HDAC6-specific inhibitor design approaches were restricted to homology models along with experimental results. A key point to gain subtype selectivity is the capping motif, which interacts with the surface of the wide basin surrounding the binding pocket of the enzyme[39]. The linker segment fits in the hydrophobic channel and bridges the zinc-binding hydroxamic acid and the cap group[39]. Given the structural feature of a benzyl linker in Tubastatin A and related inhibitors, a short bulky linker proved to be beneficial for potent and selective HDAC6 inhibition.

Based on the knowledge of the structural parameters essential for selective HDAC6 inhibitor activity, we chose to investigate new hydroxamate-based HDAC6 inhibitors that might gain the desired isoenzyme selectivity by their capping motif. To guide the design and synthesis of these inhibitors, the recently reported X-ray structures of HDAC6 in complex with benzhydroxamates were considered[5, 6, 40]. Herein, we report on the identification and development of the phenothiazine scaffold as a capping motif that confers potent and selective HDAC6 inhibitors in vitro and in cell culture.

Chart 1. Structures of selective HDAC6 inhibitors. The general structure of these inhibitors consists of a cap group (in red), a linker (in green), and a zinc-binding group (ZBG; in blue).

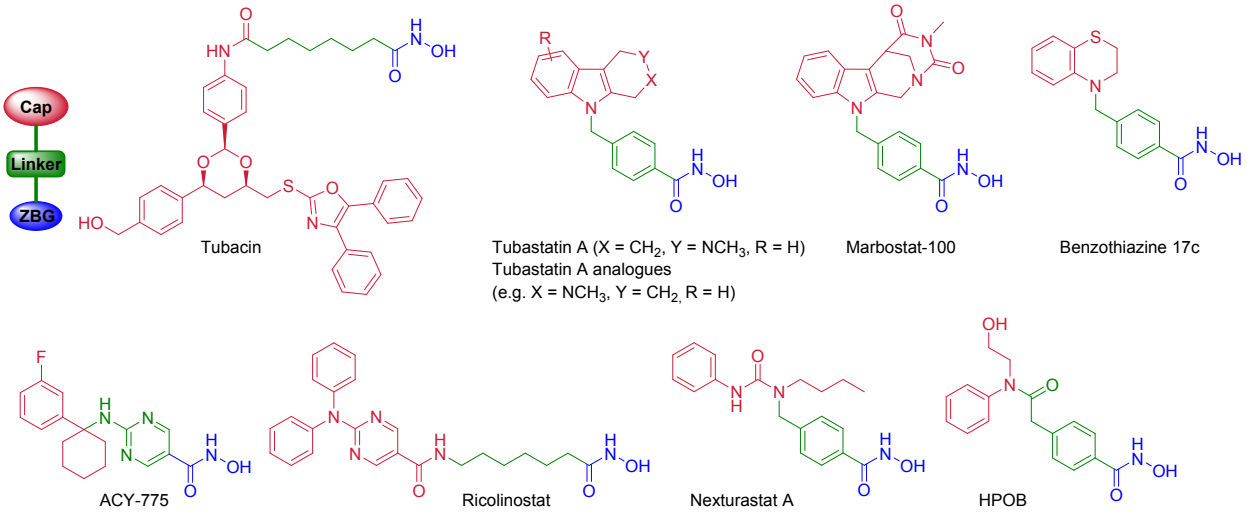

RESULTS AND DISCUSSION

CHEMISTRY

We began our studies on hydroxamate-based inhibitors with various polycyclic cap groups which were suitable for connection with the benzyl linker (see Tubastatin A, Chart 1) through benzylation of a ring nitrogen. We identified 4-[(10*H*-phenothiazin-10-yl)methyl]-*N*-hydroxybenzamide (**1a**, Chart 2) as a very potent HDAC6 inhibitor with high selectivity over HDAC1. This hit has structural similarity to a previously published selective benzothiazine-type HDAC6 inhibitor (Chart 1)[41]. On the basis of this structure, we set out for structure-activity relationships to improve selectivity and inhibitory potency.

Chart 2. Lead structure (**1a**).

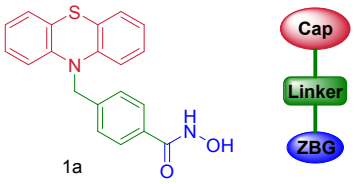

Docking of screening hit **1a** to HDAC6 showed that the tricyclic ring system is interacting with the rim of the binding tunnel but there is also space for further substitutions. Consequently, initial modifications concerned the phenothiazine ring system of compound **1a**. Various substituted phenothiazines, but also azaphenothiazines and other heterocyclic analogues were introduced as cap groups according to the synthetic route outlined in Scheme 1 and Table 1. The cap groups of choice were either commercially available or were prepared following established procedures. *N*-alkylation of the cap groups **2a-q** with methyl 4-(bromomethyl)benzoate (**3**) delivered intermediate esters **4a-q**. We first attempted to convert the esters directly into hydroxamates by treatmernt with hydroxylamine under diverse reaction conditions, but yields were very poor. Finally, we hydrolysed the esters with sodium hydroxide in aqueous dioxane to give the corresponding carboxylic acids **5a-q**. The hydroxamic acids **1a** and **7b-q** were obtained using COMU as activating agent and either hydroxylamine base[42] (**7e-q**) or *O*-(tetrahydro-2*H*-pyran-2-yl)hydroxylamine (**1a**, **7b-d**), followed by acidic cleavage of the THP protecting group. Based on our experience COMU was the most suitable coupling reagent, since only water soluble co-products arise from this reagent which are conveniently removed during aqueous work up[43]. Generally, using hydroxylamine base increased the overall yields of the desired hydroxamic acids compared to using THP-protected hydroxylamine (as for instance **7i** 41 % versus 21 % over two steps). The same coupling procedure with *N*,*O*-dimethylhydroxylamine provided *N*,*O*-dimethyl-substituted hydroxamic acid **23**.

Scheme 1[a]. General synthetic route to the target hydroxamic acids and the *N,O*-dimethyl-substituted hydroxamic acid **23**.

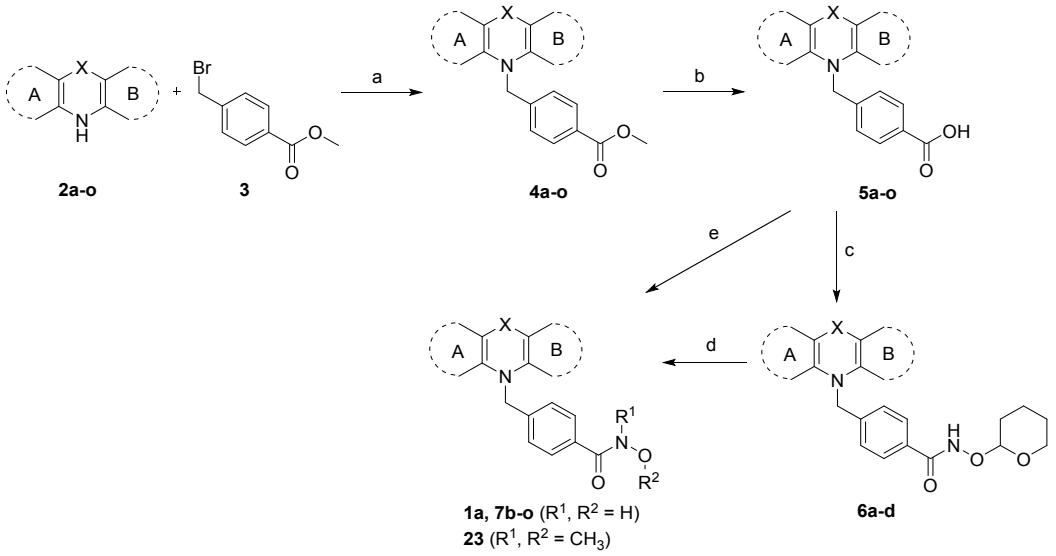

[a]Reagents and conditions: (a) LiHMDS, DMF, 0 °C → rt or 50 °C or 60 °C; (b) NaOH, H_2O/1,4-dioxane (1:1), rt or 40 °C or 50 °C or 60 °C; (c) DIPEA or Et_3N, COMU, NH_2OTHP, DMF, 0 °C → rt; (d) HCl in 1,4-dioxane, CH_2Cl_2, rt; (e) DIPEA, COMU, NH_2OH x HCl, DMF, 0 °C → rt; for **23**: **5a**, DIPEA, COMU, CH_3NHOCH_3 x HCl, DMF, 0 °C → rt.

Table 1. Line-up of cap groups defining the variations in A, B and X of the phenothiazine scaffold.

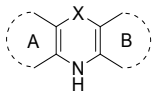

2a	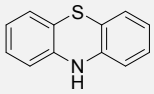	**2e**	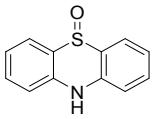	**2i**	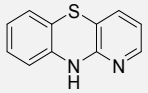	**2m**	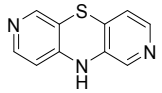
2b	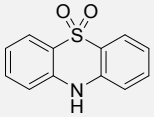	**2f**	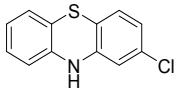	**2j**	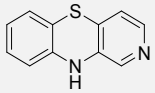	**2n**	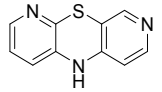
2c	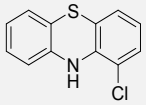	**2g**	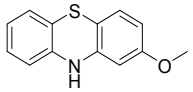	**2k**	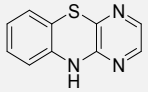	**2o**	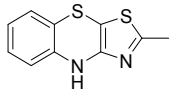
2d	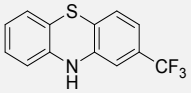	**2h**	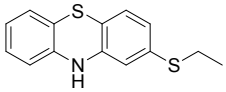	**2l**	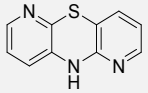	**2p/2q**	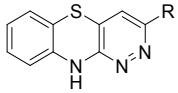 **2p** (R=H) **2q** (R=Cl)

Intriguingly, *N*-alkylation of 1,2-diazaphenothiazine (**2p**) and its 3-chloro-derivative **2q** delivered the structural isomers **8p** and **8q** besides the desired esters **4p** and **4q** (Scheme 2). The structural peculiarity in constitution of cap group and linker made **8p**/**8q** also interesting building blocks for the installation of the hydroxamic acid moiety to give compounds **10p**/**10q**.

Scheme 2[a]. Structural isomers from 1,2-diazaphenothiazines.

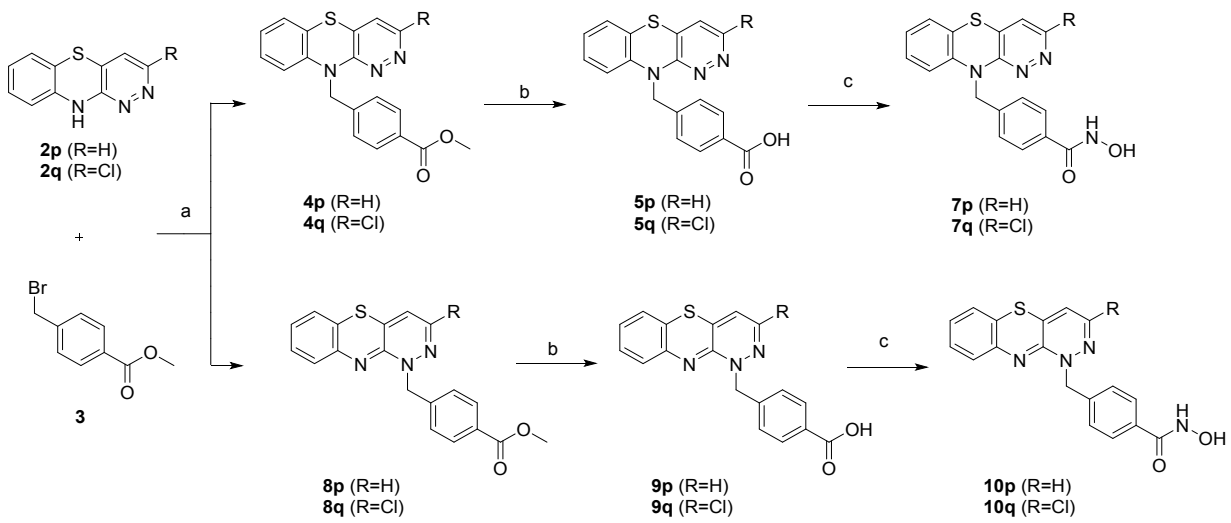

[a]Reagents and conditions: (a) LiHMDS, DMF, 0 °C → rt or 0 °C → rt → 60 °C; (b) NaOH, H_2O/1,4-dioxane (1:1), 40 °C or 60 °C; (c) DIPEA, COMU, NH_2OH x HCl, DMF, 0 °C → rt.

In order to achieve close structural similarity to the novel, highly active second-generation Tubastatin A analogues[27] (Chart 1) we prepared a tetrahydro analogue of azaphenothiazine **7j** (Scheme 3). Alkylation of 2-azaphenothiazine **2j** as described above yielded ester **4j**. This ester was further *N*-alkylated with methyl iodide to give the quaternary ammonium salt **11j**. Chemoselective reduction with $NaBH_4$[44] gave the tetrahydro derivative **12j**. Finally, ester hydrolysis and formation of the hydroxamic acid were performed as described above.

Scheme 3[a]. Synthetic route to hydroxamic acid 14j bearing a 2-methyl-1,2,3,4-tetrahydro-10*H*-pyrido[4,3-b][1,4]benzothiazine cap.

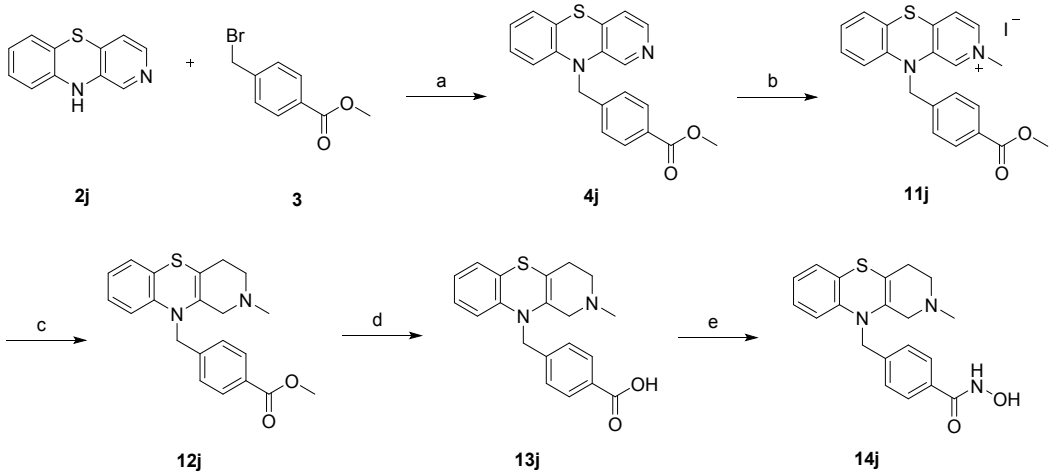

[a]Reagents and conditions: (a) LiHMDS, DMF, 0 °C → rt; (b) CH_3I, acetone/EtOH (6.5:1), reflux; (c) $NaBH_4$, EtOH, -15 °C → rt; (d) NaOH, H_2O/1,4-dioxane (1:1), rt → 60 ° C; (e) DIPEA, COMU, NH_2OH x HCl, DMF, 0 °C → rt.

Further, we conducted modifications of the linker group of the lead structure **1a**. Compound **18** consisting of a shorter and significantly less flexible phenyl linker was synthesised *via N*-arylation of parent phenothiazine **2a** with 4-fluorobenzonitrile **4** to give nitrile **16** (Scheme 4). Alkaline hydrolysis and acidic work up gave carboxylic acid **17**[45], which underwent conversion into the corresponding hydroxamic acid as aforementioned.

Scheme 4[a]. Synthetic route to the *N*-phenylphenothiazine hydroxamic acid **18**.

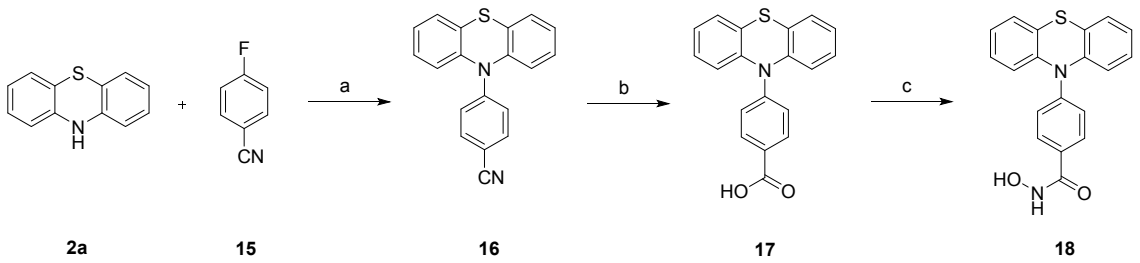

2a **15** **16** **17** **18**

[a]Reagents and conditions: (a) LiHMDS, DMF, 0 °C → rt; (b) KOH, EtOH/H_2O (7:3), reflux; (c) DIPEA, COMU, NH_2OH x HCl, DMF, 0 °C → rt

To elucidate the relevance of an extended linker compound **22** containing a phenylethyl linker was prepared (Scheme 5). A novel reductive *N*-phenylethylation of phenothiazine under acidic conditions with triethylsilane, trifluoroacetic acid and methyl 4-(2-methoxyvinyl)benzoate gave the ester **20**[46]. The required enol ether **19** was obtained by Wittig reaction of methyl 4-formylbenzoate using (methoxymethyl)triphenylphosphonium chloride and LDA. Subsequent ester hydrolysis and formation of hydroxamic acid was done as described above.

Scheme 5[a]. Synthetic route to phenylethyl hydroxamic acid **22**.

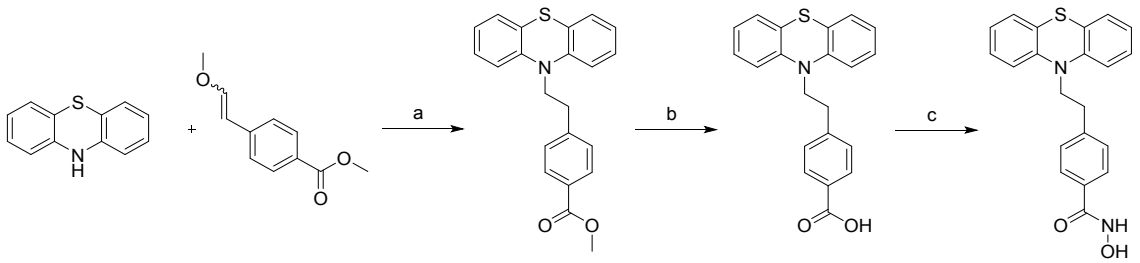

2a **19** **20** **21** **22**

[a]Reagents and conditions: (a) TFA, Et_3SiH, CH_2Cl_2 ; (b) NaOH, H_2O/1,4-dioxane (1:1), 60 °C; (c) DIPEA, COMU, NH_2OH x HCl, DMF, 0 °C → rt

INHIBITION OF HDAC1, HDAC6, AND HDAC8

All the synthesized compounds were evaluated for their inhibitory activity against human HDAC1 and HDAC6 in a biochemical in vitro assay[47]. The data are summarized in Table 2. The selective inhibitors Tubacin and Tubastatin A were included as reference substances. Already published values for Tubastatin A are listed additionally for comparison across different assay procedures. Compared to published data, Tubastatin A turned out to be 9 times more potent on HDAC1 and 2 times less potent on HDAC6 and therefore significantly less selective for HDAC6 over HDAC1 when tested in our system. These outcomes indicate that our compounds show, at least in our assay, greater selectivity for HDAC6 over HDAC1 in comparison to Tubastatin A.

Our lead structure **1a** already showed very impressive HDAC6 inhibition (IC_{50} = 22 nM) and a selectivity factor of 231 over HDAC1, thus comparing favourably with the data obtained for Tubastatin A in our assay (IC_{50} = 30 nM, selectivity factor 64). Primarily our studies focused on optimizing the capping motif of **1a** to even improve potency and selectivity for HDAC6. However, we also tested alternative linker motifs (**18** and **22**). The results demonstrated once more that a sp^3 carbon connecting the aromatic part of the linker and the cap is crucial for maintaining potent inhibition of HDAC6. While the direct connection to a phenyl linker (**18**) resulted in almost complete loss of activity and selectivity for HDAC6, the flexible phenylethyl linker (**22**) showed merely a reduced ability to inhibit HDAC6 with decreased selectivity. A similar outcome for HDAC6 inhibition was received for a phenylethyl analogue of Tubastatin

A[24]. Therefore we did not further explore the linker motif and retained the benzyl linker for the following compounds.

Regarding the modified capping motif, all congeners of **1a** containing additional substituents at positions 1 or 2 of the phenothiazine scaffold (**7c, 7d, 7f, 7g** and **7h)** also showed inhibitory activities on HDAC6 in the low nanomolar range (≤ 31 nM) and similar selectivity profiles. The same applies to the sulfone **7b**, whereas the sulfoxide **7e** suffered slightly in potency and selectivity. The incorporation of one or two nitrogen atoms into the phenothiazine scaffold (**7i** to **7n, 7p**) even enhanced the potency for HDAC. In comparison to afore mentioned compounds these (di)azaphenothiazine-containing compounds exhibited up to fourfold increase in HDAC6 inhibition accompanied by non-uniform changes in selectivity over HDAC1. Additional substitution at position 3 (chlorine) in compound **7q** resulted in a slight loss in selectivity for HDAC6. Moving the position of the linker from position 10 (thiazine nitrogen; compounds **7p** and **7q**) to N-1 of the diazaphenothiazine ring system (compounds **10p** and **10q**) resulted in the most detrimental impact on selectivity. Strikingly, compound **7i**, bearing an 1-azaphenothiazine scaffold, attained a very high level of potency (5 nM) and selectivity (538-fold). Substantial variations of the phenothiazine scaffold as demonstrated with the thiazole congener **7o**, resulted in a slight decline in potency and selectivity compared to compound **1a**.

A significant increase (from 1000 to 3700-fold) in selectivity had been reported for the tetrahydro-β-carboline regioisomer of Tubastatin A[27]. However, introduction of an analogous tetrahydropyridine motif into our phenothiazine scaffold (compound **14j**) led to a slight decrease in potency accompanied by a dramatic loss in selectivity.

Not surprisingly, the *N,O*-dimethyl-substituted hydroxamic acid **23** was completely inactive on both HDACs. Further, the carboxylic acid precursors **5a** and **5n** did not show noteworthy HDAC6 inhibition in concentrations up to 25 μM (data not shown here).

Table 2. In vitro inhibition of HDAC1 and HDAC6.

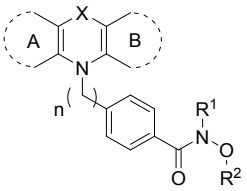

Compound	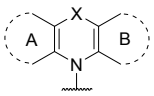	n =	R^1, R^2 =	hHDAC1[a] IC_{50} [μM]	hHDAC6[a] IC_{50} [μM]	SF 1/6[b]
Tubacin				1.01 ± 0.11	0.007 ± 0.001	144
				1.40 ± 0.24[24]	0.004 ± 0.001[24]	350
Tubastatin A	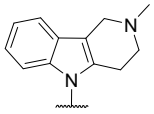	1	H	1.91 ± 0.42	0.030 ± 0.002	64
				16.4 ± 2.6[24]	0.015 ± 0.001[24]	1093
Regioisomer of Tubastatin	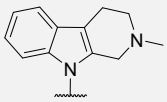	1	H	5.18 ± 0.12[27]	0.0014 ± 0.0003[27]	3700
1a	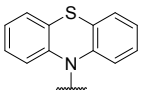	1	H	5.08 ± 0.51	0.022 ± 0.007	231
7b	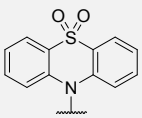	1	H	3.99 ± 1.38	0.013 ± 0.001	307
7c	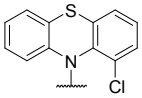	1	H	5.76 ± 1.09	0.016 ± 0.002	360

7d	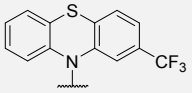	1	H	7.49 ± 1.63	0.025 ± 0.002	300
7e	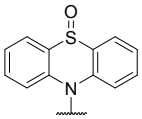	1	H	6.81 ± 2.65	0.077 ± 0.006	88
7f	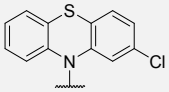	1	H	2.95 ± 0.18	0.012 ± 0.001	246
7g	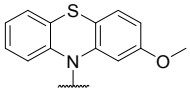	1	H	2.07 ± 0.19	0.010 ± 0.001	207
7h	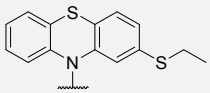	1	H	7.20 ± 0.42	0.031 ± 0.003	232
7i	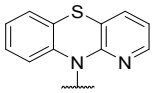	1	H	2.69 ± 1.04	0.005 ± 0.001	538
7j	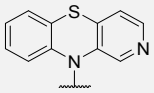	1	H	1.25 ± 0.01	0.007 ± 0.001	179
7k	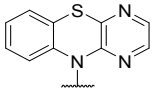	1	H	3.84 ± 0.13	0.017 ± 0.006	226
7l	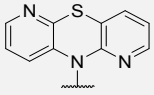	1	H	3.39 ± 0.23	0.014 ± 0.003	242
7m	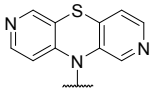	1	H	0.79 ± 0.14	0.009 ± 0.001	88
7n	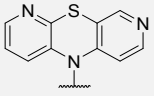	1	H	3.34 ± 0.21	0.012 ± 0.003	278
7o	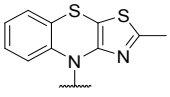	1	H	5.05 ± 0.75	0.037 ± 0.008	136
7p	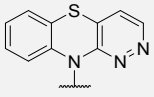	1	H	1.06 ± 0.08	0.011 ± 0.001	96
7q	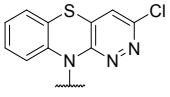	1	H	1.08 ± 0.04	0.018 ± 0.005	60

10p	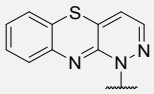	1	H	0.75 ± 0.04	0.019 ± 0.003	39
10q	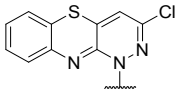	1	H	4.58 ± 0.73	0.115 ± 0.026	40
14j	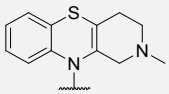	1	H	0.98 ± 0.20	0.032 ± 0.005	31
18	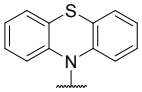	0	H	5.87 ± 0.71	2.67 ± 0.47	2
22	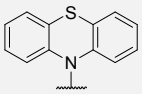	2	H	11.68 ± 2.61	0.136 ± 0.023	86
23	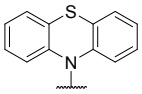	1	CH_3	n.i.	n.i.	

[a]IC_{50} values are the mean of at least two experiments. [b]SF1/6: selectivity factor for HDAC6 over HDAC1 (SF1/6 = IC_{50}(HDAC1)/IC_{50}(HCAC6)). n.i. was defined as <50% inhibition at 100 μM.

Ligand efficiency (LE) was used to estimate the relevance of achieved changes in potency regarding HDAC6 in terms of the performed modifications (Table 3). LE is a measure of the in vitro biological activity corrected for the number of heavy atoms (HA) and allows to assess how effectively the compound uses its structural features in binding to the target protein[48]. Regarding the alterations of our lead structure **1a** the highest ligand efficiencies were registered for the (di)azaphenothiazine-containing compounds (**7i** to **7n**, **7p**) with LE values ≥ 0.44 and therefore surpassing compound **1a** and Tubastatin A. Compound **7i** with an LE = 0.47 was also the most potent one and in good consistence with the mean value of published oral drugs (LE = 0.45)[48].

Table 3. IC_{50} values [μM] and ligand efficiencies (LE) [(kcal/mol)/non-H-Atom] on HDAC6. Tub A = Tubastatin A.

	Compound							
	Tub A	Tub A	**1**	**18**	**22**	**7b**	**7c**	**7d**
HA	25	25	25	24	26	27	26	29
IC_{50}, HDAC6	0.015[24]	0.030	0.022	2.67	0.136	0.013	0.016	0.025
LE, HDAC6	0.44	0.43	0.43	0.33	0.37	0.41	0.43	0.37
	Compound							
	7f	**7e**	**7g**	**7h**	**7i**	**7j**	**7k**	**7p**
HA	26	26	27	28	25	25	25	25
IC_{50}, HDAC6	0.012	0.077	0.010	0.031	0.005	0.007	0.017	0.011
LE, HDAC6	0.43	0.39	0.42	0.38	0.47	0.46	0.44	0.45
	Compound							
	7l	**7m**	**7n**	**7q**	**10p**	**10q**	**7o**	**14j**
HA	25	25	25	26	25	26	25	26
IC_{50}, HDAC6	0.014	0.009	0.012	0.018	0.019	0.115	0.037	0.032
LE, HDAC6	0.45	0.46	0.45	0.42	0.44	0.38	0.42	0.41

Some previously reported highly potent HDAC6 inhibitors exhibited moderate selectivity over HDAC8[49, 50] or even were HDAC6/8 dual inhibitors[51]. Therefore four representative compounds were selected to be also tested on HDAC8. Compound **7i** showed a selectivity profile

considerably better than those of SAHA (Vorinostat) and Tubastatin A, meaning an excellent selectivity of this compound for HDAC6 (Table 4). Compounds **1a**, **7i** and **7n** were further tested for HDAC4 inhibition, but showed less than 20% inhibition at 10 μM (data not shown here).

Table 4. In vitro inhibition of HDAC1, HDAC6, and HDAC8

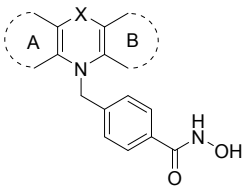

Compound	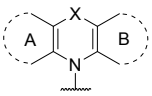	hHDAC1[a] IC_{50} [μM]	hHDAC6[a] IC_{50} [μM]	hHDAC8[a] IC_{50} [μM]	SF 1/6[b]	SF 8/6[c]
SAHA		0.117 ± 0.006	0.104 ± 0.009	0.400 ± 0.100	1	4
Tubastatin A	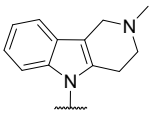	1.91 ± 0.42	0.030 ± 0.002	0.695 ± 0.060	64	23
		16.4 ± 2.6[24]	0.015 ± 0.001[24]	0.854 ± 0.040[24]	1093	57
1a	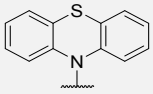	5.08 ± 0.51	0.022 ± 0.007	1.48 ± 0.04	231	67
7i	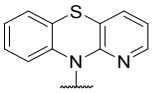	2.69 ± 1.04	0.005 ± 0.001	3.10 ± 0.09	538	620
7n	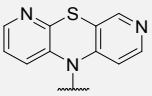	3.34 ± 0.21	0.012 ± 0.003	2.00 ± 0.03	278	167
14j	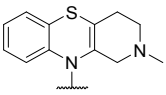	0.98 ± 0.20	0.032 ± 0.005	66% inhibition @ 1 μM	31	n.d.

[a]IC_{50} values are the mean of at least two experiments. [b]SF1/6: selectivity factor for HDAC6 over HDAC1 (SF1/6 = IC_{50}(HDAC1)/IC_{50}(HCAC6)). [c]SF8/6: selectivity factor for HDAC6 over HDAC8 (SF8/6 = IC_{50}(HDAC8)/IC_{50}(HCAC6)). n.d. not determined

CELLULAR DATA

To further validate the results obtained in the in vitro assay, Western blotting experiments were performed with two of our best compounds (**7i** and **7n**) in the leukemic cell line HL 60. The pan-HDAC inhibitor SAHA was used as a reference compound. HL60 cells were incubated for 4 h with SAHA, **7i** or **7n** in three different concentrations (10 μM, 1 μM, and 0.1 μM). Cell lysates were blotted against Ac-α-tubulin, Ac-histone H3, and GAPDH. The pan-HDAC inhibitor SAHA induced an increase of tubulin acetylation as well as of histone acetylation in HL60 cells compared to DMSO control. At least at 1 μM **7i** and **7n** induced only the acetylation of tubulin but not of histone H3 (see Figure 1), reflecting the selectivity ascertained in vitro also in the cellular setting in this range of concentration. At 10 μM some histone hyperacetylation is visible, showing the concentration dependence of selectivity in the cellular setting.

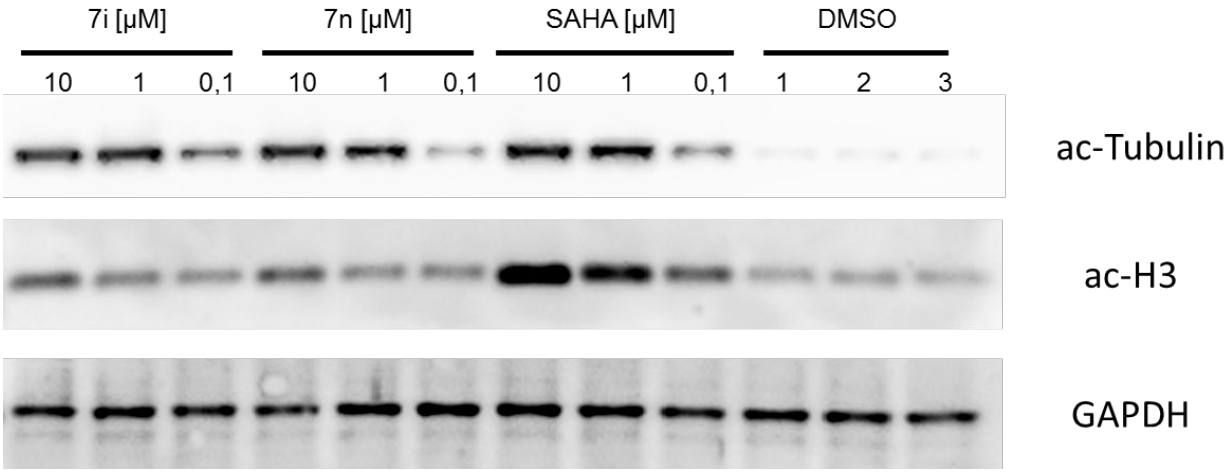

Figure 1. Western blots of acetyl-α-tubulin, acetyl-H3, and GAPDH after treatment of HL60 cells with SAHA, **7i**, and **7n**. GAPDH was the loading control. DMSO was the negative control.

The Western blots were quantified simply by determining the ratio of acetylated tubulin versus GAPDH and of acetylated histone 3 versus GAPDH (Table 5).

As shown in Figure 1 and Table 5, the induction of tubulin acetylation by **7i** and **7n** was greater than the induction of histone H3 acetylation at all concentrations tested. Compared to SAHA the level of acetylated tubulin is higher than the level of acetylated histone H3, except for **7n** at the lowest concentration. Thereby the HDAC6 selectivity of these compounds is also demonstrated and validated on a cellular level.

Table 5. Quantification of Western blots in HL60 cells

Compound	Ac-tubulin/GAPDH	Ac-H3/GAPDH	selectivity index[a]
DMSO	1.00[b]	1.00[b]	
SAHA, 10 μM	9.52	2.80	3.40
SAHA, 1 μM	9.97	1.91	5.22
SAHA, 0.1 μM	3.79	1.52	2.49
7i, 10 μM	9.20	1.28	7.19
7i, 1 μM	9.41	1.07	8.79

7i, 0.1 μM	5.42	1.14	4.75
7n, 10 μM	10.93	1.47	7.44
7n, 1 μM	7.97	0.99	8.05
7n, 0.1 μM	2.16	1.05	2.06

[a]Selectivity index defined as quotient of Ac-tubulin/GAPDH divided by Ac-H3/GAPDH. [b]All values have been normalized to DMSO.

Histone deacetylase 6 (HDAC6) is a crucial regulator of gene expression and transcription in cancer and several HDAC6 inhibitors are currently investigated in clinics as potential tumor therapeutics[16]. Likewise, we aimed at investigating the effects of **7i** and **7n** on different cancer cells, to investigate the functional effects of HDAC6 inhibition in different tumor entities. Additionally, we used non-malignant cells to assess the cancer specificity and to estimate cytotoxicity (Figure 2). **1a** and the pan-HDAC inhibitor SAHA were used as reference compounds. Firstly, CellTiter-Blue® cell viability assays indicated that **7i** and **7n** inhibited proliferation of HUH7 (hepatocellular carcinoma, Figure 2 A), MDA-MB-231 (breast adenocarcinoma, Figure 2 B) and T24 (bladder carcinoma, Figure 2 C) cells at concentrations of 10 and 100 μM after 72. SAHA treatment generally resulted in stronger antiproliferative effects, with IC_{50} values in the low micromolar range (HUH7: 1.2 μM, MDA-MB-231: 2.8 μM, T24: 2.4 μM). Similar findings were made for other breast cancer (MCF7) and leukemia (HL60, THP-1) cellular models (Figure S7, Supporting Information), showing an antiproliferative effect on cancer cells of different tissue types. Secondly, cytotoxic effects on cancer cells were analyzed by measurement of apoptotic cell death. In accordance with antiproliferative effects, the highest apoptosis rates of all tested HDAC

inhibitors were observed after treatment of MDA-MB-231 breast cancer and T24 bladder cancer cells (Figure 2 D and E) with SAHA for 48 h, as assessed with propidium iodide staining and flow cytometry . These findings further emphasized that **1a**, **7i** and **7n** are selective HDAC6 inhibitors and their application as single treatment only causes minor anticancer activity, which is in line with the low clinical activity of selective HDAC6 inhibitors[16]. The HDAC6 inhibitor with reduced class I HDAC inhibition Ricolinostat, for instance, is well tolerated but it has low clinical activity when applied as monotherapy[52], and Woan et al. showed that both genetic ablation and pharmacologic inhibition of HDAC6 decreased cancer cell proliferation without inducing apoptosis[53]. The limited anticancer activity of specific HDAC6 inhibitors is sought to be overcome by combination strategies, e.g. with immunotherapeutic agents like Lenalidomide[52] or anti-PD-L1 antibodies[54] or, alternatively, with the proteasome inhibitor Bortezomib[55, 56], for which a synergistic effect was observed[56]. Based on that, we hypothesized that **1a**, **7i** and **7n** might alter critical cancer-related pathways, namely immune checkpoints and unfolded protein response (UPR). Hence, we checked the influence of specific HDAC6 inhibition on programmed death receptor ligand-1 (PD-L1, Figure 2 F) and endoplasmatic reticulum chaperone BiP (GRP78, Figure 2 G). Interestingly, western blot analyses of bladder carcinoma lysates revealed that pharmacologic HDAC inhibition caused a clear upregulation of PD-L1 and a slight increase in GRP78 protein level. Based on that finding, we tested combinations of **1a**, **7i** and **7n** with Bortezomib and their influence on cell proliferation by impedance measurements (Figure S9 A and B, Supporting Information). However, we could not prove a synergism of **1a**, **7i** and **7n** and Bortezomib at the tested concentrations, which we related to the narrow therapeutic window of Bortezomib in our setting (Figure S9 C, Supporting Information). Moreover, our data could help to decipher the interaction of HDAC6 and PD-L1 in cancer, which is still debated. Woods et al.[57] could show that

class I HDAC inhibition enhances antitumor immunity by upregulating PD-L1 expression in melanomas, Lienlaf et al. on the other hand found a reduction of PD-L1 protein level after selective HDAC6 inhibition in melanoma cells. They reported that HDAC6 is essential for cytokine mediated expression control of PD-L1[58]. Yet, Woan et al. could not detect alterations in PD-L1 protein level after pharmacologic or genetic disruption of HDAC6 activity[53]. It is therefore obvious that more research has to be performed to clarify the role of HDAC6 in PD-L1 regulation. Adding still more complexity to the question, the regulation might also be tissue specific as tumors of different origin display distinct immunogenicity[59]. Therefore, HDAC6 inhibition can cause an upregulation of PD-L1 in bladder cancer, as reported in our study, and at the same time a downregulation in melanoma as reported by Lienlaf et al.[58]. Hence, our findings confirm the rationale for combining **1a**, **7i** and **7n** with anti-PD1/anti-PD-L1 antibodies and proteasome inhibitors.

Furthermore, toxicity of the HDAC inhibitors on non-malignant cells was assessed using HepaRG™ cells, a non-cancerous hepatic stem cell line that expresses high levels of CYP450 enzymes and thereby allows detection of CYP450-mediated toxicity. Toxicity and unfavourable tolerability associated with pan-HDAC inhibitor therapy[15] remain key unmet needs that have driven the development of specific HDAC6 inhibitors. Viability of HepaRG™ cells after 24 h of treatment was not affected even at 100 μM concentrations of **1a** and **7i**, whereas application of SAHA and **7n** slightly decreased cell viability at the highest tested concentrations to around 80% (Figure 2 H).

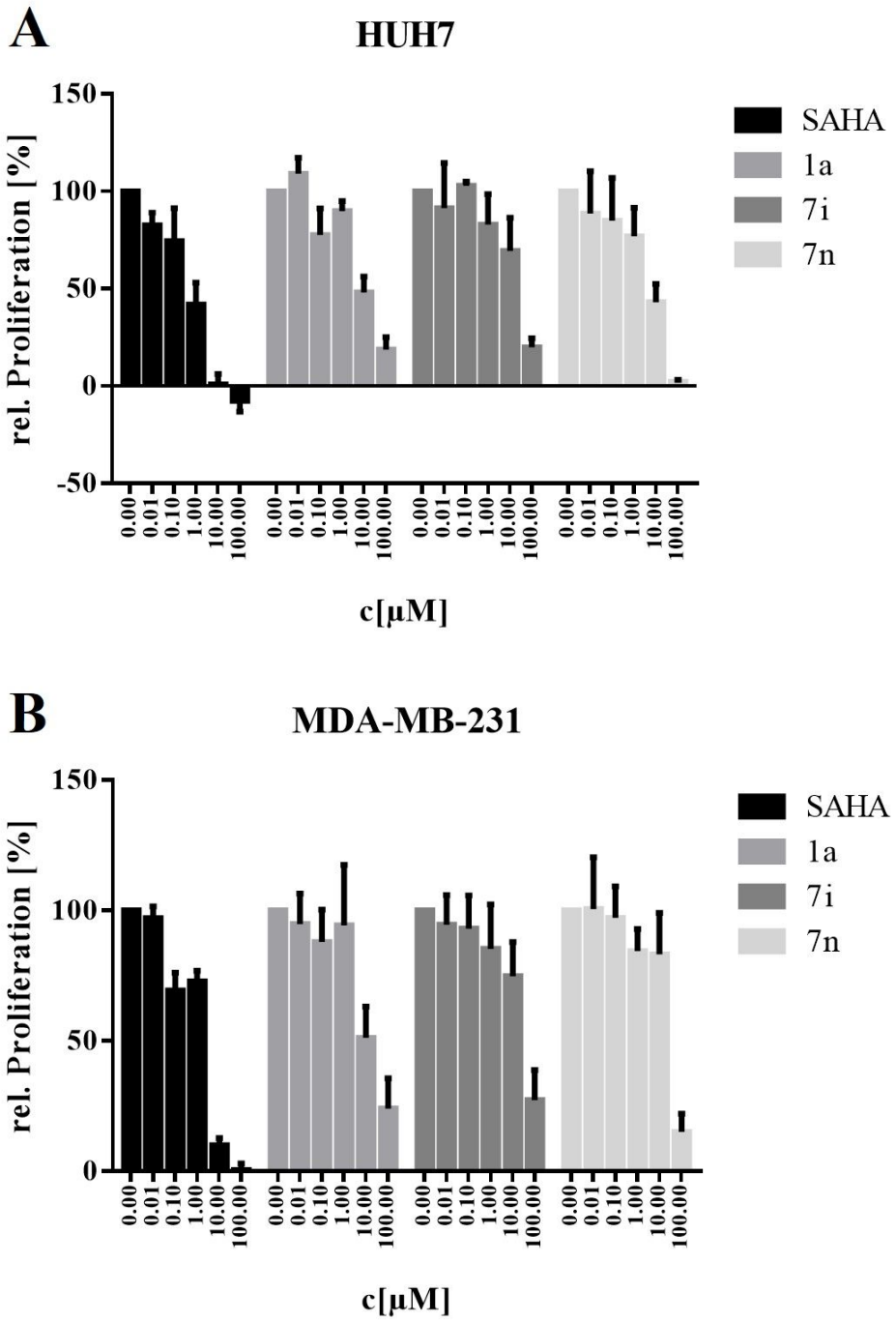
A
HUH7
rel. Proliferation [%]
150
100
50
0
-50
0.00
0.01
0.10
1.00
10.00
100.00
c[µM]
SAHA
1a
7i
7n
B
MDA-MB-231
rel. Proliferation [%]
150
100
50
0
c[µM]
SAHA
1a
7i
7n

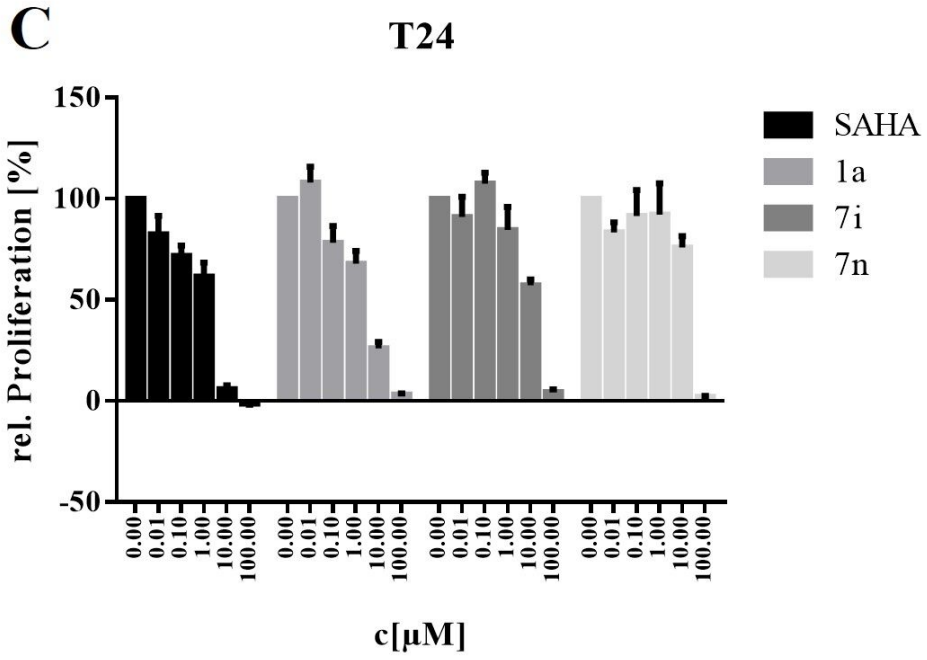
C
T24
rel. Proliferation [%]
150
100
50
0
-50
0.00
0.01
0.10
1.00
10.00
100.00
c[µM]
SAHA
1a
7i
7n

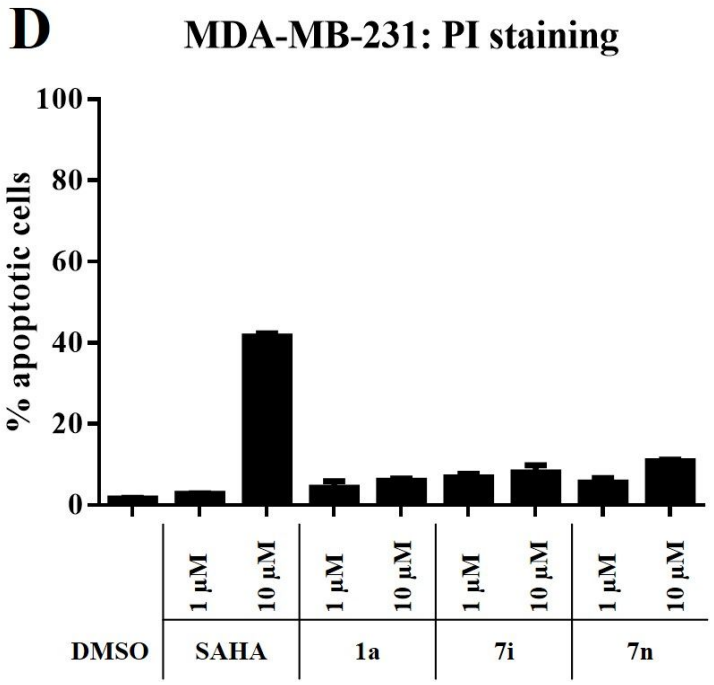
D
MDA-MB-231: PI staining
% apoptotic cells
100
80
60
40
20
0
1 µM
10 µM
DMSO
SAHA
1a
7i
7n

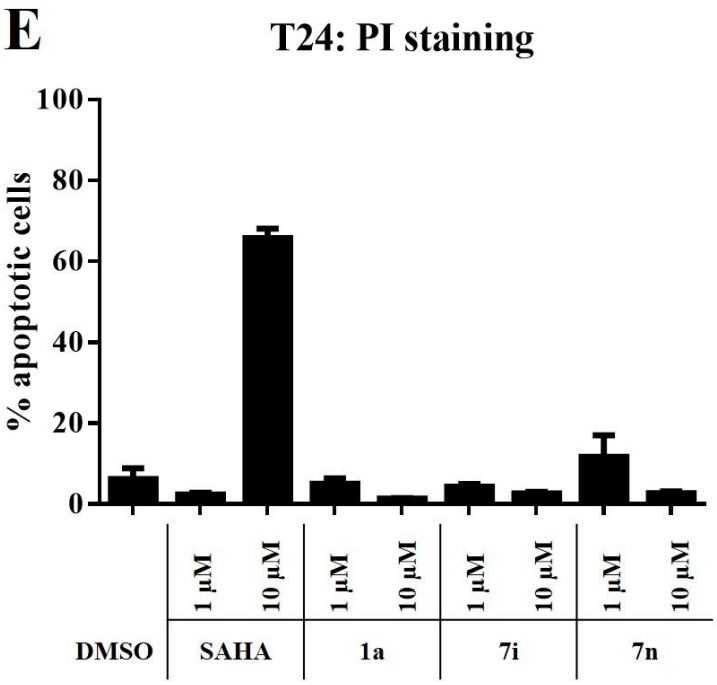

F

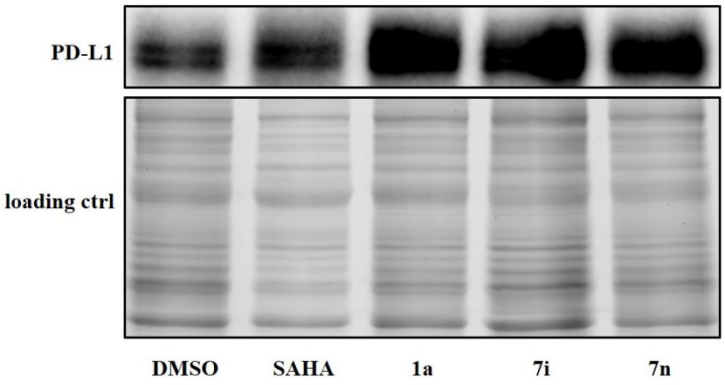

Compound	Relative normalized volume intensity
SAHA	1.94
1a	2.44
7i	1.65
7n	2.1

G

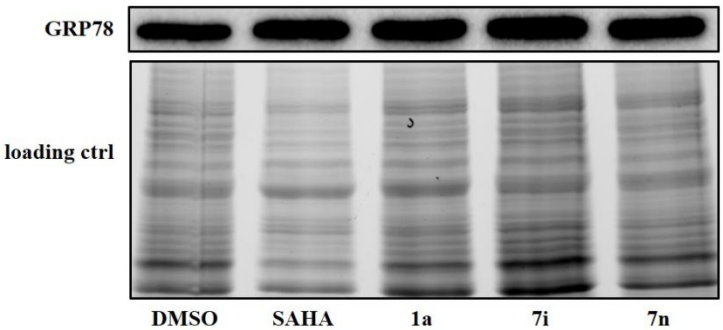

Compound	Relative normalized volume intensity
SAHA	1.90
1a	1.36
7i	1.60
7n	1.61

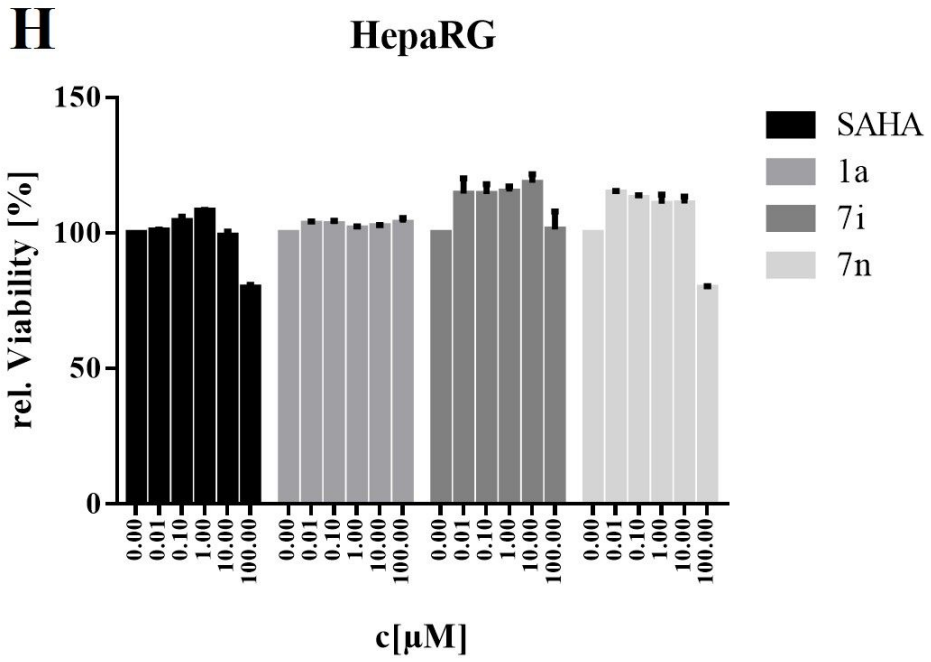

Figure 2. Biological testing of SAHA, **1a**, **7i** and **7n**. Proliferation of (A) HUH7, (B) MDA-MB-231, and (C) T24 cells was analyzed by CellTiter-Blue® cell viability assay after treatment as indicated for 72 h. Apoptosis of (D) MDA-MB-231 and (E) T24 cells was assessed by propidium iodide staining and flow cytometry after treatment as indicated for 48 h. Expression of (F) PD-L1 and (G) GRP78 was detected by western blot analysis of T24 protein lysates upon 10 µM treatment with the indicated compounds (48 h). Protein bands were normalized to whole lane protein of the DMSO control (loading control). (H) Viability of HepaRG™ cells was analyzed by CellTiter-Blue® cell viability

assay after treatment as indicated for 24 h. Data shown in (A)-(E) and (H) represent means ± SEM, performed in triplicates.

IN VITRO ASSESSMENT OF METABOLIC STABILITY AND CYP INHIBITION

Lead structure **1a** and the outstanding inhibitor **7i** were investigated regarding their metabolic stability and ability to inhibit cytochrome P450 (CYP) enzymes.

In the human liver microsomal stability assay compound **1a** showed moderate stability (Table 6, Figure S8, Supporting Information), with about 77% compound remaining after 40 min incubation. There was no evidence for a hydrolysis of the hydroxamate function, but increasing small amounts of both the sulfoxide **7e** and the sulfone **7b** were observed. Both of these metabolites still exhibit noteworthy HDAC6 inhibition (Table 2). This metabolic profile is in line with observations made for other N-substituted phenothiazines[60, 61]. In contrast, azaphenothiazine **7i** was metabolically quite stable, and degradation started only slowly after 20 min incubation.

Table 6. Metabolic stability in human microsomes

	Human microsomal stability[a]	
Compound	$t_{1/2}$ [min][b]	Cl_{int} [µL/min/mg][b]
Propranolol[c]	>40 (67)	26

Caffeine[c]	>40 (373)	4
1a	>40 (117)	14
7i	>40 (148)	11

[a]Five test points (up to 40 min) were analysed for each compound. All test points were performed in duplicates. Test concentration of compound 2 μM with human liver microsome protein 0.42 mg/mL. Amount of compound was determined by LC-MS/MS. [b]half-time ($t_{1/2}$) and clearance (Cl_{int}) were determined in plot of ln(AUC) vs. time, using linear regression analysis. [c]Propranolol as reference compound with moderate metabolic stability and Caffeine as metabolically stable reference compound.

In the fluorogenic CYP450 inhibition assay on five CYP subtypes compound **1a** showed relevant inhibition of 2C19 and 2D6 CYP isoform at the test concentration of 10 μM, whereas **7i** did not show any significant inhibition of CYP activity. Since HDAC6 inhibitors are currently investigated as potential tumor therapeutics in co-administration with other antitumor drugs and the applied CYP enzymes (CYP1A2, CYP2C9, CYP2C19, CYP2D6 and CYP3A4) are involved in about 95 % of the known drug metabolism, it is less likely that **7i** would cause metabolism-mediated interactions in a combination therapy.

Table 7. CYP450 inhibition

	CYP inhibition [%][a]				
Compound	CYP1A2	CYP2C9	CYP2C19	CYP2D6	CYP3A4
Reference inhibitor[b]	97.4	96.5	98.7	97.9	98.4
1a[c]	20.0	24.4	36.4	45.4	24.3
7i[c]	15.2	3.4	27.7	12.0	8.8

[a]all test points were performed in quadruplicates. [b]test concetrations of reference inhibitors correspond to approximately 50 fold reported IC_{50} values for the corresponding CYP450 in order to achieve 80-100 % inhibition. Reference inhibitors: CYP1A2 α-naphthoflavone, CYP2C9 sulfaphenazole, CYP2C19 ticlopidine, CYP2D6 quinidine, CYP3A4 ketoconazole. [c]test concentration of compound 10 μM.

These results indicate that the azaphenothiazine moiety in **7i** provides, compared to the parent phenothiazine cap group, enhanced metabolic stability and a decreased potential for drug-drug interactions due to inhibition of hepatic CYP enzymes.

DOCKING STUDY

To study the putative determinants of HDAC inhibitor selectivity, we performed docking studies using the solved crystal structures of hHDAC1[62] (PDB ID 5ICN), hHDAC6[5] (PDB ID, PDB ID5EDU) , HDAC6 from *Danio rerio* (zHDAC6, PDB ID 5EF7, 5G0I)[6] and hHDAC8 (PDB ID

1W22)[63]. The applied docking method was first successfully validated using the X-ray structures of hHDAC1, hHDAC6, zHDAC6 and hHDAC8 (for details see Methods section). The docking program GLIDE could perfectly reproduce the co-crystallized inhibitors in HDAC1, HDAC6 and HDAC8 (Figures S2, S3 and S4, Supporting Information). The docking of the phenothiazine-based benzhydroxamates to the catalytic domain 2 of hHDAC6 indicated that the *N*-arylmethylphenothiazine derivatives fit perfectly into the binding pocket (Figure 3, A). A similar orientation of the phenothiazine group and the 1,2,3,4-tetrahydropyrido[4,3-b]indole ring of Tubastatin A was found (Figure 3, B). As expected, the hydroxamate group coordinates the catalytic zinc ion in monodentate fashion as observed for some co-crystallized aromatic hydroxamates (*N*-hydroxy-4-{[(2-hydroxyethyl)(phenylacetyl)amino]methyl}benzamide; HPB) in zHDAC6 (PDB ID 5WGK), ACY-1083 in zHDAC6 (PDB ID 5WGM)[40], and *N*-hydroxy-4-(2-[(2-hydroxyethyl)(phenyl)amino]-2-oxoethyl)benzamide (HPOB) in zHDAC6 (PDB ID 5EF7)[6], (Figures S2 and S3, Supporting Information). A methylene spacer between the benzhydroxamate and the tricyclic ring system is required for shape complementarity between the phenothiazine and the rim of the hHDAC6 binding pocket (Figure 4). The slightly-bent phenothiazine moiety is interacting by π,π stacking with the aromatic residues H500, P501, and P620, and by van der Waals interaction with L749. The unmodified phenothiazine **1a** as well as the substituted and aza-derivatives adopt more or less the same orientation in the hHDAC6 binding pocket and yielded similar docking scores (Table S2, Supporting Information). This is in agreement with the only slight effect of these modifications on the hHDAC6 inhibition values (IC_{50} 0.005-0.037 μM). By removing the methylene group between benzhydroxamate and phenothiazine (**18**) the molecule is no longer able to adopt a kinked conformation that is required to fit perfectly into the binding pocket and to coordinate the zinc ion. As consequence, the docking score is less favorable (Table

S2, Supporting Information). An ethyl linker between the phenyl and phenothiazine (in compound **22**) is also less favorable; in this case, the phenothiazine cap protrudes from the binding pocket and loses the interaction with H500 and P620.

In contrast, the docking of the inhibitors to hHDAC1 showed that in this enzyme the benzhydroxamate is not able to perfectly coordinate to the catalytic zinc ion due to the narrow binding pocket (Figure 5). The distances between the hydroxamate group and the zinc ion are generally larger than in the hHDAC6 complexes. Thus, these docking studies reveal the structural basis for the HDAC6 selectivity of the synthesized inhibitors.

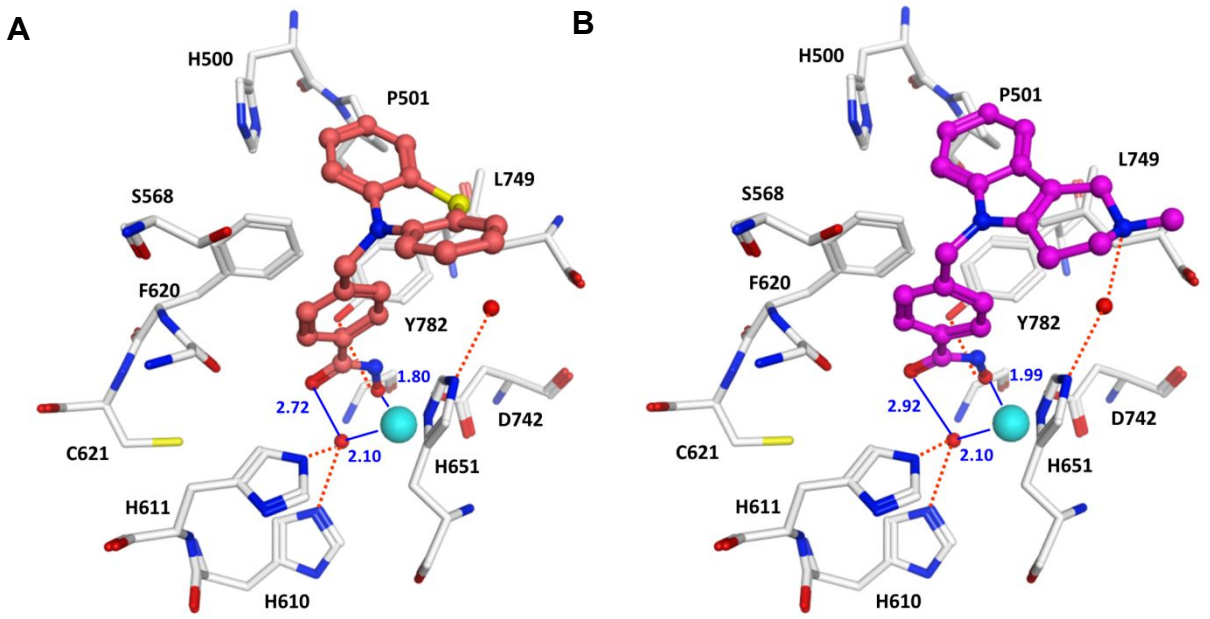

Figure 3. Docking poses calculated for inhibitor **1a** (colored salmon) (**A**), and Tubastatin A (colored magenta) (**B**) at hHDAC6 (PDB ID 5EDU). Only surrounding amino acid residues are shown for clarity. Hydrogen bonds are shown as orange dashed lines. The zinc ion is shown as cyan ball and water molecules are shown as red balls. Distances between the hydroxamate and zinc ion/water are given in Å (blue colored lines).

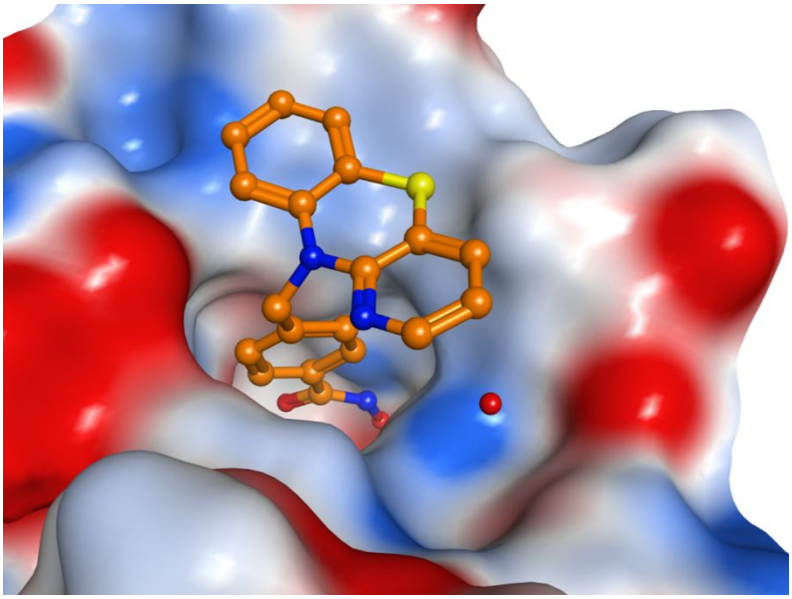

Figure 4. Docking pose calculated for inhibitor **7i** (colored orange). The molecular surface of the hHDAC6 (PDB ID 5EDU) binding pocket is colored according to the electrostatic potential (blue = electropositive, red = electronegative).

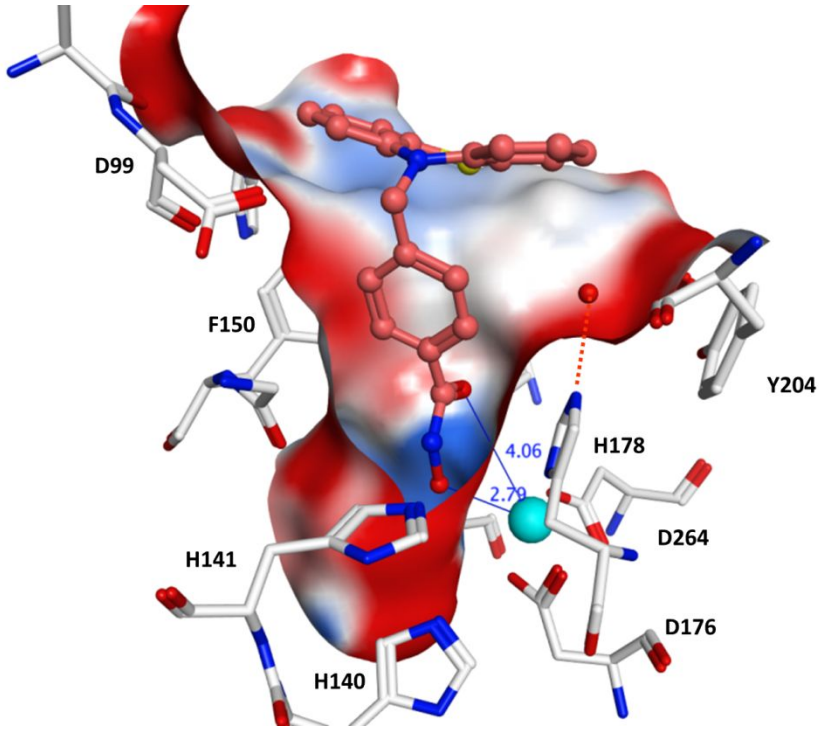

Figure 5. Molecular surface of the hHDAC1 binding pocket (PDB ID 5ICN) colored according to the electrostatic potential (blue = electropositive, red = electronegative). The docking pose of inhibitor **1a** is colored salmon. Hydrogen bonds are shown as dashed orange colored lines. The distances between the hydroxamate group and the zinc ion are given in Å and are drawn as blue colored lines.

As a negative control we prepared the *N,O*-dimethyl-substituted hydroxamic acid **23**. This compound is not able to to coordinate to the zinc ion (Figure 6), and consequently is completely inactive on both HDACs. Free carboxylic acids **5a** and **5n** were inactive on HDAC6 as well. Docking of **5a** to either zHDAC6 or hHDAC6 showed that due to the steric bulk of the capping group the carboxylate oxygen is not able to interact directly with the zinc ion (Figure S5, Supporting Information).

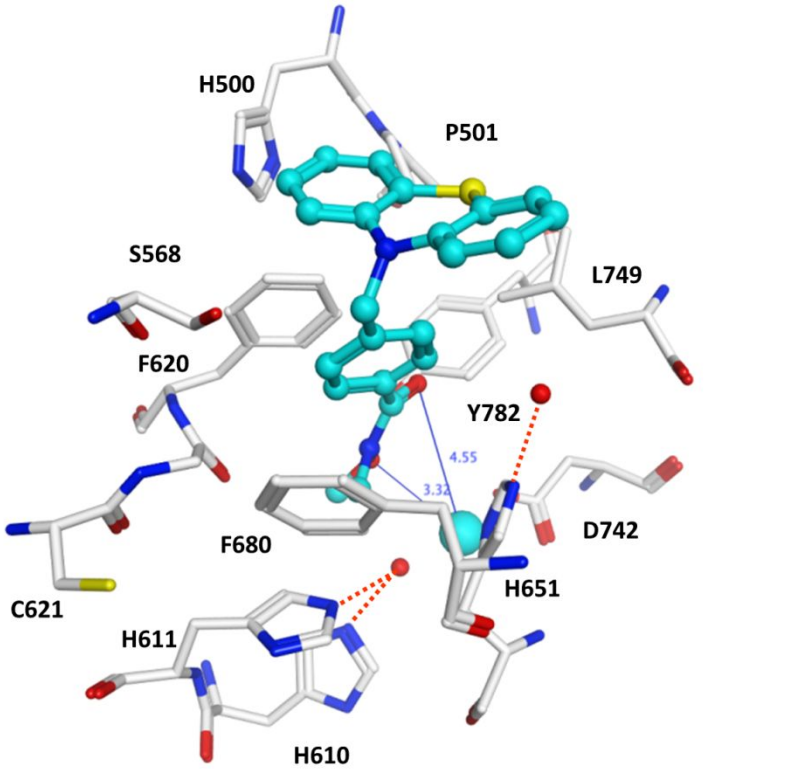

Figure 6. Docking poses of the inactive inhibitor **23** (colored cyan) at hHDAC6 (PDB ID 5EDU). Due to the full methylation of the hydroxamate group this compound is not able to coordinate to the zinc ion. Only surrounding amino acid residues are shown for clarity. Hydrogen bonds are shown as orange dashed lines. The zinc ion is shown as cyan ball. The distances between the hydroxamate group and the zinc ion are given in Å and are drawn as blue colored lines.

To rationalize the observed selectivity for hHDAC6 over hHDAC8 we docked the inhibitors **1a, 7i, 7n, 14j** and Tubastatin A (Table 4) to hHDAC8. For the docking we took the hHDAC8 X-ray structure co-crystallized with a benzhydroxamate bearing a sulfonamide linker at the para position as observed in the synthesized phenothiazine based benzhydroxamates. Docking of the inhibitors showed that all are able to coordinate to the zinc ion in a bidentate fashion as observed for the co-

crystallized inhibitor. In the case of hHDAC8, the interaction of the tricylic system of the inhibitors is less favorable compared to HDAC6 due to the different shape of the pocket rim (Figure 7). The main reasons for the different binding mode observed for HDAC6 and HDAC8 is the longer L1 loop in HDAC6 that harbors H500 and P501 which interact with the phenothiazine ring of the inhibitors in hHDAC6 as well as the substitution of M682 (hHDAC6) to G210 in hHDAC8. These modifications significantly alter the shape of the rim region in HDAC6/8. Tubastatin A as well as **14j** contain a basic amine in the cap group that shows ionic interaction with D101 in HDAC8 (Figure S6, Supporting Information) whereas the compounds with a neutral/aromatic tricycle (e.g. **1a, 7i, 7n**) are not able to interact with D101 and are therefore less active against hHDAC8.

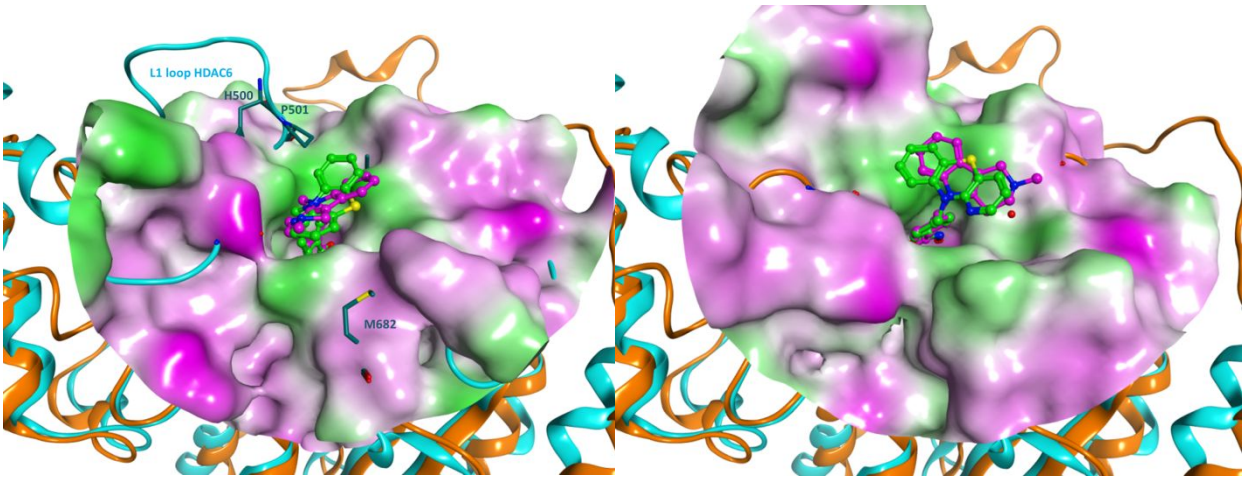

Figure 7. Comparison of the shape of the pocket rim in hHDAC8 (left side) and hHDAC6 (right side). Docking poses of Tubastatin A (magenta) and **7i** (green) are shown for both HDACs. H500, P501 (Loop L1) and M682 in hHDAC6 are shown in petrol. hHDAC6 backbone is displayed as cyan colored ribbon, hHDAC8 backbone ribbon is colored orange. Molecular surface of both

binding pockets is colored according to the hydrophobicity (magenta indicates polar, green hydrophobic regions).

CRYSTALLIZATION STUDIES

The crystal structure of *Danio rerio* HDAC6 catalytic domain 2 (zHDAC6) complexed with **7i** was solved (PDB 5W5K). The overall fold of zHDAC6 CD2 is relatively unchanged upon **7i** binding in comparison with unliganded zHDAC6 (PDB 5EEM), with a root mean square deviation (rmsd) of 0.20 Å over 313 Cα atoms. Poor electron density is observed for residues D771 and H772, so these residues are omitted from the final model. Crystallographic data collection and refinement statistics are given in Table S1 in the Supporting Information.

The hydroxamate moiety of **7i** adopts the monodentate Zn^{2+} coordination mode previously observed for the zHDAC6 complex with the isoenzyme-selective inhibitor N-hydroxy-4-(2-[(2-hydroxyethyl)(phenyl)amino]-2-oxoethyl)benzamide (HPOB) (Figure 8; an electron density map showing the bound inhibitor appears in Figure S2). The hydroxamate N-O– group coordinates to Zn^{2+} with a Zn^{2+}---O separation of 2.0 Å, while the hydroxamate C=O forms a hydrogen bond with the Zn^{2+}-bound water molecule (O---O separation = 2.9 Å). The catalytic tyrosine, Y745, interacts with the hydroxamate NH and OH groups with O---O and O---N separations of 2.7 Å each, as well as the hydroxamate C=O with an O---O separation of 3.0 Å. The Zn^{2+}-bound water molecule remains hydrogen bonded to the side chains of the catalytic histidine dyad, H573 and H574, with O---N separations of 2.6 Å and 2.5 Å, respectively. The aromatic side chains of F583 and F643 (corresponding to F620 and F680 in hHDAC6) interact with the aromatic linker group of **7i**. The azaphenothiazine capping group bends slightly with a 163˚ angle between the two aromatic planes,

meaning that the thiazine nitrogen is slightly pyramidalized with C-N-C bond angles of 115˚ between ring carbons and the methylene linker carbon. One of the aromatic rings makes van der Waals contacts with the side chains of H463, P464, and F583 (corresponding to H500, P501, and F620 in hHDAC6).

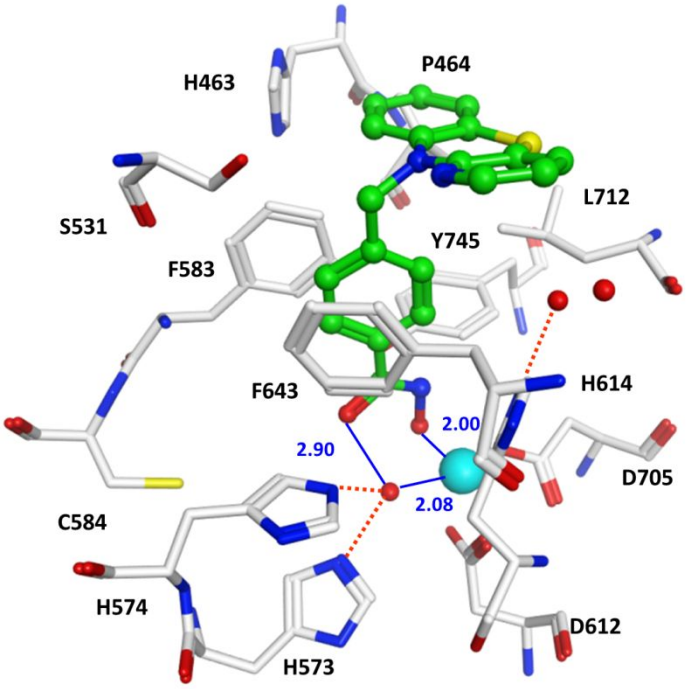

Figure 8. X-ray structure of zHDAC6 complexed with **7i** (colored green) (PDB ID 5W5K). Only surrounding amino acid residues are shown for clarity. Hydrogen bonds are shown as orange dashed lines. The zinc ion is shown as cyan ball and water molecules are shown as red balls. Distances between the hydroxamate and zinc ion/water molecule are given in Å (blue colored lines).

CONCLUSION

On the basis of a widely accepted HDAC pharmacophore model (containing cap group, linker, and zinc-binding group we developed a series of new potent and selective hydroxamate-based HDAC6 inhibitors with the phenothiazine system as cap group scaffold. We confirmed the beneficial effect of the previously published benzylic linker[24] on potency and selectivity compared to phenyl and phenylethyl linkers. The variations of the phenothiazine cap group comprising various substituents or the oxidation state of the sulphur atom yielded superb potency and selectivity. The introduction of nitrogen atoms into the phenothiazine system led to inhibitors featuring excellent potency and selectivity for HDAC6 with 1-azaphenothiazine **7i** as the most potent and selective compound among them. Docking studies carried out for hHDAC1, HDAC6 and HDAC8 gave a rationale for the high selectivity of the phenothiazine-based hydroxamates and their aromatic aza-analogues. Crystallization of the most potent and selective inhibitor **7i**, one of the very few available X-ray structures for HDAC6 with an inhibitor, clearly confirmed the binding mode to zHDAC6. The selective inhibition of HDAC6 by **7i** and **7n** was also validated in cell culture with Western blotting of tubulin versus histone acetylation. This assay has clearly a lower dynamic range than the in-vitro assay and the observed selectivity factors should be viewed semi-quantitatively, showing that the high HDAC6 selectivity was retained in cell culture. As HDAC6 represents a potential target in cancer, we investigated the effects of HDAC6 inhibition on several cancer cell lines. This study confirmed that selective HDAC6 inhibition results in low to moderate antitumor activity, which is in line with the currently available preclinical and clinical study data. However, compounds **7i** and **7n** affected immune checkpoints and proteasome-dependent degradation, which suggests them as potential candidates for combination therapies with anticancer agents. Concurrently, their acute toxic effects were low to non-existent on non-malignant cells.

It is noteworthy that several of these highly potent and selective HDAC6 inhibitors including prominent **7i** can be synthesised in a 3-step synthesis starting from commercially available or easily accessible (aza)phenothiazine building blocks.

EXPERIMENTAL SECTION

In vitro testing on HDAC1, HDAC4, HDAC6, and HDAC8.

For HDAC1 and 6 activity testing OptiPlate-96 black microplates (PerkinElmer) were used. Assay volume was 60 µL. 52 µL of human recombinant HDAC1 (BPS Bioscience, catalog no. 50051) or human recombinant HDAC6 (BPS Bioscience, catalog no. 50006) in incubation buffer (50 mM Tris-HCl, pH 8.0, 137 mM NaCl, 2.7 mM KCl, 1 mM $MgCl_2$, and 1 mg/mL BSA) were incubated with increasing concentrations of inhibitors in DMSO and 5 µL of the fluorogenic substrate ZMAL (Z-(Ac)Lys-AMC) (126 µM) for 90 min at 37 °C. After incubation time an amount of 60 µL of the stop solution, comprising 5 µl Trichostatin A (TSA) (33 µM) and 10 µl trypsin (6 mg/mL) in trypsin buffer (Tris-HCl 50 mM, pH 8.0, NaCl 100 mM), was added. The plate was incubated again at 37 °C for 30 min, and fluorescence was measured on a BMG LABTECH POLARstar OPTIMA plate reader (BMG Labtechnologies, Germany) with an excitation wavelength of 390 nm and an emission wavelength of 460 nm[47].

The HDAC4 assay was performed in 96-well half area plates with an assay volume of 30 µL. 5 µL ZMTFAL (150 µM) as fluorogenic substrate, HDAC4 (BPS Bioscience, catalog no. 50004) (0.01 µg/well) in incubation buffer (15 mM Tris-HCl, pH 7.5, 50 mM KH_2PO_4, 3 mM $MgSO_4$, 10 mM KCl) and different concentrations of inhibitors in DMSO (2.5 µL) were used. After 90 min of

incubation the assay was stopped by adding 30 µL stop solution containing 5 µL trypsin (6 mg/mL) and 2.5 µL Quisinostat (33 µM) in trypsin buffer (Tris-HCl 50 mM, pH 8.0, NaCl 100 mM). The fluorescence was measured in a plate reader (BMGPolarstar) with λ_{ex} 390 nm and λ_{em} 460 nm.

Testing on HDAC8 inhibition was performed using commercial available Fluor de Lys (FDL) drug discovery kit (BML-KI178). Corresponding to manufacturer's instructions increasing inhibitor concentrations (10 µl), enzyme (hHDAC8) solution (15 µl) and FDL substrate (25 µl) were incubated for 90 min at 37 °C. Followed by a second incubation step (45 min, 30°C) after adding of 50 µL of developer solution, fluorescence measuring was conducted as mentioned before. Enzyme was obtained as previously described[64].

Cell culture experiments

Cell culture with HL60 cells. HL60 cells (ATCC CCL-240) were cultured in RPMI medium 1640 containing 10% FBS gold, 2 mM L-glutamine, 100 U/mL penicillin, and 100 µg/mL streptomycin. 2.5 x 10^5 cells per well were seeded in a 12-well plate and immediately incubated with different concentrations of test compounds for 4 h. After incubation cells were collected in Eppendorf tubes and centrifuged with 500 g for 5 minutes at room temperature. Cells were washed with PBS and lysed in 90 µL of SDS sample buffer (Cell Signaling, 62.5 mM Tris-HCl (pH 6.8 at 25 °C), 2% w/v SDS, 10% v/v glycerol, 50 mM dithiothreitol, 0.01% bromophenol blue). After sonicating for 5 min, to shear DNA and reduce sample viscosity, the samples were heated to 95 °C for 1 min. Cell extracts were used directly for SDS−PAGE or kept frozen at −20 °C until usage. For the SDS−PAGE an amount of 7 µL of cell extracts was loaded onto a 12.5% SDS gel and run at 160 V followed by the transfer to a nitrocellulose membrane via Western

blotting for antibody-based detection. After transfer the nonspecific binding was blocked by incubating the membrane in 25 mL of blocking buffer (5% nonfat dry milk in Tris buffered saline with 0.1% Tween 20 (TBS-T)) for 1 h at room temperature or at 4 °C overnight. After washing the membrane 3 times for 5 min with TBS-T, the primary antibody (antiacetylated α-tubulin (Sigma-Aldrich T7451-200UL, 1:1000)) was added in 3% milk in TBS-T for 3 h at room temperature or overnight at 4 °C. Before exposing the membrane with the secondary antibody, it was washed again three times for 5 min with TBS-T to remove unbound primary antibody. The secondary antibody anti-mouse-IgG-HRP (Sigma-Aldrich, 1:2000) was added in 3% milk in TBS-T at room temperature for 1 h. Afterward the membrane was washed again. The detection was performed via enhanced chemiluminescence (ECL Prime) after incubation for 5 min in the dark with a FUSION-SL (PEQLAB) and the FUSION-CAPT software. After detection of acetylated tubulin the whole procedure was repeated with the primary antibody antiacetyl-histone H3 (Millipore 06.599, 1:2000) and the secondary antibody anti-rabbit IgG-HRP (Sigma-Aldrich, 1:5000) to detect the acetylation of histone H3 and again with the primary antibody antiGAPDH (Sigma-Aldrich 69545-200UL, 1:5000) and the secondary antibody antirabbit IgG-HRP (Sigma-Aldrich, 1:10 000) to control the loading amount.

Cell culture with HUH7, MDA-MB-231, and T24 cells. HUH7 and MDA-MB-231 cells were purchased from Japanese Collection of Research Bioresources (JCRB) and from Cell Line Service Eppelheim, respectively. T24 cells were obtained from Dr. B. Mayer (Surgical Clinic, LMU, Munich). HUH7, MDA-MB-231 and T24 cells were maintained in in DMEM High Glucose containing 10% FCS. HepaRG™ cells were obtained from Life Technologies and they were plated and maintained in Williams' medium E supplemented with GlutaMAX™ and HepaRG™ Thaw,

Plate, & General Purpose Medium Supplement (Thaw, Plate, & General Purpose Working Medium), purchased from Life Technologies.

Cell viability and proliferation assays. Cell viability and proliferation were assessed using CellTiter-Blue® Cell Viability Assay (Promega, Madison, WI, USA). For determination of cell viability, HepaRG cells were seeded at a density of 1 x 10^4 cells per well into 96 well plates and allowed to adhere for 4 h. Treatment was performed for 24 h at the indicated concentrations. For assessment of cell proliferation, HUH7, MDA-MB-231 or T24 cells were seeded at a density of 0.5 x 10^4 cells per well into 96 well plates and allowed to adhere overnight. 4 h after seeding, initial metabolic activity was determined. Treatment was performed for 72 h at the indicated concentrations. 2 h before the end of stimulation time, CellTiter-Blue® reagent was added and fluorescence at 590 nm was detected with a Sunrise ELISA reader (Tecan, Maennerdorf, Austria).

Analysis of apoptosis. Flow cytometric analysis based on the fluorochrome Propidium iodide was performed as described previously[65]. Briefly, MDA-MB-231 or T24 cells were seeded at a density of 0.4 x 10^6 cells per well into 24 well plates and allowed to adhere overnight. After 48 h of treatment at the indicated concentrations, cells were harvested, stained and analyzed by flow cytometry on a FACSCalibur (Becton Dickinson, Heidelberg, Germany) as described before[66].

Western blot analysis. MDA-MB-231 or T24 cells were seeded at a density of 0.8 x 10^6 cells per well into 6 well plates and allowed to adhere overnight. After 48 h of treatment at the indicated concentrations, Western blot analysis was conducted as described previously[66]. Following antibodies were used: PD-L1 (Cell Signalling Technology, #13684) and GRP78 (BD Biosciences,

BD 610978). The stain free technology (Bio-Rad, Munich, Germany) was used as loading control, which enables quantification of whole lane protein and thereby the normalization of protein bands.

In vitro metabolism

Metabolic stability assay in human liver microsomes and cytochrome P450 inhibition assay were performed under contract by Bienta (Enamine Biology Services, Kyiv, Ukraine), and more detailed information about the assays are given at bienta.net.

Ligand efficiency

For the calculation of the ligand efficiency or binding energy per atom (LE, Δg) the metric presented by Hopkins et al[67] was used. LE is described by dividing the free energy of binding by the number of heavy atoms ($\Delta g = \Delta G/N_{HA}$). The free energy of ligand binding is defined as follows: $\Delta G = -RT \ln K_d$, where R is the ideal gas constant (1.987×10^{-3} kcal/K/mol), T is the temperature in Kelvin (K) and K_d is the dissociation constant. Following the common practice we substituted the K_d value by the IC_{50} values and assumed a temperature of T = 310 K.

Computational methods

Crystal structures of human HDAC1 (hHDAC1, PDB ID 5ICN)[62], human HDAC6 (hHDAC6, PDB ID 5EDU)[5], *Danio rerio* (zebrafish) HDAC6 (zHDAC6, PDB ID 5EF7, 5G0I)[6] and human HDAC8 (hHDAC8, PDB ID 1W22)) were downloaded from the Protein Data Bank PDB[68]. In case

of HDAC6 33 crystal structures have been solved recently. We took the HDAC6 crystal structures co-crystallized with aromatic benzhydroxamates due to the similarity with the inhibitors under study. Protein preparation was done using Schrödinger's Protein Preparation Wizard[69] by adding hydrogen atoms, assigning protonation states and minimizing the protein. Ligands were prepared in MOE[70] from smiles. Protonation states of the inhibitors were adjusted to pH 7 using the Protonate3D protocol in MOE (hydroxamic acids were considered as deprotonated). Multiple low energy starting conformations were generated with MOE within an energy window of 5 kcal/mol. Molecular docking was performed using the program GLIDE[69]. The same protocol was applied successfully in previous studies[33, 71]. The top-ranked docking poses were selected based on the GLIDE SP score. In case of the crystal structures of zHDAC6 and hHDAC6 a water molecule bound to the zinc ion was considered for ligand docking. This water molecule bridges the interaction between the hydroxamate group and the zinc ion. This special type of zinc-binding has been described for aromatic benzhydroxamtes co-crystallized with zHDAC6[5, 6]. This water molecule was also considered for docking the inhibitors to hHDAC6. A second water molecule bound to H651 (hHDAC6) and H614 (zHDAC6) was considered for the inhibitor docking. GLIDE SP score was used as scoring function. In the case of hHDAC8, the water molecules bound in the foot pocket and to H180 were considered for the inhibitor docking. Using the described docking protocol, the experimentally derived structure of a benzhydroxamate co-crystallized with hHDAC8 (PDB ID 1W22) could be reproduced with an rmsd value of 1.87 Å (see Figure S1, Supporting Information). The bidentate coordination of the zinc ion in hHDAC8 was correctly reproduced by the docking program.

Interestingly, the binding mode of co-crystallized aromatic hydroxamates in zHDAC6 is slightly different. In case of HPOB bound to zHDAC6 (PDB 5EF7), the hydroxamate group is bound with

its terminal hydroxyl group to the zinc ion and the water molecule. In the zHDAC6 structure complexed with the structurally similar inhibitor Nexturastat A (PDB ID 5G0I) the hydroxamate is rotated by 180 degrees resulting in an interaction between the carbonyl group and the zinc ion/water molecule. In both complexes the hydroxamate shows a monodentate chelating of the zinc ion whereas in the hHDAC6 crystal structure complexed with SAHA the hydroxamte group is showing the typical bidentate chelating. Docking of the phenothiazine-based hydroxamates always gave for human and zebrafish HDAC6 both orientations of the hydroxamate with marginal differences of the docking score (see Figure S2 and S3, Supporting Information). Using the described docking protocol, the experimentally derived structure of Nexturastat A bound in catalytic domain 2 of zHDAC6 (PDB ID 5G0I) and HPOB bound to catalytic domain 2 of zHDAC6 (PDB ID 5EF7) could be reproduced with rmsd values of 0.56 Å and 0.89 Å, respectively.

Crystallization and structure determination of the zHDAC6-7i complex

The isolated C-terminal catalytic domain from *Danio rerio* HDAC6 (zHDAC6) was expressed and purified as previously described[40]. For the co-crystallization of the zHDAC6–**7i** complex, a 5 µL drop of protein solution [5 mg/mL zHDAC6, 50 mM HEPES (pH 7.5), 100 mM KCl, 5% glycerol (v/v), 1 mM TCEP, 2 mM **7i**, and 5% DMSO (v/v)] was added to a 3 µL drop of precipitant solution [50 mM $Mg(OAc)_2$, 100 mM sodium cacodylate, and 25% PEG 8,000 (w/v)] at 4˚C. This sitting drop was equilibrated against a 500 µL reservoir of precipitant solution by vapour diffusion. Crystals appeared within 3 days.

X-ray diffraction data were collected from crystals on beamline 17-ID-2 (FMX) at the National Synchrotron Light Source II (NSLS2), Brookhaven National Laboratory. Data were indexed and

integrated using the iMosflm[72] software and scaled using Aimless in the CCP4 Program Suite[73]. The structure was solved by molecular replacement using the structure of unliganded HDAC6 (PDB 5EEM)[6] as a search model within the program Phaser[74]. Atomic models were built and altered using the graphics software Coot[75] and structure refinement was performed using PHENIX[76]. Due to the lower resolution of the structure, main chain structural restraints were obtained from the 1.05 Å-resolution crystal structure of zHDAC6 complexed with TSA (PDB 5WGI)[40]. Compound **7i** was modelled into the structure when clearly resolved electron density was observed. Model quality was assessed using MolProbity[77] and PROCHECK[78]. Crystallographic data and refinement statistics as recorded in Table S1.

Authors will release the atomic coordinates upon article publication.

Compound characterization

Chemistry. General Information. Melting points were determined by open tube capillary method with a Büchi Melting Point B-540 apparatus and are uncorrected. ^{1}H and ^{13}C NMR spectra were recorded either with JNM-Eclipse+400 Joel (400 MHz) or Avance III HD 400 MHz Bruker BioSpin (400 MHz) or Avance III HD 500 MHz Bruker BioSpin (500 MHz) spectrometers. NMR-Spectra were recorded in deuterated solvents. Chemical shifts (δ) are reported in parts per million (ppm) relative to TMS or residual undeuteriated solvent, and coupling constants (*J*) are given in hertz (Hz). Multiplicities are abbreviated as follows: s = singlet; d = doublet; t = triplet; q = quartet; dd = doublet of doublet; m = multiplet, br s = broad singlet. Signal assignments were carried out based on ^{1}H, ^{13}C, HMBC, HMQC and COSY spectra. ESI-Mass spectra were recorded on a Thermo Finnigan LTQ FT. Thin-layer chromatography (TLC) was performed using pre-coated polyester sheets POLYGRAM® SIL

G/UV_{254} from Macherey-Nagel. Purification by flash column chromatography (FCC) was performed using Silica Gel 60 or RP-18 from Merck KGaA. Solutions were concentrated *in vacuo* on a Heidolph rotary evaporator. HPLC purity analysis was individually performed on an Agilent 1100 Series apparatus with a G1311A QuatPump, and a G1329A ALS autosampler, and a G1316A ColComp column oven, and Agilent ChemStation Rev. B04.02 as software. A G1315A DAD detector was set to 210 nm and 254 for detection. Injection volume was 10 µL of a dilution of 100 µg/mL (sample in MeOH). Column temperature was 50 °C, flow either 0.5 mL/min, 1.0 mL/min, or 1.2 mL/min. Different solvent mixtures were used as mobile phase, from 15 % to 40 % water and from 85 % to 60 % acetonitrile or MeOH respectively. The water used for preparation of the mobile phase contained 2 % THF. The following column was used: Agilent Poroshell 120, EC-C18 2.7 µm, (3.0x100 mm). All tested substances showed a purity ≥ 95 %.

PAINS Analysis

PAINS1, PAINS2 and PAINS3 filter as implemented in Schrödinger's Canvas[69] program were employed to identify possible Pan Assay Interference compounds. Three compounds were flagged as PAINS: Tubastatin A, regioisomer of Tubastatin A, and **22**.

Standard synthetic protocols

Details concerning number of equivalents, solvent volume, reaction time and eluents for flash column chromatography are presented below for any single compound.

Standard protocol 1 (*N*-alkylation of unsubstituted or substituted (aza)phenothiazines and heterocyclic analogues): Typically, the (aza)phenothiazine or heterocyclic analogue was dissolved in anhydrous DMF under nitrogen atmosphere and deprotonated by adding gradually 1 M LiHMDS in toluene at 0 °C. After 15 min methyl 4-(bromomethyl)benzoate, dissolved in anhydrous DMF, was added and the reaction was allowed to proceed with stirring at room temperature. The reaction mixture was poured into water and extracted repeatedly with CH_2Cl_2. The combined organic layers were washed with brine, dried over $MgSO_4$, concentrated *in vacuo*, and purified by flash column chromatography.

Standard protocol 2 (hydrolysis of methyl esters to carboxylic acids): Typically, the methyl ester was hydrolysed by suspending it in 1,4-dioxane/H_2O (1:1), adding 2 M NaOH and stirring at room temperature or elevated temperature under TLC control. Upon completion of the reaction the solution was, if applicable, cooled down to room temperature and acidified with 2 M citric acid or 2 M HCl to pH 4. The resulting precipitate was collected by filtration, washed with water, and dried. If no precipitation emerged, the carboxylic acid was extracted with ethyl acetate. The combined organic layers were washed with brine, dried over $MgSO_4$, and concentrated *in vacuo*.

Standard protocol 3 (conversion of the carboxylic acids into THP protected hydroxamic acids): Typically, the carboxylic acid was dissolved in anhydrous DMF under nitrogen atmosphere and deprotonated by addition of Et_3N or DIPEA at 0 °C. To the resulting carboxylate a solution of COMU in anhydrous DMF was added at 0 °C and the mixture stirred for 5 minutes. Then a solution of NH_2OTHP in anhydrous DMF was added and the mixture was stirred for one hour at 0 °C and subsequently at room temperature. The reaction mixture was poured into water

and extracted with CH_2Cl_2. The combined organic layers were washed with brine, dried over $MgSO_4$, concentrated *in vacuo*, and purified by flash column chromatography.

Standard protocol 4 (cleavage of the THP protecting group): Typically, to a solution of THP protected hydroxamic acid in CH_2Cl_2, 4 M HCl in 1,4-dioxane was added and the reaction mixture was stirred at room temperature. The precipitated hydroxamic acid was collected by filtration and washed with a small amount of cold CH_2Cl_2. If no precipitation occurred, the solvent was evaporated *in vacuo* and the crude product was purified by flash column chromatography.

Standard protocol 5 (direct conversion of carboxylic acids into hydroxamic acids): Typically, the carboxylic acid was dissolved in anhydrous DMF under nitrogen atmosphere and activated for 1 hour by adding DIPEA and a solution of COMU in anhydrous DMF at 0 °C. To the activated carboxylic acid a solution of hydroxylamine in anhydrous DMF (freshly prepared by stirring equimolar amounts of hydroxylamine hydrochloride and DIPEA in DMF for 15 min at room temperature) was added and the reaction was allowed to proceed with stirring at room temperature. Then the mixture was partitioned between ethyl acetate and water, and the combined organic layers were dried over Na_2SO_4, concentrated *in vacuo*, and purified by flash column chromatography (work-up A). Alternatively (work-up B), the reaction mixture was evaporated *in vacuo* to dryness and the residue was directly purified by flash column chromatography. However, coproducts arising from the coupling reagent COMU were not completely removed in both work-up protocols A and B, therefore additional washing or precipitation steps had to be performed in some cases.

4-[(10*H*-Phenothiazin-10-yl)methyl]-*N*-hydroxybenzamide (1a). Standard protocol 4 with 102 mg (0.236 mmol) of **6a** in 3.0 mL of CH_2Cl_2 and 310 µL (1.24 mmol, 5.3 equiv) of HCl (4 M) in 1,4-dioxane. The reaction mixture was stirred for 5 hours. Precipitation yielded 56 mg (0.161 mmol, 68 %) of **1a** as a grey solid. Mp: 195 - 197 °C. ^{1}H NMR (500 MHz, DMSO-d_6): δ (ppm) = 11.16 (s, 1H, NHOH), 9.02 (bs, 1H, NHOH), 7.72 – 7.67 (m, 2H, 2'-H, 6'-H), 7.41 – 7.36 (m, 2H, 3'-H, 5'-H), 7.15 (dd, *J* = 7.6, 1.5 Hz, 2H, 4'''-H, 6'''-H), 7.07 (td, *J* = 7.8, 1.5 Hz, 2H, 2'''-H, 8'''-H), 6.91 (td, *J* = 7.5, 1.0 Hz, 2H, 3'''-H, 7'''-H), 6.78 (dd, *J* = 8.2, 1.1 Hz, 2H, 1'''-H, 9'''-H), 5.18 (s, 2H, 1''-H). ^{13}C NMR (126 MHz, DMSO-d_6): δ (ppm) = 164.1 (C-1), 144.1 (C-9a''', C-10a'''), 140.4 (C-4'), 131.6 (C-1'), 127.6 (C-2''', C-8'''), 127.2 (C-2', C-6'), 126.9 (C-4''', C-6'''), 126.7 (C-3', C-5'), 122.8 (C-3''', C-7'''), 122.6 (C-4a''', C-5a'''), 115.9 (C-1''', C-9'''), 50.7 (C-1''). MS (ESI−): m/z calcd for $[(C_{20}H_{15}N_2O_2S)^-]$ 347.0860, found 347.0858.

Methyl 4-[(10*H*-phenothiazin-10-yl)methyl]benzoate (4a). Standard protocol 1 with 1.05 g (5.27 mmol) of 10*H*-phenothiazine (**2a**) in 6.0 mL of anhydrous DMF, 10.5 mL (10.5 mmol, 2.0 equiv) of LiHMDS (1 M) and 2.03 g (8.86 mmol, 1.7 equiv) of methyl 4-(bromomethyl)benzoate (**3**) in 4.0 mL of anhydrous DMF. Reaction mixture was stirred for 93 hours at 50 °C and was extracted with CH_2Cl_2 (4 x 60 mL). Flash column chromatography with CH_2Cl_2 and hexanes (7:3, R_f 0.7) gave 1.28 g (3.68 mmol, 70 %) of **4a** as a beige solid. Mp: 125 - 126 °C. ^{1}H NMR (400 MHz, CD_2Cl_2): δ (ppm) = 8.02 – 7.92 (m, 2H, 2'-H, 6'-H), 7.47 – 7.38 (m, 2H, 3'-H, 5'-H), 7.11 (dd, *J* = 7.6, 1.6 Hz, 2H, 4'''-H, 6'''-H), 7.00 (td, *J* = 7.7, 1.3 Hz, 2H, 2'''-H, 8'''-H), 6.88 (td, *J* = 7.5, 1.2 Hz, 2H, 3'''-H, 7'''-H), 6.63 (dd, *J* = 8.1, 1.1 Hz, 2H, 1'''-H, 9'''-H), 5.14 (s, 2H, 1''-H), 3.86 (s, 3H, $COOCH_3$). ^{13}C NMR (101 MHz, CD_2Cl_2): δ (ppm) = 167.1 (C-1), 144.9 (C-9a''', C-10a'''), 142.9 (C-4'), 130.3 (C-2', C-6'), 129.7 (C-1'), 127.8 (C-2''', C-8'''), 127.4 (C-3', C-5'),

127.4 (C-4‴, C-6‴), 124.1 (C-4a‴, C-5a‴), 123.2 (C-3‴, C-7‴), 116.0 (C-1‴, C-9‴), 52.7 (C-1″), 52.5 (COO$\underline{C}H_3$). MS (ESI+): m/z calcd for [$(C_{21}H_{18}NO_2S)^+$] 348.1053, found 348.1052

Methyl 4-[(5,5-dioxido-10*H*-phenothiazin-10-yl)methyl]benzoate (4b). Standard protocol 1 with 452 mg (1.95 mmol) of 10*H*-phenothiazine 5,5-dioxide (**2b**; synthesized according to Sharma *et al.*[79]) in 3.0 mL of anhydrous DMF, 3.88 mL (3.88 mmol, 2.0 equiv) of LiHMDS (1 M) and 763 mg (3.33 mmol, 1.7 equiv) of methyl 4-(bromomethyl)benzoate (**3**) in 2.0 mL of anhydrous DMF. Reaction mixture was stirred for 19 hours and was extracted with CH_2Cl_2 (3 x 30 mL). Flash column chromatography with CH_2Cl_2 and hexanes (9:1, R_f 0.3) gave 581 mg (1.53 mmol, 79 %) of **4b** as a white solid. Mp: 204 - 205 °C. ^{1}H NMR (400 MHz, CD_2Cl_2): δ (ppm) = 8.11 (dd, J = 7.9, 1.5 Hz, 2H, 4‴-H, 6‴-H), 8.05 – 7.97 (m, 2H, 2'-H, 6'-H), 7.52 (ddd, J = 8.8, 7.2, 1.7 Hz, 2H, 2‴-H, 8‴-H), 7.35 – 7.25 (m, 4H, 3'-H, 5'-H, 3‴-H, 7‴-H), 7.11 (d, J = 8.6 Hz, 2H, 1‴-H, 9‴-H), 5.49 (s, 2H, 1″-H), 3.88 (s, 3H, $COOCH_3$). ^{13}C NMR (126 MHz, CD_2Cl_2) δ (ppm) = 166.9 (C-1), 141.4 (C-9a‴, C-10a‴), 141.0 (C-4'), 133.9 (C-2‴, C-8‴), 130.8 (C-2', C-6'), 130.4 (C-1'), 126.7 (C-3', C-5'), 125.2 (C-4a‴, C-5a‴), 123.8 (C-4‴, C-6‴), 122.9 (C-3‴, C-7‴), 117.1 (C-1‴, C-9‴), 53.3 (C-1″), 52.6 (COO$\underline{C}H_3$). MS (ESI+): m/z calcd for [$(C_{21}H_{18}NO_4S)^+$] 380.0951, found 380.0951.

Methyl 4-[(1-chloro-10*H*-phenothiazin-10-yl)methyl]benzoate (4c). Standard protocol 1 with 450 mg (1.93 mmol) of 1-chloro-10*H*-phenothiazine (**2c**; synthesized according to Sharma *et al.*[80]) in 3.0 mL of anhydrous DMF, 3.85 mL (3.85 mmol, 2.0 equiv) of LiHMDS (1 M) and 770 mg (3.36 mmol, 1.7 equiv) of methyl 4-(bromomethyl)benzoate (**3**) in 2.0 mL of anhydrous DMF. Reaction mixture was stirred for 19 hours and was extracted with CH_2Cl_2 (3 x 30 mL). Iterated flash column chromatography with hexanes and EtOAc (19:1, R_f 0.4) and then hexanes and acetone (9:1, R_f 0.5) gave 465 mg (1.22 mmol, 63 %) of **4c** as a white solid. Mp: 159 - 161

°C. ^{1}H NMR (500 MHz, DMSO-d_6): δ (ppm) = 7.81 – 7.76 (m, 2H, 2'-H, 6'-H), 7.50 – 7.46 (m, 2H, 3'-H, 5'-H), 7.34 (dd, J = 8.0, 1.4 Hz, 1H, 4'''-H), 7.22 (dd, J = 7.9, 1.3 Hz, 2H, 2'''-H, 9'''-H), 7.15 (dd, J = 7.7, 1.5 Hz, 1H, 6'''-H), 7.15 (td, J = 7.7, 1.5 Hz, 1H, 8'''-H), 7.07 (t, J = 7.8 Hz, 1H, 3'''-H), 6.96 (td, J = 7.5, 1.2 Hz, 1H, 7'''-H), 5.22 (s, 2H, 1''-H), 3.79 (s, 3H, $COOCH_3$). ^{13}C NMR (126 MHz, DMSO-d_6): δ (ppm) = 165.9 (C-1), 145.0 (C-9a'''), 143.4 (C-4'), 140.6 (C-10a'''), 133.4 (C-1'''), 129.7 (C-4'''), 129.0 (C-2', C-6'), 128.6 (C-1'), 128.2 (C-3', C-5'), 128.2 (C-5a'''), 127.6 (C-6'''/C-8'''), 126.8 (C-8'''/C-6'''), 126.2 (C-2'''), 125.8 (C-4a'''), 125.4 (C-3'''), 124.1 (C-7'''), 121.2 (C-9'''), 56.6 (C-1''), 52.0 ($COO\underline{C}H_3$). MS (ESI+): m/z calcd for [$(C_{21}H_{17}ClNO_2S)^+$] 382.0663, found 382.0663.

Methyl 4-{[2-(trifluoromethyl)-10*H*-phenothiazin-10-yl]methyl}benzoate (4d). Standard protocol 1 with 450 mg (1.68 mmol) of 2-(trifluoromethyl)-10*H*-phenothiazine (**2d**) in 2.0 mL of anhydrous DMF, 3.35 mL (3.35 mmol, 2.0 equiv) of LiHMDS (1 M) and 652 mg (2.85 mmol, 1.7 equiv) of methyl 4-(bromomethyl)benzoate (**3**) in 1.0 mL of anhydrous DMF. Reaction mixture was stirred for 3 hours and was extracted with CH_2Cl_2 (3 x 30 mL). Flash column chromatography with CH_2Cl_2 and hexanes (1:1, R_f 0.3) gave 468 mg (1.13 mmol, 67 %) of **4d** as a white solid. Mp: 51 - 53 °C. ^{1}H NMR (400 MHz, CD_2Cl_2): δ (ppm) = 8.01 – 7.96 (m, 2H, 2'-H, 6'-H), 7.47 – 7.41 (m, 2H, 3'-H, 5'-H), 7.22 (d, J = 8.0 Hz, 1H, 4'''-H), 7.16 – 7.10 (m, 2H, 3'''-H, 6'''-H), 7.03 (td, J = 7.8, 1.6 Hz, 1H, 8'''-H), 6.93 (td, J = 7.5, 1.2 Hz, 1H, 7'''-H), 6.83 (d, J = 0.8 Hz, 1H, 1'''-H), 6.68 (dd, J = 8.1, 1.1 Hz, 1H, 9'''-H), 5.15 (s, 2H, 1''-H), 3.87 (s, 3H, $COOCH_3$). ^{13}C NMR (101 MHz, CD_2Cl_2): δ (ppm) = 167.0 (C-1), 145.6 (C-10a'''), 144.3 (C-9a'''), 142.0 (C-4'), 130.5 (C-2', C-6'), 130.1 (C-1'), 129.8 (q, ^2J = 32.4 Hz, C-2'''), 129.7 (C-4a'''), 128.2 (C-8'''), 127.7 (C-4'''), 127.7 (C-6'''), 127.4 (C-3', C-5'), 124.6 (q, ^1J = 272.3 Hz, CF_3), 123.9 (C-7'''),

123.5 (C-5a'''), 119.9 (q, ^3J = 3.9 Hz, C-3'''), 116.5 (C-9'''), 112.3 (q, ^3J = 3.9 Hz, C-1'''), 52.8 (C-1''), 52.5 (COO<u>C</u>H$_3$). MS (ESI+): m/z calcd for [($C_{22}H_{17}F_3NO_2S$)$^+$] 416.0927, found 416.0930.

Methyl 4-[(5-oxido-10*H*-phenothiazin-10-yl)methyl]benzoate (4e). Standard protocol 1 with 523 mg (2.43 mmol) of 10*H*-phenothiazine 5-oxide (**2e**; synthesized according to Gilman *et al.*[81]) in 2.0 mL of anhydrous DMF, 2.41 mL (2.41 mmol, 1.0 equiv) of LiHMDS (1 M) and 936 g (4.09 mmol, 1.7 equiv) of methyl 4-(bromomethyl)benzoate (**3**) in 1.0 mL of anhydrous DMF. Reaction mixture was stirred for 18 hours and was extracted with CH_2Cl_2 (4 x 30 mL). Flash column chromatography with CH_2Cl_2 with 2 % MeOH (R_f 0.2) gave 673 mg (1.85 mmol, 76 %) of **4e** as a white solid. Mp: 178 °C. ^{1}H NMR (400 MHz, CD_2Cl_2): δ (ppm) = 8.03 – 7.94 (m, 4H, 2'-H, 6'-H, 4'''-H, 6'''-H), 7.51 (ddd, J = 8.7, 7.3, 1.7 Hz, 2H, 2'''-H, 8'''-H), 7.31 – 7.24 (m, 4H, 3'-H, 5'-H, 3'''-H, 7'''-H), 7.17 (d, J = 8.5 Hz, 2H, 1'''-H, 9'''-H), 5.56 (s, 2H, 1''-H), 3.88 (s, 3H, COOCH$_3$). ^{13}C NMR (101 MHz, CD_2Cl_2): δ (ppm) = 167.0 (C-1), 141.4 (C-4'), 139.2 (C-9a''', C-10a'''), 133.4 (C-2''', C-8'''), 131.8 (C-4''', C-6'''), 130.7 (C-2', C-6'), 130.3 (C-1'), 126.7 (C-3', C-5'), 125.8 (C-4a''', C-5a'''), 122.8 (C-3''', C-7'''), 117.0 (C-1''', C-9'''), 52.9 (C-1''), 52.6 (COO<u>C</u>H$_3$). MS (ESI+): m/z calcd for [($C_{21}H_{18}NO_3S$)$^+$] 364.1002, found 364.0998.

Methyl 4-[(2-chloro-10*H*-phenothiazin-10-yl)methyl]benzoate (4f). Standard protocol 1 with 599 mg (2.56 mmol) of 2-chloro-10*H*-phenothiazine (**2f**) in 1.5 mL of anhydrous DMF, 5.11 mL (5.11 mmol, 2.0 equiv) of LiHMDS (1 M) and 995 mg (4.34 mmol, 1.7 equiv) of methyl 4-(bromomethyl)benzoate (**3**) in 1.0 mL of anhydrous DMF. Reaction mixture was stirred for 20 hours and was extracted with CH_2Cl_2 (3 x 30 mL). Flash column chromatography with CH_2Cl_2 and hexanes (1:1, R_f 0.3) gave 490 mg (1.28 mmol, 50 %) of **4f** as a white solid. Mp: 56 - 58 °C. ^{1}H NMR (400 MHz, CD_2Cl_2): δ (ppm) = 8.05 – 7.90 (m, 2H, 2'-H, 6'-H), 7.48 – 7.36 (m, 2H, 3'-H, 5'-H), 7.10 (dd, J = 7.6, 1.6 Hz, 1H, 6'''-H), 7.02 (d, J = 8.2 Hz, 1H, 4'''-H), 7.00 (td, J = 7.8,

1.6 Hz, 1H, 8'''-H), 6.91 (td, *J* = 7.7, 1.2 Hz, 1H, 7'''-H), 6.87 (dd, *J* = 8.2, 2.1 Hz, 1H, 3'''-H), 6.63 (dd, *J* = 8.2, 1.2 Hz, 1H, 9'''-H), 6.61 (d, *J* = 2.1 Hz, 1H, 1'''-H), 5.10 (s, 2H, 1''-H), 3.87 (s, 3H, $COOCH_3$). ^{13}C NMR (101 MHz, CD_2Cl_2): δ (ppm) = 167.1 (C-1), 146.3 (C-10a'''), 144.3 (C-9a'''), 142.2 (C-4'), 133.6 (C-2'''), 130.5 (C-2', C-6'), 130.0 (C-1'), 128.1 (C-4'''), 128.0 (C-8'''), 127.6 (C-6'''), 127.4 (C-3', C-5'), 124.0 (C-5a'''), 123.7 (C-7'''), 123.0 (C-3'''), 123.0 (C-4a'''), 116.4 (C-1'''), 116.2 (C-9'''), 52.9 (C-1''), 52.5 ($COO\underline{C}H_3$). MS (ESI+): m/z calcd for $[(C_{21}H_{17}ClNO_2S)^+]$ 382.0663, found 382.0667.

Methyl 4-[(2-methoxy-10*H*-phenothiazin-10-yl)methyl]benzoate (4g). Standard protocol 1 with 607 mg (2.65 mmol) of 2-methoxy-10*H*-phenothiazine (**2g**) in 3.0 mL of anhydrous DMF, 5.21 mL (5.21 mmol, 2.0 equiv) of LiHMDS (1 M) and 1.05 g (4.58 mmol, 1.7 equiv) of methyl 4-(bromomethyl)benzoate (**3**) in 2.0 mL of anhydrous DMF. Reaction mixture was stirred for 44 hours and was extracted with CH_2Cl_2 (3 x 30 mL). Flash column chromatography with CH_2Cl_2 and hexanes (1:1, R_f 0.3) gave 661 mg (1.75 mmol, 66 %) of **4g** as a white solid. Mp: 147 °C. ^1H NMR (500 MHz, CD_2Cl_2): δ (ppm) = 8.02 – 7.90 (m, 2H, 2'-H, 6'-H), 7.48 – 7.35 (m, 2H, 3'-H, 5'-H), 7.11 (dd, *J* = 7.6, 1.6 Hz, 1H, 6'''-H), 7.04 – 6.94 (m, 2H, 4'''-H, 8'''-H), 6.88 (td, *J* = 7.5, 1.1 Hz, 1H, 7'''-H), 6.65 (dd, *J* = 8.2, 1.1 Hz, 1H, 9'''-H), 6.45 (dd, *J* = 8.4, 2.5 Hz, 1H, 3'''-H), 6.22 (d, *J* = 2.5 Hz, 1H, 1'''-H), 5.12 (s, 2H, 1''-H), 3.86 (s, 3H, $COOCH_3$), 3.61 (s, 3H, OCH_3). ^{13}C NMR (126 MHz, CD_2Cl_2): δ (ppm) = 167.1 (C-1), 160.3 (C-2'''), 146.3 (C-10a'''), 144.8 (C-9a'''), 142.9 (C-4'), 130.4 (C-2', C-6'), 129.8 (C-1'), 127.8 (C-4'''), 127.6 (C-8'''), 127.4 (C-6'''), 127.4 (C-3', C-5'), 124.8 (C-5a'''), 123.3 (C-7'''), 116.1 (C-9'''), 115.0 (C-4a'''), 107.5 (C-3'''), 104.0 (C-1'''), 55.8 (OCH_3), 52.8 (C-1''), 52.5 ($COO\underline{C}H_3$). MS (ESI+): m/z calcd for $[(C_{22}H_{20}NO_3S)^+]$ 378.1158, found 378.1159.

Methyl 4-{[2-(ethylthio)-10*H*-phenothiazin-10-yl]methyl}benzoate (4h). Standard protocol 1 with 700 mg (2.70 mmol) of 2-(ethylthio)-10*H*-phenothiazine (**2h**) in 1.5 mL of anhydrous DMF, 2.64 mL (2.64 mmol, 1.0 equiv) of LiHMDS (1 M) and 1.06 g (4.63 mmol, 1.7 equiv) of methyl 4-(bromomethyl)benzoate (**3**) in 1.5 mL of anhydrous DMF. Reaction mixture was stirred for 47 hours and was extracted with CH_2Cl_2 (3 x 50 mL). Flash column chromatography with CH_2Cl_2 and hexanes (1:1, R_f 0.2) gave 765 mg (1.88 mmol, 70 %) of **4h** as a pale yellow oil. ^{1}H NMR (400 MHz, CD_2Cl_2): δ (ppm) = 8.01 – 7.95 (m, 2H, 2'-H, 6'-H), 7.46 – 7.40 (m, 2H, 3'-H, 5'-H), 7.11 (dd, *J* = 7.6, 1.6 Hz, 1H, 6'''-H), 7.01 (d, *J* = 8.0 Hz, 1H, 4'''-H), 7.01 (td, *J* = 7.8, 1.6 Hz, 1H, 8'''-H), 6.90 (td, *J* = 7.5, 1.1 Hz, 1H, 7'''-H), 6.85 (dd, *J* = 8.0, 1.8 Hz, 1H, 3'''-H), 6.66 (dd, *J* = 8.0, 1.3 Hz, 1H, 9'''-H), 6.58 (d, *J* = 1.8 Hz, 1H, 1'''-H), 5.13 (s, 2H, 1''-H), 3.87 (s, 3H, $COOCH_3$), 2.68 (q, *J* = 7.3 Hz, 2H, $SC\underline{H}_2CH_3$), 1.08 (t, *J* = 7.3 Hz, 3H, $SCH_2C\underline{H}_3$). ^{13}C NMR (101 MHz, CD_2Cl_2): δ (ppm) = 167.1 (C-1), 145.3 (C-10a'''), 144.8 (C-9a'''), 142.7 (C-4'), 136.3 (C-2'''), 130.5 (C-2', C-6'), 129.9 (C-1'), 127.8 (C-8'''), 127.5 (C-4''', C-6'''), 127.4 (C-3', C-5'), 124.3 (C-5a'''), 124.0 (C-3'''), 123.4 (C-7'''), 121.9 (C-4a'''), 116.9 (C-1'''), 116.2 (C-9'''), 52.8 (C-1''), 52.5 ($COO\underline{C}H_3$), 28.4 ($S\underline{C}H_2CH_3$), 14.7 ($SCH_2\underline{C}H_3$). MS (ESI+): m/z calcd for [$(C_{23}H_{22}NO_2S_2)^+$] 408.1087, found 408.1091.

Methyl 4-[(10*H*-benzo[*b*]pyrido[2,3-*e*][1,4]thiazin-10-yl)methyl]benzoate (4i). Standard protocol 1 with 507 mg (2.53 mmol) of 10*H*-benzo[*b*]pyrido[2,3-e][1,4]thiazine (**2i**; synthesized according to Kutscher *et al.*[82]) in 3.0 mL of anhydrous DMF, 4.98 mL (4.98 mmol, 2.0 equiv) of LiHMDS (1 M) and 976 mg (4.26 mmol, 1.7 equiv) of methyl 4-(bromomethyl)benzoate (**3**) in 2.0 mL of anhydrous DMF. Reaction mixture was stirred for 24 hours and was extracted with CH_2Cl_2 (3 x 50 mL). Flash column chromatography with hexanes and EtOAc (9:1, R_f 0.3) gave 593 mg (1.70 mmol, 67 %) of **4i** as a beige solid. Mp: 127 - 128 °C. ^{1}H NMR (500 MHz,

CD_2Cl_2): δ (ppm) = 7.97 – 7.91 (m, 2H, 2'-H, 6'-H), 7.90 (dd, *J* = 4.9, 1.7 Hz, 1H, 2'''-H), 7.41 – 7.36 (m, 2H, 3'-H, 5'-H), 7.30 (dd, *J* = 7.5, 1.7 Hz, 1H, 4'''-H), 7.04 (dd, *J* = 7.6, 1.6 Hz, 1H, 6'''-H), 6.94 (td, *J* = 7.8, 1.6 Hz, 1H, 8'''-H), 6.86 (td, *J* = 7.5, 1.2 Hz, 1H, 7'''-H), 6.78 (dd, *J* = 7.5, 4.9 Hz, 1H, 3'''-H), 6.58 (dd, *J* = 8.3, 1.2 Hz, 1H, 9'''-H), 5.37 (s, 2H, 1''-H), 3.86 (s, 3H, $COOCH_3$). ^{13}C NMR (126 MHz, CD_2Cl_2): δ (ppm) = 167.2 (C-1), 154.8 (C-10a'''), 145.6 (C-2'''), 144.0 (C-4'), 142.9 (C-9a'''), 134.6 (C-4'''), 130.2 (C-2', C-6'), 129.3 (C-1'), 128.0 (C-8'''), 127.2 (C-6'''), 127.2 (C-3', C-5'), 123.6 (C-7'''), 121.4 (C-5a'''), 118.8 (C-3'''), 117.3 (C-4a'''), 116.5 (C-9'''), 52.4 ($COO\underline{C}H_3$), 49.5 (C-1''). MS (ESI+): m/z calcd for [($C_{20}H_{17}N_2O_2S)^+$] 349.1005, found 349.1007.

Methyl 4-[(10*H*-benzo[*b*]pyrido[3,4-*e*][1,4]thiazin-10-yl)methyl]benzoate (4j). Standard protocol 1 with 1.21 g (6.04 mmol) of 10*H*-benzo[*b*]pyrido[3,4-*e*][1,4]thiazine (**2j**; synthesized according to Saggiomo *et al.*[83]) in 3.0 mL of anhydrous DMF, 6.00 mL (6.00 mmol, 1.0 equiv) of LiHMDS (1 M) and 2.32 g (10.1 mmol, 1.7 equiv) of methyl 4-(bromomethyl)benzoate (**3**) in 2.0 mL of anhydrous DMF. Reaction mixture was stirred for 39 hours and was extracted with CH_2Cl_2 (3 x 150 mL). Flash column chromatography with hexanes and EtOAc (3:2, R_f 0.2) gave 1.52 g (4.36 mmol, 72 %) of **4j** as a pale beige solid. Mp: 169 - 170 °C. ^{1}H NMR (400 MHz, CD_2Cl_2): δ (ppm) = 8.03 – 7.95 (m, 3H, 2'-H, 6'-H, 3'''-H), 7.79 (s, 1H, 1'''-H), 7.45 – 7.38 (m, 2H, 3'-H, 5'-H), 7.06 (dd, *J* = 7.6, 1.5 Hz, 1H, 6'''-H), 7.02 (td, *J* = 8.0, 1.5 Hz, 1H, 8'''-H), 6.99 (d, *J* = 4.9 Hz, 1H, 4'''-H), 6.90 (td, *J* = 7.6, 1.1 Hz, 1H, 7'''-H), 6.63 (dd, *J* = 8.2, 1.1 Hz, 1H, 9'''-H), 5.14 (s, 2H, 1''-H), 3.87 (s, 3H, $COOCH_3$). ^{13}C NMR (101 MHz, CD_2Cl_2): δ (ppm) = 167.0 (C-1), 144.2 (C-3'''), 144.1 (C-9a'''), 142.0 (C-4'), 140.6 (C-10a'''), 136.4 (C-1'''), 134.8 (C-4a'''), 130.6 (C-2', C-6'), 130.1 (C-1'), 128.4 (C-8'''), 127.6 (C-6'''), 127.2 (C-3', C-5'), 123.7 (C-7'''),

121.8 (C-5a'''), 121.4 (C-4'''), 116.3 (C-9'''), 52.6 (C-1''), 52.5 (COO<u>C</u>H$_3$). MS (ESI+): m/z calcd for [($C_{20}H_{17}N_2O_2S$)$^+$] 349.1005, found 349.1004.

Methyl 4-[(10*H*-benzo[*b*]pyrazino[2,3-*e*][1,4]thiazin-10-yl)methyl]benzoate (4k). Standard protocol 1 with 601 mg (2.99 mmol) of 10*H*-benzo[*b*]pyrazino[2,3-*e*][1,4]thiazine (**2k**; synthesized according to Okafor[84]) in 2.0 mL of anhydrous DMF, 5.95 mL (5.95 mmol, 2.0 equiv) of LiHMDS (1 M) and 1.15 g (5.02 mmol, 1.7 equiv) of methyl 4-(bromomethyl)benzoate (**3**) in 1.0 mL of anhydrous DMF. Reaction mixture was stirred for 3 hours and was extracted with CH_2Cl_2 (3 x 50 mL). Flash column chromatography with hexanes and EtOAc (9:1, R_f 0.3) gave 473 mg (1.35 mmol, 45 %) of **4k** as a yellow solid. Mp: 153 - 154 °C. ^{1}H NMR (400 MHz, CD_2Cl_2): δ (ppm) = 7.99 – 7.94 (m, 2H, 2'-H, 6'-H), 7.74 (d, J = 2.8 Hz, 1H, 3'''-H), 7.66 (d, J = 2.8 Hz, 1H, 2'''-H), 7.38 – 7.32 (m, 2H, 3'-H, 5'-H), 7.00 (dd, J = 7.5, 1.7 Hz, 1H, 6'''-H), 6.93 (td, J = 7.8, 1.8 Hz, 1H, 8'''-H), 6.87 (td, J = 7.5, 1.3 Hz, 1H, 7'''-H), 6.54 (dd, J = 8.1, 1.2 Hz, 1H, 9'''-H), 5.26 (s, 2H, 1''-H), 3.87 (s, 3H, $COOCH_3$). ^{13}C NMR (101 MHz, CD_2Cl_2): δ (ppm) = 167.1 (C-1), 150.5 (C-10a'''), 143.1 (C-4a'''), 142.9 (C-4'), 140.5 (C-9a'''), 139.0 (C-2'''), 137.4 (C-3'''), 130.3 (C-2', C-6'), 129.6 (C-1'), 128.3 (C-8'''), 127.5 (C-6'''), 126.9 (C-3', C-5'), 124.1 (C-7'''), 120.2 (C-5a'''), 116.6 (C-9'''), 52.5 (COO<u>C</u>H$_3$), 49.4 (C-1''). MS (ESI+): m/z calcd for [($C_{19}H_{16}N_3O_2S$)$^+$] 350.0958, found 350.0960.

Methyl 4-[(10*H*-dipyrido[2,3-*b*:2',3'-*e*][1,4]thiazin-10-yl)methyl]benzoate (4l). Standard protocol 1 with 510 mg (2.53 mmol) of 10*H*-dipyrido[2,3-*b*:2',3'-*e*][1,4]thiazine (**2l**; synthesized according to Rodig *et al.*[85]) in 2.0 mL of anhydrous DMF, 2.50 mL (2.50 mmol, 1.0 equiv) of LiHMDS (1 M) and 998 mg (4.36 mmol, 1.7 equiv) of methyl 4-(bromomethyl)benzoate (**3**) in 1.0 mL of anhydrous DMF. Reaction mixture was stirred for 7 hours and was extracted with CH_2Cl_2 (3 x 50 mL). Flash column chromatography with CH_2Cl_2 with 2 % MeOH (R_f 0.5) gave

447 mg (1.28 mmol, 51 %) of **4l** as a beige solid. Mp: 137 °C. ^{1}H NMR (500 MHz, CD_2Cl_2): δ (ppm) = 7.98 – 7.94 (m, 2H, 2'-H, 6'-H), 7.90 – 7.83 (m, 2H, 2'''-H, 7'''-H), 7.38 – 7.34 (m, 2H, 3'-H, 5'-H), 7.28 (dd, *J* = 7.5, 1.7 Hz, 1H, 4'''-H), 6.81 – 6.76 (m, 2H, 3'''-H, 8'''-H), 6.64 (dd, *J* = 8.3, 1.3 Hz, 1H, 9'''-H), 5.29 (s, 2H, 1''-H), 3.87 (s, 3H, $COOCH_3$). ^{13}C NMR (126 MHz, CD_2Cl_2): δ (ppm) = 167.1 (C-1), 152.7 (C-10a'''), 145.7 (C-2'''/C-7'''), 144.8 (C-5a'''), 143.3 (C-7'''/C-2'''), 143.0 (C-4'), 138.7 (C-9a'''), 135.0 (C-4'''), 130.3 (C-2', C-6'), 129.6 (C-1'), 127.0 (C-3', C-5'), 122.3 (C-8'''), 121.6 (C-9'''), 119.1 (C-3'''), 116.8 (C-4a'''), 52.5 ($COO\underline{C}H_3$), 49.2 (C-1''). MS (ESI+): m/z calcd for [$(C_{19}H_{16}N_3O_2S)^+$] 350.0958, found 350.0960.

Methyl 4-[(10*H*-dipyrido[3,4-*b*:3',4'-*e*][1,4]thiazin-10-yl)methyl]benzoate (4m). Standard protocol 1 with 346 mg (1.72 mmol) of 10*H*-dipyrido[3,4-*b*:3',4'-*e*][1,4]thiazine (**2m**; synthesized according to Morak *et al.*[86]) in 1.8 mL of anhydrous DMF, 1.74 mL (1.74 mmol, 1.0 equiv) of LiHMDS (1 M) and 675 mg (2.95 mmol, 1.7 equiv) of methyl 4-(bromomethyl)benzoate (**3**) in 0.6 mL of anhydrous DMF. Reaction mixture was stirred for 20 hours and was extracted with CH_2Cl_2 (3 x 30 mL). Flash column chromatography with CH_2Cl_2 with 5 % MeOH (R_f 0.4) gave 330 mg (0.944 mmol, 55 %) of **4m** as a pale yellow solid. Mp: 192 - 193 °C. ^{1}H NMR (400 MHz, CD_2Cl_2): δ (ppm) = 8.07 (d, *J* = 5.9 Hz, 1H, 8'''-H), 8.06 (s, 1H, 6'''-H), 8.04 (d, *J* = 4.9 Hz, 1H, 3'''-H), 8.05 – 7.97 (m, 2H, 2'-H, 6'-H), 7.78 (s, 1H, 1'''-H), 7.39 – 7.33 (m, 2H, 3'-H, 5'-H), 6.99 (dd, *J* = 4.9, 0.5 Hz, 1H, 4'''-H), 6.40 (d, *J* = 5.6 Hz, 1H, 9'''-H), 5.12 (s, 2H, 1''-H), 3.88 (s, 3H, $COOCH_3$). ^{13}C NMR (101 MHz, CD_2Cl_2): δ (ppm) = 166.9 (C-1), 150.6 (C-9a'''), 150.1 (C-8'''), 147.1 (C-6'''), 145.3 (C-3'''), 140.5 (C-4'), 138.7 (C-10a'''), 136.5 (C-1'''), 133.7 (C-4a'''), 130.8 (C-2', C-6'), 130.4 (C-1'), 126.9 (C-3', 5'), 121.9 (C-4'''), 117.5 (C-5a'''), 110.2 (C-9'''), 52.6 ($COO\underline{C}H_3$), 52.1 (C-1''). MS (ESI+): m/z calcd for [$(C_{19}H_{16}N_3O_2S)^+$] 350.0958, found 350.0954.

Methyl 4-[(5*H*-dipyrido[2,3-*b*:4',3'-*e*][1,4]thiazin-5-yl)methyl]benzoate (4n). Standard protocol 1 with 370 mg (1.84 mmol) of 5*H*-dipyrido[2,3-*b*:4',3'-*e*][1,4]thiazine (**2n**; synthesized according to Rodig *et al.*[85]) in 1.8 mL of anhydrous DMF, 1.84 mL (1.84 mmol, 1.0 equiv) of LiHMDS (1 M) and 719 mg (3.14 mmol, 1.7 equiv) of methyl 4-(bromomethyl)benzoate (**3**) in 0.6 mL of anhydrous DMF. Reaction mixture was stirred for 20 hours and was extracted with CH_2Cl_2 (3 x 30 mL). Flash column chromatography with CH_2Cl_2 with 5 % MeOH (R_f 0.4) gave 312 mg (0.893 mmol, 49 %) of **4n** as a beige solid. Mp: 179 - 180 °C. ^{1}H NMR (400 MHz, CD_2Cl_2): δ (ppm) = 8.08 (s, 1H, 4'''-H), 8.04 (d, *J* = 5.6 Hz, 1H, 2'''-H), 8.03 – 7.99 (m, 2H, 2'-H, 6'-H), 7.96 (dd, *J* = 4.7, 1.3 Hz, 1H, 7'''-H), 7.37 – 7.31 (m, 2H, 3'-H, 5'-H), 6.86 (dd, *J* = 8.2, 4.7 Hz, 1H, 8'''-H), 6.71 (dd, *J* = 8.2, 1.3 Hz, 1H, 9'''-H), 6.36 (d, *J* = 5.6 Hz, 1H, 1'''-H), 5.03 (s, 2H, 1''-H), 3.88 (s, 3H, $COOCH_3$). ^{13}C NMR (101 MHz, CD_2Cl_2): δ (ppm) = 166.9 (C-1), 149.7 (C-2'''), 149.3 (C-10a'''), 147.3 (C-4'''), 146.1 (C-5a'''), 144.1 (C-7'''), 140.4 (C-4'), 138.7 (C-9a'''), 130.8 (C-2', C-6'), 130.4 (C-1'), 126.8 (C-3', C-5'), 122.5 (C-8'''), 121.7 (C-9'''), 118.8 (C-4a'''), 109.9 (C-1'''), 52.6 ($COO\underline{C}H_3$), 52.2 (C-1''). MS (ESI+): m/z calcd for [($C_{19}H_{16}N_3O_2S$)$^+$] 350.0958, found 350.0954.

Methyl 4-[(2-methyl-4*H*-benzo[*b*]thiazolo[4,5-*e*][1,4]thiazin-4-yl)methyl]benzoate (4o). Standard protocol 1 with 802 mg (3.64 mmol) of 2-methyl-4*H*-benzo[*b*]thiazolo[4,5-*e*][1,4]thiazine (**2o**; synthesized according to FR1401481A[87]) in 2.8 mL of anhydrous DMF, 3.63 mL (3.63 mmol, 1.0 equiv) of LiHMDS (1 M) and 1.41 g (6.16 mmol, 1.7 equiv) of methyl 4-(bromomethyl)benzoate (**3**) in 1.4 mL of anhydrous DMF. Reaction mixture was stirred for 2 hours and was extracted with CH_2Cl_2 (3 x 80 mL). Flash column chromatography with CH_2Cl_2 and hexanes (7:3, R_f 0.3) gave 697 mg (1.89 mmol, 52 %) of **4o** as a yellow solid. Mp: 149 °C. ^{1}H NMR (400 MHz, CD_2Cl_2): δ (ppm) = 8.00 – 7.93 (m, 2H, 2'-H, 6'-H), 7.48 – 7.43 (m, 2H, 3'-

H, 5'-H), 6.97 – 6.87 (m, 2H, 6'''-H, 8'''-H), 6.79 (td, *J* = 7.5, 1.2 Hz, 1H, 7'''-H), 6.47 (dd, *J* = 8.2, 1.2 Hz, 1H, 5'''-H), 5.23 (s, 2H, 1''-H), 3.87 (s, 3H, $COOCH_3$), 2.52 (s, 3H, CH_3). ^{13}C NMR (101 MHz, CD_2Cl_2): δ (ppm) = 167.2 (C-1), 163.6 (C-2'''), 152.8 (C-3a'''), 144.3 (C-4a'''), 144.1 (C-4'), 130.3 (C-2', C-6'), 129.6 (C-1'), 128.2 (C-6'''/C-8'''), 127.6 (C-8'''/C-6'''), 127.1 (C-3', C-5'), 123.3 (C-7'''), 120.2 (C-8a'''), 115.3 (C-5'''), 96.6 (C-9a'''), 52.5 ($COO\underline{C}H_3$), 50.9 (C-1''), 19.9 (CH_3). MS (ESI+): m/z calcd for [$(C_{19}H_{17}N_2O_2S_2)^+$] 369.0726, found 369.0727.

Methyl 4-[(10*H*-benzo[*b*]pyridazino[3,4-*e*][1,4]thiazin-10-yl)methyl]benzoate (4p) and methyl 4-[(1*H*-benzo[*b*]pyridazino[3,4-*e*][1,4]thiazin-1-yl)methyl]benzoate (8p). Standard protocol 1 with 694 mg (3.45 mmol) of 10*H*-benzo[*b*]pyridazino[3,4-*e*][1,4]thiazine (**2p**; synthesized according to Yoneda *et al.*[88]) in 3.0 mL of anhydrous DMF, 6.82 mL (6.82 mmol, 2.0 equiv) of LiHMDS (1 M) and 1.34 g (5.85 mmol, 1.7 equiv) of methyl 4-(bromomethyl)benzoate (**3**) in 2.0 mL of anhydrous DMF. Reaction mixture was stirred for 13 hours at room temperature and was extracted with CH_2Cl_2 (3 x 80 mL). Iterated flash column chromatography with CH_2Cl_2 with 2 % MeOH (R_f 0.3 (**4p**) and 0.7 (**8p**)) and then CH_2Cl_2 and hexanes (19:1, R_f 0.0 (**4p**) and 0.3 (**8p**)) gave 564 mg (1.61 mmol, 47 %) of **4p** as a beige solid (mp: 179 °C) and 171 mg (0.489 mmol, 14 %) of **8p** as an orange-red solid (mp: 145 – 146 °C). **4p**: ^1H NMR (400 MHz, CD_2Cl_2): δ (ppm) = 8.43 (d, *J* = 4.9 Hz, 1H, 3'''-H), 8.00 – 7.93 (m, 2H, 2'-H, 6'-H), 7.42 – 7.36 (m, 2H, 3'-H, 5'-H), 7.03 – 6.96 (m, 3H, 4'''-H, 6'''-H, 8'''-H), 6.89 (td, *J* = 7.5, 1.2 Hz, 1H, 7'''-H), 6.65 (dd, *J* = 8.1, 1.2 Hz, 1H, 9'''-H), 5.46 (s, 2H, 1''-H), 3.87 (s, 3H, $COOCH_3$). ^{13}C NMR (101 MHz, CD_2Cl_2): δ (ppm) = 167.2 (C-1), 156.0 (C-10a'''), 147.6 (C-3'''), 143.0 (C-4'), 141.5 (C-9a'''), 130.3 (C-2', C-6'), 129.6 (C-1'), 128.8 (C-8'''), 128.1 (C-4a'''), 127.3 (C-6'''), 127.1 (C-3', C-5') 124.1 (C-7'''), 123.5 (C-4'''), 118.9 (C-5a'''), 117.2 (C-9'''), 52.5 ($COO\underline{C}H_3$), 50.0 (C-1''). MS (ESI+): m/z calcd for [$(C_{19}H_{16}N_3O_2S)^+$] 350.0958, found 350.0960.

8p: ^{1}H NMR (400 MHz, CD_2Cl_2): δ (ppm) = 8.03 – 7.97 (m, 2H, 2'-H, 6'-H), 7.55 – 7.49 (m, 2H, 3'-H, 5'-H), 6.90 (d, *J* = 4.3 Hz, 1H, 4'''-H), 6.85 (td, *J* = 7.6, 1.6 Hz, 1H, 9'''-H), 6.69 – 6.62 (m, 2H, 8'''-H, 10'''-H), 6.56 (dd, *J* = 7.6, 1.5 Hz, 1H, 7'''-H), 5.93 (d, *J* = 4.3 Hz, 1H, 5'''-H), 5.06 (s, 2H, 1''-H), 3.88 (s, 3H, $COOCH_3$). ^{13}C NMR (101 MHz, CD_2Cl_2): δ (ppm) = 167.2 (C-1), 150.6 (C-1a'''), 144.5 (C-10a'''), 142.8 (C-4'), 138.3 (C-4'''), 136.3 (C-5a'''), 130.0 (C-2', C-6'), 130.0 (C-1'), 129.1 (C-3', C-5'), 128.6 (C-9'''), 126.6 (C-10'''), 125.0 (C-7'''), 124.3 (C-8'''), 118.3 (C-6a'''), 116.1 (C-5'''), 55.9 (C-1''), 52.5 ($COO\underline{C}H_3$). MS (ESI+): m/z calcd for [($C_{19}H_{16}N_3O_2S$)$^+$] 350.0958, found 350.0961.

Methyl 4-[(3-chloro-10*H*-benzo[*b*]pyridazino[3,4-*e*][1,4]thiazin-10-yl)methyl]benzoate (4q) and methyl 4-[(3-chloro-1*H*-benzo[*b*]pyridazino[3,4-*e*][1,4]thiazin-1-yl)methyl]benzoate (8q). Standard protocol 1 with 501 mg (2.13 mmol) of 3-chloro-10*H*-benzo[*b*]pyridazino[3,4-*e*][1,4]thiazine (**2q**; synthesized according to Yoneda *et al.*[88]) in 6.0 mL of anhydrous DMF, 4.31 mL (4.31 mmol, 2.0 equiv) of LiHMDS (1 M) and 836 mg (3.65 mmol, 1.7 equiv) of methyl 4-(bromomethyl)benzoate (**3**) in 1.0 mL of anhydrous DMF. Reaction mixture was stirred for 16 hours at room temperature, then for 2 hours at 60 °C and was extracted with CH_2Cl_2 (3 x 80 mL). Iterated flash column chromatography with hexanes and EtOAc (4:1, R_f 0.2 (**4q**) and 0.5 (**8q**)) and then CH_2Cl_2 and hexanes (4:1, R_f 0.1 (**4q**) and 0.4 (**8q**)) gave 383 mg (1.00 mmol, 47 %) of **4q** as a yellow solid (mp: 180 - 181 °C) and 142 mg (0.370 mmol, 17 %) of **8q** as an orange-red solid (mp: 195 -196 °C). **4q**: ^{1}H NMR (500 MHz, CD_2Cl_2): δ (ppm) = 8.00 – 7.95 (m, 2H, 2'-H, 6'-H), 7.40 – 7.35 (m, 2H, 3'-H, 5'-H), 7.04 – 6.98 (m, 3H, 4'''-H, 6'''-H, 8'''-H), 6.91 (td, *J* = 7.3, 1.1 Hz, 1H, 7'''-H), 6.66 (dd, *J* = 8.2, 1.2 Hz, 1H, 9'''-H), 5.41 (s, 2H, 1''-H), 3.87 (s, 3H, $COOCH_3$). ^{13}C NMR (126 MHz, CD_2Cl_2): δ (ppm) = 167.1 (C-1), 155.1 (C-10a'''), 151.2 (C-3'''), 142.4 (C-4'), 140.9 (C-9a'''), 131.7 (C-4a'''), 130.3 (C-2', C-6'), 129.7 (C-1'), 129.1 (C-8'''), 127.4

(C-6'''), 127.0 (C-3', C-5'), 124.4 (C-7'''), 123.8 (C-4'''), 117.9 (C-5a'''), 117.4 (C-9'''), 52.5 (COO<u>C</u>H$_3$), 50.2 (C-1''). MS (ESI+): m/z calcd for [($C_{19}H_{15}ClN_3O_2S$)$^+$] 384.0568, found 384.0569. **8q**: ^{1}H NMR (500 MHz, CD_2Cl_2): δ (ppm) = 8.03 – 7.98 (m, 2H, 2'-H, 6'-H), 7.56 – 7.50 (m, 2H, 3'-H, 5'-H), 6.90 (td, *J* = 7.7, 1.5 Hz, 1H, 9'''-H), 6.75 – 6.69 (m, 2H, 8'''-H, 10'''-H), 6.62 (dd, *J* = 8.0, 1.5 Hz, 1H, 7'''-H), 5.95 (s, 1H, 5'''-H), 5.01 (s, 2H, 1''-H), 3.88 (s, 3H, $COOCH_3$). ^{13}C NMR (126 MHz, CD_2Cl_2): δ (ppm) = 167.1 (C-1), 148.6 (C-1a'''), 143.6 (C-10a'''), 142.1 (C-4'), 139.1 (C-4'''/C-5a'''), 138.9 (C-5a'''/C-4'''), 130.2 (C-1'), 130.1 (C-2', C-6'), 129.1 (C-3', C-5'), 128.9 (C-9'''), 127.2 (C-10'''), 125.0 (C-7'''), 124.8 (C-8'''), 117.4 (C-6a'''), 116.4 (C-5'''), 55.9 (C-1''), 52.5 (COO<u>C</u>H$_3$). MS (ESI+): m/z calcd for [($C_{19}H_{15}ClN_3O_2S$)$^+$] 384.0568, found 384.0568.

4-[(10*H*-Phenothiazin-10-yl)methyl]benzoic acid (5a). Standard protocol 2 with 1.07 g (3.08 mmol) of **4a** in 20.0 mL of 1,4-dioxane/H_2O (1:1) and 3.78 mL (7.56 mmol, 2.5 equiv) of NaOH (2 M). The reaction mixture was stirred for 4 hours at 50 °C. The precipitate was collected and dried in high vacuum to yield 840 mg (2.52 mmol, 82 %) of **5a** as a white solid. Mp: 210 °C. ^{1}H NMR (500 MHz, DMSO-d_6): δ (ppm) = 12.88 (bs, 1H, COOH), 7.92 – 7.87 (m, 2H, 2'-H, 6'-H), 7.46 – 7.41 (m, 2H, 3'-H, 5'-H), 7.15 (dd, *J* = 7.6, 1.5 Hz, 2H, 4'''-H, 6'''-H), 7.06 (td, *J* = 7.8, 1.5 Hz, 2H, 2'''-H, 8'''-H), 6.91 (td, *J* = 7.5, 1.0 Hz, 2H, 3'''-H, 7'''-H), 6.76 (dd, *J* = 8.3, 0.9 Hz, 2H, 1'''-H, 9'''-H), 5.20 (s, 2H, 1''-H). ^{13}C NMR (126 MHz, DMSO-d_6): δ (ppm) = 167.1 (C-1), 144.1 (C-9a''', C-10a'''), 142.4 (C-4'), 129.6 (C-2', C-6'), 129.5 (C-1'), 127.5 (C-2''', C-8'''), 126.9 (C-3', C-5'), 126.9 (C-4''', C-6'''), 122.7 (C-3''', C-7'''), 122.6 (C-4a''', C-5a'''), 115.8 (C-1''', C-9'''), 50.9 (C-1''). MS (ESI−): m/z calcd for [($C_{20}H_{14}NO_2S$)$^-$] 332.0751, found 332.0750.

4-[(5,5-Dioxido-10*H*-phenothiazin-10-yl)methyl]benzoic acid (5b). Standard protocol 2 with 526 mg (1.39 mmol) of **4b** in 17.0 mL of 1,4-dioxane/H_2O (1:1) and 1.71 mL (3.42 mmol, 2.5

equiv) of NaOH (2 M). The reaction mixture was stirred for 5 hours at 50 °C. The precipitate was collected and dried at 60 °C in a drying oven to yield 355 mg (0.972 mmol, 70 %) of **5b** as a white solid. Mp: 250 - 253 °C. ^{1}H NMR (500 MHz, DMSO-d_6): δ (ppm) = 12.98 (bs, 1H, COOH), 8.05 (dd, *J* = 7.9, 1.5 Hz, 2H, 4'''-H, 6'''-H), 7.95 – 7.84 (m, 2H, 2'-H, 6'-H), 7.65 (ddd, *J* = 8.7, 7.3, 1.6 Hz, 2H, 2'''-H, 8'''-H), 7.36 (t, *J* = 7.6 Hz, 2H, 3'''-H, 7'''-H), 7.32 (d, *J* = 8.7 Hz, 2H, 1'''-H, 9'''-H), 7.29 – 7.22 (m, 2H, 3'-H, 5'-H), 5.69 (s, 2H, 1''-H). ^{13}C NMR (126 MHz, DMSO-d_6): δ = 167.2 (C-1), 140.7 (C-4'), 140.4 (C-9a''', C-10a'''), 133.7 (C-2''', C-8'''), 130.4 (C-1'), 129.8 (C-2', C-6'), 126.2 (C-3', C-5'), 123.6 (C-4a''', C-5a'''), 122.6 (C-4''', C-6'''), 122.4 (C-3''', C-7'''), 117.2 (C-1''', C-9'''), 51.2 (C-1''). MS (ESI−): m/z calcd for [($C_{20}H_{14}NO_4S$)$^-$] 364.0649, found 364.0650.

4-[(1-Chloro-10*H*-phenothiazin-10-yl)methyl]benzoic acid (5c). Standard protocol 2 with 303 mg (0.793 mmol) of **4c** in 10.0 mL of 1,4-dioxane/H_2O (1:1) and 980 µL (1.96 mmol, 2.5 equiv) of NaOH (2 M). The reaction mixture was stirred for 48 hours at 50 °C. The precipitate was collected and dried in high vacuum to yield 235 mg (0.639 mmol, 80 %) of **5c** as a white solid. Mp: 218 °C. ^{1}H NMR (400 MHz, DMSO-d_6): δ (ppm) = 12.87 (bs, 1H, COOH), 7.82 – 7.70 (m, 2H, 2'-H, 6'-H), 7.50 – 7.40 (m, 2H, 3'-H, 5'-H), 7.34 (dd, *J* = 8.0, 1.4 Hz, 1H, 4'''-H), 7.22 (dd, *J* = 7.5, 1.2 Hz, 2H, 2'''-H, 9'''-H), 7.15 (dd, *J* = 7.6, 1.5 Hz, 1H, 6'''-H), 7.15 (dd, *J* = 7.7, 1.4 Hz, 1H, 8'''-H), 7.06 (t, *J* = 7.8 Hz, 1H, 3'''-H), 6.96 (td, *J* = 7.5, 1.3 Hz, 1H, 7'''-H), 5.21 (s, 2H, 1''-H). ^{13}C NMR (126 MHz, DMSO-d_6): δ (ppm) = 167.1 (C-1), 145.1 (C-9a'''), 142.9 (C-4'), 140.7 (C-10a'''), 133.4 (C-1'''), 129.9 (C-1'), 129.7 (C-4'''), 129.2 (C-2', C-6'), 128.1 (C-5a'''), 128.0 (C-3', C-5'), 127.6 (C-6'''/C-8'''), 126.8 (C-8'''/C-6'''), 126.3 (C-2'''), 125.8 (C-4a'''), 125.4 (C-3'''), 124.1 (C-7'''), 121.1 (C-9'''), 56.6 (C-1''). MS (ESI−): m/z calcd for [($C_{20}H_{13}ClNO_2S$)$^-$] 366.0361, found 366.0364.

4-[(2-(Trifluoromethyl)-10*H*-phenothiazin-10-yl)methyl]benzoic acid (5d). Standard protocol 2 with 333 mg (0.802 mmol) of **4d** in 5.0 mL of 1,4-dioxane/H_2O (1:1) and 990 µL (1.98 mmol, 2.5 equiv) of NaOH (2 M). The reaction mixture was stirred for 16 hours at 60 °C. The precipitate was collected and dried in high vacuum to yield 255 mg (0.635 mmol, 79 %) of **5d** as a white solid. Mp: 173 - 174 °C. ^{1}H NMR (400 MHz, DMSO-d_6): δ (ppm) = 12.91 (bs, 1H, COOH), 7.97 – 7.84 (m, 2H, 2'-H, 6'-H), 7.50 – 7.42 (m, 2H, 3'-H, 5'-H), 7.37 (d, J = 8.0 Hz, 1H, 4'''-H), 7.24 (dd, J = 8.0, 1.8 Hz, 1H, 3'''-H), 7.19 (dd, J = 7.6, 1.5 Hz, 1H, 6'''-H), 7.12 (td, J = 7.8, 1.5 Hz, 1H, 8'''-H), 6.99 (d, J = 1.8 Hz, 1H, 1'''-H), 6.97 (td, J = 7.5, 1.1 Hz, 1H, 7'''-H), 6.84 (dd, J = 8.2, 1.1 Hz, 1H, 9'''-H), 5.29 (s, 2H, 1''-H). ^{13}C NMR (101 MHz, DMSO-d_6): δ (ppm) = 167.0 (C-1), 144.7 (C-10a'''), 143.4 (C-9a'''), 141.8 (C-4'), 129.7 (C-2', C-6'), 128.6 (C-1'/C-4a'''), 128.5 (C-4a'''/C-1'), 128.1 (q, ^2J = 31.9 Hz, C-2'''), 128.0 (C-8'''), 127.5 (C-4'''), 127.1 (C-6'''), 127.0 (C-3', C-5'), 124.0 (q, ^1J = 272.1 Hz, CF_3), 123.4 (C-7'''), 121.8 (C-5a'''), 119.3 (q, ^3J = 4.0 Hz, C-3'''), 116.3 (C-9'''), 112.0 (q, ^3J = 3.6 Hz, C-1'''), 50.8 (C-1''). MS (ESI−): m/z calcd for [$(C_{21}H_{13}F_3NO_2S)^-$] 400.0625, found 400.0626.

4-[(5-Oxido-10*H*-phenothiazin-10-yl)methyl]benzoic acid (5e). Standard protocol 2 with 303 mg (0.834 mmol) of **4e** in 6.0 mL of 1,4-dioxane/H_2O (1:1) and 510 µL (1.02 mmol, 1.2 equiv) of NaOH (2 M). The reaction mixture was stirred for 3 hours at 60 °C. The precipitate was collected and dried at 60 °C in a drying oven to yield 275 mg (0.787 mmol, 95 %) of **5e** as a white solid. Mp: 328 °C. ^{1}H NMR (500 MHz, DMSO-d_6): δ (ppm) = 12.91 (s, 1H, COOH), 8.02 (dd, J = 7.6, 1.6 Hz, 2H, 4'''-H, 6'''-H), 7.95 – 7.82 (m, 2H, 2'-H, 6'-H), 7.60 (ddd, J = 8.6, 7.2, 1.5 Hz, 2H, 2'''-H, 8'''-H), 7.37 – 7.27 (m, 4H, 1'''-H, 3'''-H, 7'''-H, 9'''-H), 7.27 – 7.20 (m, 2H, 3'-H, 5'-H), 5.74 (s, 2H, 1''-H). ^{13}C NMR (126 MHz, DMSO-d_6): δ (ppm) = 167.0 (C-1), 141.3 (C-4'), 138.3 (C-9a''', C-10a'''), 133.0 (C-2''', C-8'''), 131.1 (C-4''', C-6'''), 129.8 (C-2', C-6'), 129.7 (C-1'),

126.3 (C-3', C-5'), 124.3 (C-4a''', C-5a'''), 122.1 (C-3''', C-7'''), 116.6 (C-1''', C-9'''), 50.7 (C-1''). MS (ESI−): m/z calcd for [$(C_{20}H_{14}NO_3S)^-$] 348.0700, found 348.0699.

4-[(2-Chloro-10*H*-phenothiazin-10-yl)methyl]benzoic acid (5f). Standard protocol 2 with 360 mg (0.943 mmol) of **4f** in 6.0 mL of 1,4-dioxane/H_2O (1:1) and 1.18 mL (2.36 mmol, 2.5 equiv) of NaOH (2 M). The reaction mixture was stirred for 2 hours at 60 °C. The precipitate was collected and dried in high vacuum to yield 317 mg (0.862 mmol, 91 %) of **5f** as a white solid. Mp: 123 - 125 °C. ^{1}H NMR (500 MHz, DMSO-d_6): δ (ppm) = 13.18 (bs, 1H, COOH), 7.95 – 7.85 (m, 2H, 2'-H, 6'-H), 7.46 – 7.38 (m, 2H, 3'-H, 5'-H), 7.17 (d, J = 7.6 Hz, 1H, 6'''-H), 7.16 (d, J = 8.1 Hz, 1H, 4'''-H), 7.08 (td, J = 7.8, 1.5 Hz, 1H, 8'''-H), 6.97 (dd, J = 8.1, 1.8 Hz, 1H, 3'''-H), 6.94 (t, J = 7.5 Hz, 1H, 7'''-H), 6.86 – 6.74 (m, 2H, 1'''-H, 9'''-H), 5.22 (s, 2H, 1''-H). ^{13}C NMR (126 MHz, DMSO-d_6): δ (ppm) = 167.2 (C-1), 145.6 (C-10a'''), 143.4 (C-9a'''), 141.4 (C-4'), 132.2 (C-2'''), 130.5 (C-1'), 129.6 (C-2', C-6'), 127.9 (C-4'''), 127.7 (C-8'''), 127.0 (C-6'''), 126.8 (C-3', C-5'), 123.2 (C-7'''), 122.3 (C-3''', C-5a'''), 121.7 (C-4a'''), 116.2 (C-9'''), 115.8 (C-1'''), 50.8 (C-1''). MS (ESI−): m/z calcd for [$(C_{20}H_{13}ClNO_2S)^-$] 366.0361, found 366.0368.

4-[(2-Methoxy-10*H*-phenothiazin-10-yl)methyl]benzoic acid (5g). Standard protocol 2 with 569 mg (1.51 mmol) of **4g** in 15.0 mL of 1,4-dioxane/H_2O (1:1) and 1.85 mL (3.70 mmol, 2.5 equiv) of NaOH (2 M). The reaction mixture was stirred for 2 hours at 60 °C. The precipitate was collected and dried in high vacuum to yield 479 mg (1.32 mmol, 87 %) of **5g** as a white solid. Mp: 179 - 182 °C. ^{1}H NMR (400 MHz, DMSO-d_6): δ (ppm) = 12.87 (s, 1H, COOH), 7.99 – 7.81 (m, 2H, 2'-H, 6'-H), 7.54 – 7.36 (m, 2H, 3'-H, 5'-H), 7.15 (dd, J = 7.6, 1.5 Hz, 1H, 6'''-H), 7.07 (td, J = 7.5, 1.5 Hz, 1H, 8'''-H), 7.05 (d, J = 8.4 Hz, 1H, 4'''-H), 6.91 (td, J = 7.5, 1.1 Hz, 1H, 7'''-H), 6.79 (dd, J = 8.3, 1.1 Hz, 1H, 9'''-H), 6.53 (dd, J = 8.5, 2.4 Hz, 1H, 3'''-H), 6.35 (d, J = 2.4 Hz, 1H, 1'''-H), 5.21 (s, 2H, 1''-H), 3.61 (s, 3H, OCH_3). ^{13}C NMR (101 MHz, DMSO-d_6): δ(ppm)

= 167.0 (C-1), 159.3 (C-2'''), 145.4 (C-10a'''), 144.0 (C-9a'''), 142.4 (C- 4'), 129.6 (C-2', C-6'), 129.5 (C-1'), 127.4 (C-8'''), 127.2 (C-4'''), 126.9 (C-3', C-5'), 126.8 (C-6'''), 123.3 (C-5a'''), 122.7 (C-7'''), 115.9 (C-9'''), 113.4 (C-4a'''), 107.4 (C-3'''), 103.5 (C-1'''), 55.1 (OCH_3), 50.9 (C-1''). MS (ESI−): m/z calcd for [$(C_{21}H_{16}NO_3S)^-$] 362.0856, found 362.0860.

4-[(2-(Ethylthio)-10*H*-phenothiazin-10-yl)methyl]benzoic acid (5h). Standard protocol 2 with 700 mg (1.72 mmol) of **4h** in 11.0 mL of 1,4-dioxane/H_2O (1:1) and 2.15 mL (4.30 mmol, 2.5 equiv) of NaOH (2 M). The reaction mixture was stirred for 12 hours at 60 °C. Extraction with EtOAc (2 x 100 mL) yielded 591 mg (1.50 mmol, 87 %) of **5h** as a pale yellow solid. Mp: 76 - 78 °C. ^{1}H NMR (400 MHz, DMSO-d_6): δ (ppm) = 12.92 (bs, 1H, COOH), 7.98 – 7.82 (m, 2H, 2'-H, 6'-H), 7.51 – 7.37 (m, 2H, 3'-H, 5'-H), 7.16 (dd, J = 7.6, 1.5 Hz, 1H, 6'''-H), 7.09 (td, J = 7.8, 1.5 Hz, 1H, 8'''-H), 7.07 (d, J = 8.0 Hz, 1H, 4'''-H), 6.93 (t, J = 7.5 Hz, 1H, 7'''-H), 6.85 (dd, J = 8.0, 1.7 Hz, 1H, 3'''-H), 6.82 (d, J = 7.4 Hz, 1H, 9'''-H), 6.64 (d, J = 1.7 Hz, 1H, 1'''-H), 5.22 (s, 2H, 1''-H), 2.73 (q, J = 7.3 Hz, 2H, $SC\underline{H}_2CH_3$), 0.97 (t, J = 7.3 Hz, 3H, $SCH_2C\underline{H}_3$). ^{13}C NMR (101 MHz, DMSO-d_6): δ (ppm) = 167.1 (C-1), 144.4 (C-10a'''), 144.0 (C-9a'''), 142.2 (C-4'), 135.4 (C-2'''), 129.6 (C-1', C-2', C-6'), 127.6 (C-8'''), 127.1 (C-4'''), 126.9 (C-3', C-5', C-6'''), 122.9 (C-7'''), 122.7 (C-5a'''), 122.6 (C-3'''), 120.0 (C-4a'''), 116.0 (C-9'''), 115.7 (C-1'''), 50.8 (C-1''), 26.3 ($S\underline{C}H_2CH_3$), 14.0 ($SCH_2\underline{C}H_3$). MS (ESI−): m/z calcd for [$(C_{22}H_{18}NO_2S_2)^-$] 392.0784, found 392.0784.

4-[(10*H*-Benzo[*b*]pyrido[2,3-*e*][1,4]thiazin-10-yl)methyl]benzoic acid (5i). Standard protocol 2 with 312 mg (0.895 mmol) of **4i** in 10.0 mL of 1,4-dioxane/H_2O (1:1) and 1.11 mL (2.22 mmol, 2.5 equiv) of NaOH (2 M). The reaction mixture was stirred for 5 hours at 60 °C. The precipitate was collected and dried at 40 °C in a drying oven to yield 263 mg (0.787 mmol, 88 %) of **5i** as a pale beige solid. Mp: 175 - 177 °C. ^{1}H NMR (400 MHz, DMSO-d_6): δ (ppm) =

12.92 (bs, 1H, COOH), 7.93 (dd, *J* = 4.9, 1.6 Hz, 1H, 2'''-H), 7.90 – 7.84 (m, 2H, 2'-H, 6'-H), 7.48 (dd, *J* = 7.5, 1.6 Hz, 1H, 4'''-H), 7.39 – 7.33 (m, 2H, 3'-H, 5'-H), 7.10 (dd, *J* = 7.6, 1.5 Hz, 1H, 6'''-H), 7.01 (td, *J* = 7.8, 1.6 Hz, 1H, 8'''-H), 6.93 – 6.86 (m, 2H, 3'''-H, 7'''-H), 6.68 (dd, *J* = 8.3, 1.1 Hz, 1H, 9'''-H), 5.37 (s, 2H, 1''-H). ^{13}C NMR (101 MHz, DMSO-d_6): δ (ppm) = 167.3 (C-1), 153.5 (C-10a'''), 145.2 (C-2'''), 142.8 (C-4'), 141.7 (C-9a'''), 134.6 (C-4'''), 129.6 (C-1'), 129.4 (C-2', C-6'), 127.7 (C-8'''), 126.7 (C-6'''), 126.5 (C-3', C-5'), 123.2 (C-7'''), 119.7 (C-5a'''), 118.6 (C-3'''), 116.0 (C-9'''), 115.6 (C-4a'''), 47.9 (C-1''). MS (ESI−): m/z calcd for [$(C_{19}H_{13}N_2O_2S)^-$] 333.0703, found 333.0706.

4-[(10*H*-Benzo[b]pyrido[3,4-e][1,4]thiazin-10-yl)methyl]benzoic acid (5j). Standard protocol 2 with 229 mg (0.657 mmol) of **4j** in 6.0 mL of 1,4-dioxane/H_2O (1:1) and 820 µL (1.64 mmol, 2.5 equiv) of NaOH (2 M). The reaction mixture was stirred for 2 hours at 60 °C. Extraction with EtOAc (3 x 50 mL) yielded 198 mg (0.592 mmol, 90 %) of **5j** as a yellow solid. Mp: 134 - 137 °C. ^{1}H NMR (500 MHz, DMSO-d_6): δ (ppm) = 12.90 (s, 1H, COOH), 8.02 (d, *J* = 4.9 Hz, 1H, 3'''-H), 7.95 – 7.89 (m, 2H, 2'-H, 6'-H), 7.87 (s, 1H, 1'''-H), 7.48 – 7.40 (m, 2H, 3'-H, 5'-H), 7.18 (d, *J* = 4.9 Hz, 1H, 4'''-H), 7.15 (dd, *J* = 7.7, 1.5 Hz, 1H, 6'''-H), 7.10 (td, *J* = 7.8, 1.5 Hz, 1H, 8'''-H), 6.94 (t, *J* = 7.5 Hz, 1H, 7'''-H), 6.78 (d, *J* = 8.2 Hz, 1H, 9'''-H), 5.25 (s, 2H, 1''-H). ^{13}C NMR (126 MHz, DMSO-d_6): δ (ppm) = 167.0 (C-1), 143.4 (C-3'''), 143.2 (C-9a'''), 141.7 (C-4'), 139.6 (C-10a'''), 135.9 (C-1'''), 133.1 (C-4a'''), 129.7 (C-2', C-6'), 129.7 (C-1'), 128.2 (C-8'''), 127.1 (C-6'''), 126.8 (C-3', C-5'), 123.2 (C-7'''), 121.1 (C-4'''), 120.2 (C-5a'''), 116.1 (C-9'''), 50.4 (C-1''). MS (ESI+): m/z calcd for [$(C_{19}H_{15}N_2O_2S)^+$] 335.0849, found 335.0850.

4-[(10*H*-Benzo[*b*]pyrazino[2,3-*e*][1,4]thiazin-10-yl)methyl]benzoic acid (5k). Standard protocol 2 with 405 mg (1.16 mmol) of **4k** in 10.0 mL of 1,4-dioxane/H_2O (1:1) and 1.43 mL (2.86 mmol, 2.5 equiv) of NaOH (2 M). The reaction mixture was stirred for 2 hours at 60 °C.

The precipitate was collected and dried at 60 °C in a drying oven to yield 354 mg (1.06 mmol, 91 %) of **5k** as a yellow solid. Mp: 204 - 205 °C. ^{1}H NMR (500 MHz, DMSO-d_6): δ (ppm) = 12.88 (bs, 1H, COOH), 7.91 – 7.84 (m, 2H, 2'-H, 6'-H), 7.82 (d, J = 2.8 Hz, 1H, 3'''-H), 7.79 (d, J = 2.8 Hz, 1H, 2'''-H), 7.40 – 7.35 (m, 2H, 3'-H, 5'-H), 7.09 (dd, J = 7.6, 1.5 Hz, 1H, 6'''-H), 7.01 (td, J = 7.8, 1.6 Hz, 1H, 8'''-H), 6.91 (td, J = 7.5, 1.1 Hz, 1H, 7'''-H), 6.62 (dd, J = 8.3, 1.1 Hz, 1H, 9'''-H), 5.27 (s, 2H, 1''-H). ^{13}C NMR (126 MHz, DMSO-d_6): δ (ppm) = 167.1 (C-1), 149.2 (C-10a'''), 141.9 (C-4'), 141.2 (C-4a'''), 139.3 (C-9a'''), 138.8 (C-2'''), 136.8 (C-3'''), 129.6 (C-2', C-6'), 129.4 (C-1'), 128.1 (C-8'''), 126.8 (C-6'''), 126.4 (C-3', C-5'), 123.6 (C-7'''), 118.4 (C-5a'''), 116.2 (C-9'''), 47.9 (C-1''). MS (ESI−): m/z calcd for [$(C_{18}H_{12}N_3O_2S)^-$] 334.0656, found 334.0661.

4-[(10*H*-Dipyrido[2,3-*b*:2',3'-*e*][1,4]thiazin-10-yl)methyl]benzoic acid (5l). Standard protocol 2 with 287 mg (0.821 mmol) of **4l** in 6.0 mL of 1,4-dioxane/H_2O (1:1) and 500 µL (1.00 mmol, 1.2 equiv) of NaOH (2 M). The reaction mixture was stirred for 38 hours at room temperature. The precipitate was dried at 60 °C in a drying oven to yield 226 mg (0.674 mmol, 82 %) of **5l** as a pale yellow solid. Mp: 250 - 251 °C. ^{1}H NMR (500 MHz, DMSO-d_6): δ (ppm) = 12.86 (s, 1H, COOH), 7.94 – 7.86 (m, 4H, 2'-H, 6'-H, 2'''-H, 7'''-H), 7.48 (dd, J = 7.5, 1.6 Hz, 1H, 4'''-H), 7.40 – 7.35 (m, 2H, 3'-H, 5'-H), 6.98 (dd, J = 8.3, 4.7 Hz, 1H, 8'''-H), 6.89 (dd, J = 7.6, 4.9 Hz, 1H, 3'''-H), 6.84 (dd, J = 8.4, 1.3 Hz, 1H, 9'''-H), 5.32 (s, 2H, 1''-H). ^{13}C NMR (126 MHz, DMSO-d_6): δ (ppm) = 167.1 (C-1), 151.4 (C-10a'''), 145.3 (C-2'''), 142.8 (C-5a'''), 142.6 (C-7'''), 142.2 (C-4'), 137.6 (C-9a'''), 134.8 (C-4'''), 129.6 (C-2', C-6'), 129.3, (C-1'), 126.5, (C-3', C-5'), 122.4, (C-8'''), 121.6, (C-9'''), 118.8, (C-3'''), 115.1, (C-4a'''), 47.5, (C-1''). MS (ESI−): m/z calcd for [$(C_{18}H_{12}N_3O_2S)^-$] 334.0656, found 334.0657.

4-[(10*H*-Dipyrido[3,4-*b*:3',4'-*e*][1,4]thiazin-10-yl)methyl]benzoic acid (5m). Standard protocol 2 with 312 mg (0.893 mmol) of **4m** in 6.0 mL of 1,4-dioxane/H_2O (1:1) and 550 µL

(1.10 mmol, 1.2 equiv) of NaOH (2 M). The reaction mixture was stirred for 2 hours at 60 °C. The precipitate was dried at 50 °C in a drying oven to yield 245 mg (0.731 mmol, 82 %) of **5m** as a yellow solid. Mp: 131 - 134 °C. ^{1}H NMR (500 MHz, DMSO-d_6): δ (ppm) = 12.94 (bs, 1H, COOH), 8.12 (d, J = 5.6 Hz, 1H, 8'''-H), 8.12 (s, 1H, 6'''-H), 8.05 (d, J = 4.9 Hz, 1H, 3'''-H), 7.96 – 7.90 (m, 2H, 2'-H, 6'-H), 7.85 (s, 1H, 1'''-H), 7.43 – 7.37 (m, 2H, 3'-H, 5'-H), 7.20 (d, J = 4.9 Hz, 1H, 4'''-H), 6.65 (d, J = 5.6 Hz, 1H, 9'''-H), 5.28 (s, 2H, 1''-H). ^{13}C NMR (126 MHz, DMSO-d_6): δ (ppm) = 167.0 (C-1), 149.7 (C-9a'''), 149.6 (C-6'''/C-8'''), 146.3 (C-8'''/C-6'''), 144.5 (C-3'''), 140.5 (C-4'), 137.6 (C-10a'''), 136.1 (C-1'''), 132.0 (C-4a'''), 129.8 (C-1', C-2', C-6'), 126.6 (C-3', C-5'), 121.6 , (C-4'''), 116.0 (C-5a'''), 110.1 (C-9'''), 49.8 (C-1''). MS (ESI+): m/z calcd for [($C_{18}H_{14}N_3O_2S$)$^+$] 336.0801, found 336.0801.

4-[(5*H*-Dipyrido[2,3-*b*:4',3'-*e*][1,4]thiazin-5-yl)methyl]benzoic acid (5n). Standard protocol 2 with 272 mg (0.778 mmol) of **4n** in 6.0 mL of 1,4-dioxane/H_2O (1:1) and 480 µL (0.960 mmol, 1.2 equiv) of NaOH (2 M). The reaction mixture was stirred for 3 hours at 60 °C. The precipitate was collected and dried at 50 °C in a drying oven to yield 208 mg (0.620 mmol, 80 %) of **5n** as a pale yellow solid. Mp: 129 - 132 °C. ^{1}H NMR (500 MHz, DMSO-d_6): δ (ppm) = 12.94 (bs, 1H, COOH), 8.12 (s, 1H, 4'''-H), 8.09 (d, J = 5.7 Hz, 1H, 2'''-H), 7.97 (d, J = 4.7 Hz, 1H, 7'''-H), 7.95 – 7.88 (m, 2H, 2'-H, 6'-H), 7.41 – 7.34 (m, 2H, 3'-H, 5'-H), 7.05 (dd, J = 8.3, 4.7 Hz, 1H, 8'''-H), 6.94 (d, J = 8.2 Hz, 1H, 9'''-H), 6.58 (d, J = 5.6 Hz, 1H, 1'''-H), 5.18 (s, 2H, 1''-H). ^{13}C NMR (126 MHz, DMSO-d_6): δ (ppm) = 167.0 (C-1), 149.3 (C-2'''), 148.3 (C-10a'''), 146.3 (C-4'''), 143.9 (C-5a'''), 143.4 (C-7'''), 140.4 (C-4'), 137.7 (C-9a'''), 129.8 (C-1', C-2', C-6'), 126.6 (C-3', C-5'), 122.6 (C-8'''), 122.0 (C-9'''), 117.0 (C-4a'''), 109.8 (C-1'''), 50.0 (C-1''). MS (ESI+): m/z calcd for [($C_{18}H_{14}N_3O_2S$)$^+$] 336.0801, found 336.0799.

4-[(2-Methyl-4*H*-benzo[*b*]thiazolo[4,5-*e*][1,4]thiazin-4-yl)methyl]benzoic acid (5o). Standard protocol 2 with 255 mg (0.692 mmol) of **4o** in 5.0 mL of 1,4-dioxane/H_2O (1:1) and 430 µL (0.860 mmol, 1.2 equiv) of NaOH (2 M). The reaction mixture was stirred for 3 hours at 60 °C and 11 hours at room temperature. The precipitate was collected and dried at 60 °C in a drying oven to yield 207 mg (0.584 mmol, 84 %) of **5o** as a beige solid. Mp: 223 - 224 °C. ^{1}H NMR (400 MHz, DMSO-d_6): δ (ppm) = 12.86 (bs, 1H, COOH), 7.93 – 7.87 (m, 2H, 2'-H, 6'-H), 7.48 – 7.41 (m, 2H, 3'-H, 5'-H), 7.02 – 6.94 (m, 2H, 6'''-H, 8'''-H), 6.82 (td, *J* = 7.5, 1.1 Hz, 1H, 7'''-H), 6.60 (dd, *J* = 8.2, 1.1 Hz, 1H, 5'''-H), 5.24 (s, 2H, 1''-H), 2.52 (s, 3H, CH_3). ^{13}C NMR (101 MHz, DMSO-d_6): δ (ppm) = 167.1 (C-1), 163.3 (C-2'''), 151.7 (C-3a'''), 143.1 (C-4'), 143.0 (C-4a'''), 129.6 (C-2', C-6'), 129.5 (C-1'), 128.0 (C-6'''/C-8'''), 127.1 (C-8'''/C-6'''), 126.5 (C-3', C-5'), 122.9 (C-7'''), 118.4 (C-8a'''), 114.9 (C-5'''), 94.7 (C-9a'''), 49.3 (C-1''), 19.3 (CH_3). MS (ESI+): m/z calcd for [($C_{18}H_{15}N_2O_2S_2$)$^+$] 355.0570, found 355.0569.

4-[(10*H*-Benzo[*b*]pyridazino[3,4-*e*][1,4]thiazin-10-yl)methyl]benzoic acid (5p). Standard protocol 2 with 433 mg (1.24 mmol) of **4p** in 10.0 mL of 1,4-dioxane/H_2O (1:1) and 1.53 mL (3.06 mmol, 2.5 equiv) of NaOH (2 M). The reaction mixture was stirred for 2 hours at 60 °C. Extraction with EtOAc (3 x 100 mL) yielded 353 mg (1.05 mmol, 85 %) of **5p** as a yellow solid. Mp: 229 - 230 °C. ^{1}H NMR (400 MHz, DMSO-d_6): δ (ppm) = 12.75 (bs, 1H, COOH), 8.51 (d, *J* = 4.9 Hz, 1H, 3'''-H), 7.92 – 7.86 (m, 2H, 2'-H, 6'-H), 7.43 – 7.37 (m, 2H, 3'-H, 5'-H), 7.34 (d, *J* = 5.0 Hz, 1H, 4'''-H), 7.11 (dd, *J* = 7.6, 1.5 Hz, 1H, 6'''-H), 7.06 (td, *J* = 7.8, 1.6 Hz, 1H, 8'''-H), 6.92 (td, *J* = 7.5, 1.1 Hz, 1H, 7'''-H), 6.73 (dd, *J* = 8.3, 1.1 Hz, 1H, 9'''-H), 5.45 (s, 2H, 1''-H). ^{13}C NMR (101 MHz, DMSO-d_6): δ (ppm) = 167.1 (C-1), 154.6 (C-10a'''), 147.3 (C-3'''), 142.2 (C-4'), 140.3 (C-9a'''), 129.5 (C-2', C-6'), 129.2 (C-1'), 128.4 (C-8'''), 126.8 (C-6'''), 126.5 (C-3', C-5'),

126.3 (C-4a'''), 123.6 (C-7'''), 123.6 (C-4'''), 117.4 (C-5a'''), 116.6 (C-9'''), 48.4 (C-1''). MS (ESI+): m/z calcd for [$(C_{18}H_{14}N_3O_2S)^+$] 336.0801, found 336.0802.

4-[(3-Chloro-10*H*-benzo[*b*]pyridazino[3,4-*e*][1,4]thiazin-10-yl)methyl]benzoic acid (5q). Standard protocol 2 with 311 mg (0.810 mmol) of **4q** in 7.0 mL of 1,4-dioxane/H_2O (1:1) and 1.01 mL (2.02 mmol, 2.5 equiv) of NaOH (2 M). The reaction mixture was stirred for 14 hours at 40 °C. The precipitate was collected and dried in high vacuum to yield 257 mg (0.695 mmol, 86 %) of **5q** as a yellow solid. Mp: 254 °C. ^{1}H NMR (400 MHz, DMSO-d_6): δ (ppm) = 12.87 (s, 1H, COOH), 7.92 – 7.86 (m, 2H, 2'-H, 6'-H), 7.59 (s, 1H, 4'''-H), 7.42 – 7.36 (m, 2H, 3'-H, 5'-H), 7.13 (dd, *J* = 7.7, 1.5 Hz, 1H, 6'''-H), 7.06 (td, *J* = 7.8, 1.6 Hz, 1H, 8'''-H), 6.93 (td, *J* = 7.6, 1.0 Hz, 1H, 7'''-H), 6.69 (dd, *J* = 8.4, 1.1 Hz, 1H, 9'''-H), 5.37 (s, 2H, 1''-H). ^{13}C NMR (101 MHz, DMSO-d_6): δ (ppm) = 167.1 (C-1), 153.9 (C-10a'''), 150.0 (C-3'''), 141.7 (C-4'), 139.7 (C-9a'''), 130.6 (C-4a'''), 129.5 (C-2', C-6'), 129.3 (C-1'), 128.6 (C-8'''), 126.8 (C-6'''), 126.5 (C-3', C-5'), 123.8 (C-7'''), 123.7 (C-4'''), 116.7 (C-9'''), 116.6 (C-5a'''), 48.7 (C-1''). MS (ESI+): m/z calcd for [$(C_{18}H_{13}ClN_3O_2S)^+$] 370.0412, found 370.0412.

(±)-4-[(10*H*-Phenothiazin-10-yl)methyl]-*N*-[(tetrahydro-2*H*-pyran-2-yl)oxy]benzamide (6a). Standard protocol 3 with 213 mg (0.639 mmol) of **5a** in 2.0 mL of anhydrous DMF, 180 µL (1.30 mmol, 2.0 equiv) of Et_3N, 405 mg (0.946 mmol, 1.5 equiv) of COMU in 1.0 mL of anhydrous DMF and 111 mg (0.948 mmol, 1.5 equiv) of NH_2OTHP in 1.0 mL of anhydrous DMF. The reaction mixture was stirred for 16 hours and was extracted with CH_2Cl_2 (3 x 20 mL). Iterated flash column chromatography with hexanes and EtOAc (7:3, R_f 0.2 to 1:1, R_f 0.4) and then CH_2Cl_2 with 1 % MeOH (R_f 0.2) gave 151 mg (0.349 mmol, 55 %) of **6a** as a white solid. Mp: 187 - 188 °C. ^{1}H NMR (400 MHz, CD_2Cl_2): δ (ppm) = 8.92 (s, 1H, NH), 7.71 – 7.65 (m, 2H, 2'-H, 6'-H), 7.45 – 7.39 (m, 2H, 3'-H, 5'-H), 7.11 (dd, *J* = 7.6, 1.5 Hz, 2H, 4''''-H, 6''''-H),

7.00 (td, J = 7.8, 1.6 Hz, 2H, 2""-H, 8""-H), 6.89 (td, J = 7.5, 1.1 Hz, 2H, 3""-H, 7""-H), 6.63 (dd, J = 8.2, 1.1 Hz, 2H, 1""-H, 9""-H), 5.12 (s, 2H, 1'"-H), 5.01 (t, J = 3.0 Hz, 1H, 2"-H), 3.96 (ddd, J = 11.9, 8.9, 3.0 Hz, 1H, 6"-H_a), 3.59 (dtd, J = 11.0, 4.0, 1.4 Hz, 1H, 6"-H_e), 1.87 – 1.74 (m, 3H, 3"-H_a, 3"-H_e, 4"-H_a/4"-H_e), 1.67 – 1.51 (m, 3H, 4"-H_a/4"-H_e, 5"-H_a, 5"-H_e). ^{13}C NMR (101 MHz, CD_2Cl_2): δ (ppm) = 166.0 (C-1), 145.0 (C-9a"", C-10a""), 141.9 (C-4'), 131.7 (C-1'), 128.1 (C-2', C-6'), 127.8 (C-2"", C-8""), 127.7 (C-3', C-5'), 127.5 (C-4"", C-6""), 124.3 (C-4a"", C-5a""), 123.3 (C-3"", C-7""), 116.0 (C-1"", C-9""), 103.1 (C-2"), 63.2 (C-6"), 52.6 (C-1'"), 28.7 (C-3"), 25.6 (C-5"), 19.3 (C-4"). (ESI+): m/z calcd for [$(C_{25}H_{25}N_2O_3S)^+$] 433.1580, found 433.1584.

(±)-4-[(5,5-Dioxido-10*H*-phenothiazin-10-yl)methyl]-*N*-[(tetrahydro-2*H*-pyran-2-yl)oxy]benzamide (6b). Standard protocol 3 with 201 mg (0.550 mmol) of **5b** in 1.5 mL of anhydrous DMF, 190 µL (1.12 mmol, 2.0 equiv) of DIPEA, 355 mg (0.829 mmol, 1.5 equiv) of COMU in 1.0 mL of anhydrous DMF and 99 mg (0.85 mmol, 1.5 equiv) of NH_2OTHP in 1.0 mL of anhydrous DMF. The reaction mixture stirred for 91 hours and was extracted with CH_2Cl_2 (3 x 20 mL). Iterated flash column chromatography with CH_2Cl_2 with 2 % MeOH (R_f 0.2) and then hexanes and EtOAc (7:3, R_f 0.4) gave 137 mg (0.295 mmol, 54 %) of **6b** as a white solid. Mp: 206 °C. ^{1}H NMR (500 MHz, CD_2Cl_2): δ (ppm) = 8.91 (s, 1H, NH), 8.10 (dd, J = 7.9, 1.6 Hz, 2H, 4""-H, 6""-H), 7.74 – 7.69 (m, 2H, 2'-H, 6'-H), 7.51 (ddd, J = 8.8, 7.2, 1.7 Hz, 2H, 2""-H, 8""-H), 7.32 – 7.24 (m, 4H, 3'-H, 5'-H, 3""-H, 7""-H), 7.10 (d, J = 8.6 Hz, 2H, 1""-H, 9""-H), 5.47 (s, 2H, 1'"-H), 5.01 (t, J = 2.9 Hz, 1H, 2"-H), 3.95 (ddd, J = 12.0, 9.3, 3.0 Hz, 1H, 6"-H_a), 3.59 (dtd, J = 11.2, 4.1, 1.6 Hz, 1H, 6" H_e), 1.86 – 1.75 (m, 3H, 3"-H_a, 3"-H_e, 4"-H_a/4"-H_e), 1.67 – 1.52 (m, 3H, 4"-H_a/4"-H_e, 5"-H_a, 5"-H_e). ^{13}C NMR (126 MHz, CD_2Cl_2): δ (ppm) = 165.7 (C-1), 141.5 (C-9a"", C-10a""), 140.1 (C-4'), 133.9 (C-2"", C-8""), 132.3 (C-1'), 128.5 (C-2', C-6'), 126.9 (C-3', C-5'), 125.2 (C-4a"", C-5a""), 123.8 (C-4"", C-6""), 122.9 (C-3"", C-7""), 117.1 (C-1"", C-9""), 103.1

(C-2''), 63.2 (C-6''), 53.2 (C-1'''), 28.6 (C-3''), 25.6 (C-5''), 19.2 (C-4''). MS (ESI−): m/z calcd for [($C_{25}H_{23}N_2O_5S$)$^-$] 463.1333, found 463.1334.

(±)-4-[(1-Chloro-10*H*-phenothiazin-10-yl)methyl]-*N*-[(tetrahydro-2*H*-pyran-2-yl)oxy]benzamide (6c). Standard protocol 3 with 225 mg (0.612 mmol) of **5c** in 1.5 mL of anhydrous DMF, 210 µL (1.23 mmol, 2.0 equiv) of DIPEA, 393 mg (0.918 mmol, 1.5 equiv) of COMU in 1.0 mL of anhydrous DMF and 107 mg (0.913 mmol, 1.5 equiv) of NH_2OTHP in 1.0 mL of anhydrous DMF. The reaction mixture was stirred for 24 hours and was extracted with CH_2Cl_2 (3 x 20 mL). Iterated flash column chromatography with hexanes and EtOAc (7:3, R_f 0.2) and then 100 % CH_2Cl_2 (R_f 0.2) gave 159 mg (0.340 mmol, 56 %) of **6c** as a light pink solid. Mp: 78 - 80 °C. ^{1}H NMR (500 MHz, DMSO-d_6): δ (ppm) = 11.53 (s, 1H, NH), 7.63 – 7.57 (m, 2H, 2'-H, 6'-H), 7.47 – 7.41 (m, 2H, 3'-H, 5'-H), 7.34 (dd, J = 8.0, 1.3 Hz, 1H, 4''''-H), 7.23 (dd, J = 7.7, 1.3 Hz, 1H, 2''''-H), 7.22 (dd, J = 8.3, 1.1 Hz, 1H, 9''''-H), 7.15 (dd, J = 7.7, 1.5 Hz, 1H, 6''''-H), 7.15 (dd, J = 7.7, 1.4 Hz, 1H, 8''''-H), 7.06 (t, J = 7.8 Hz, 1H, 3''''-H), 6.95 (td, J = 7.5, 1.2 Hz, 1H, 7''''-H), 5.21 (s, 2H, 1'''-H), 4.94 (t, J = 3.0 Hz, 1H, 2''-H), 4.09 – 3.93 (m, 1H, 6''-H_a), 3.54 – 3.43 (m, 1H, 6''-H_e), 1.75 – 1.63 (m, 3H, 3''-H_a, 3''-H_e, 4''-H_a/4''-H_e), 1.59 – 1.46 (m, 3H, 4''-H_a/4''-H_e, 5''-H_a, 5''-H_e). ^{13}C NMR (126 MHz, DMSO-d_6): δ (ppm) = 163.8 (C-1), 145.1 (C-9a''''), 141.5 (C-4'), 140.7 (C-10a''''), 133.3 (C-1''''), 131.3 (C-1'), 129.8 (C-4''''), 128.0 (C-5a''''), 127.8 (C-3', C-5'), 127.6 (C-8''''), 127.1 (C-2', C-6'), 126.8 (C-6''''), 126.3 (C-2''''), 125.7 (C-4a''''), 125.3 (C-3''''), 124.1 (C-7''''), 121.0 (C-9''''), 100.8 (C-2''), 61.3 (C-6''), 56.6 (C-1'''), 27.8 (C-3''), 24.7 (C-5''), 18.2 (C-4''). MS (ESI−): m/z calcd for [($C_{25}H_{22}ClN_2O_3S$)$^-$] 465.1045, found 465.1046.

(±)-*N*-[(Tetrahydro-2*H*-pyran-2-yl)oxy]-4-{[2-(trifluoromethyl)-10*H*-phenothiazin-10-yl]methyl}benzamide (6d). Standard protocol 3 with 233 mg (0.580 mmol) of **5d** in 1.5 mL of

anhydrous DMF, 200 µL (1.18 mmol, 2.0 equiv) of DIPEA, 373 mg (0.871 mmol, 1.5 equiv) of COMU in 1.0 mL of anhydrous DMF and 103 mg (0.879 mmol, 1.5 equiv) of NH_2OTHP in 1.0 mL of anhydrous DMF. Reaction mixture was stirred for 48 hours and was extracted with CH_2Cl_2 (3 x 20 mL). Flash column chromatography with *n*-pentane and EtOAc (3:2, R_f 0.3) gave 195 mg (0.390 mmol, 67 %) of **6d** as a pale pink solid. Mp: 80 - 82 °C. ^{1}H NMR (500 MHz, CD_2Cl_2): δ (ppm) = 8.99 (s, 1H, NH), 7.73 – 7.68 (m, 2H, 2'-H, 6'-H), 7.45 – 7.40 (m, 2H, 3'-H, 5'-H), 7.22 (d, J = 8.0 Hz, 1H, 4""-H), 7.14 (dd, J = 8.0, 1.7 Hz, 1H, 3""-H), 7.11 (dd, J = 7.6, 1.5 Hz, 1H, 6""-H), 7.02 (td, J = 7.8, 1.6 Hz, 1H, 8""-H), 6.92 (td, J = 7.5, 1.1 Hz, 1H, 7""-H), 6.84 (d, J = 1.7 Hz, 1H, 1""-H), 6.66 (dd, J = 8.2, 1.1 Hz, 1H, 9""-H), 5.14 (s, 2H, 1'"-H), 5.01 (t, J = 3.0 Hz, 1H, 2"-H), 3.96 (ddd, J = 11.9, 9.2, 3.0 Hz, 1H, 6"-H_a), 3.59 (dtd, J = 11.1, 4.1, 1.6 Hz, 1H, 6"-H_b), 1.87 – 1.77 (m, 3H, 3"-H_a, 3"-H_e, 4"-H_a/4"-H_e), 1.64 – 1.52 (m, 3H, 4"-H_a/4"-H_e, 5"-H_a, 5"-H_e). ^{13}C NMR (126 MHz, CD_2Cl_2): δ (ppm) = 165.9 (C-1), 145.6 (C-10a""), 144.2 (C-9a""), 141.1 (C-4'), 131.9 (C-1'), 129.9 (q, ^2J = 32.3 Hz, C-2""), 129.7 (C-4a""), 128.2 (C-8""), 128.2 (C-2', C-6'), 127.7 (C-4""), 127.6 (C-6""), 127.6 (C-3', C-5'), 124.6 (q, ^1J = 272.0 Hz, CF_3), 123.9 (C-7""), 123.5 (C-5a""), 119.9 (q, ^3J = 3.9 Hz, C-3""), 116.5 (C-9""), 112.3 (q, ^3J = 3.9 Hz, C-1""), 103.2 (C-2"), 63.2 (C-6"), 52.7 (C-1'"), 28.7 (C-3"), 25.6 (C-5"), 19.3 (C-4"). MS (ESI+): m/z calcd for [($C_{26}H_{24}F_3N_2O_3S$)$^+$] 501.1454, found 501.1457.

4-[(5,5-Dioxido-10*H*-phenothiazin-10-yl)methyl]-*N*-hydroxybenzamide (7b). Standard protocol 4 with 95 mg (0.20 mmol) of **6b** in 2.0 mL of CH_2Cl_2 and 260 µL (1.04 mmol, 5.2 equiv) of HCl (4 M) in 1,4-dioxane. The reaction mixture was stirred for 30 minutes. Precipitation yielded 50 mg (0.13 mmol, 66 %) of **7b** as a beige solid. Mp: 94 - 95 °C. ^{1}H NMR (400 MHz, DMSO-d_6): δ (ppm) = 11.16 (s, 1H, NHOH), 9.02 (s, 1H, NHOH), 8.05 (dd, J = 7.9, 1.5 Hz, 2H, 4'"-H, 6'"-H), 7.74 – 7.68 (m, 2H, 2'-H, 6'-H), 7.65 (ddd, J = 8.7, 7.2, 1.6 Hz, 2H, 2'"-

H, 8'''-H), 7.36 (t, *J* = 7.5 Hz, 2H, 3'''-H, 7'''-H), 7.32 (d, *J* = 8.6 Hz, 2H, 1'''-H, 9'''-H), 7.26 – 7.19 (m, 2H, 3'-H, 5'-H), 5.67 (s, 2H, 1''-H). ^{13}C NMR (101 MHz, DMSO-d_6): δ (ppm) = 163.9 (C-1), 140.4 (C-9a''', C-10a'''), 139.1 (C-4'), 133.6 (C-2''', C-8'''), 131.9 (C-1'), 127.4 (C-2', C-6'), 126.1 (C-3', C-5'), 123.6 (C-4a''', C-5a'''), 122.6 (C-4''', C-6'''), 122.3 (C-3''', C-7'''), 117.2 (C-1''', C-9'''), 51.0 (C-1''). MS (ESI−): m/z calcd for [$(C_{20}H_{15}N_2O_4S)^-$] 379.0758, found 379.0765.

4-[(1-Chloro-10*H*-phenothiazin-10-yl)methyl]-*N*-hydroxybenzamide (7c). Standard protocol 4 with 62 mg (0.13 mmol) of **6c** in 2.0 mL of CH_2Cl_2 and 0.17 mL (0.68 mmol, 5.2 equiv) of HCl (4 M) in 1,4-dioxane. No precipitate was obtained. Flash column chromatography of the crude residue with 100 % MeOH on RP_{18} silica gel yielded 23 mg (60 µmol, 46 %) of **7c** as a beige solid. Mp: 75 – 77 °C. ^{1}H NMR (500 MHz, DMSO-d_6): δ (ppm) = 11.09 (s, 1H, NHO<u>H</u>), 8.95 (s, 1H, N<u>H</u>OH), 7.63 – 7.53 (m, 2H, 2'-H, 6'-H), 7.47 – 7.39 (m, 2H, 3'-H, 5'-H), 7.34 (dd, *J* = 8.0, 1.3 Hz, 1H, 4'''-H), 7.23 (dd, *J* = 5.0, 1.3 Hz, 1H, 2'''-H), 7.22 (dd, *J* = 5.8, 1.2 Hz, 1H, 9'''-H), 7.19 – 7.12 (m, 2H, 6'''-H, 8'''-H), 7.06 (t, *J* = 7.8 Hz, 1H, 3'''-H), 6.95 (td, *J* = 7.5, 1.2 Hz, 1H, 7'''-H), 5.21 (s, 2H, 1''-H). ^{13}C NMR (126 MHz, DMSO-d_6): δ (ppm) = 163.9 (C-1), 145.2 (C-9a'''), 141.1 (C-4'), 140.7 (C-10a'''), 133.3 (C-1'''), 131.8 (C-1'), 129.8 (C-4'''), 128.0 (C-5a'''), 127.8 (C-3', C-5'), 127.6 (C-6'''/ C-8'''), 126.9 (C-8'''/ C-6'''), 126.8 (C-2', C-6'), 126.3 (C-2'''), 125.7 (C-4a'''), 125.3 (C-3'''), 124.0 (C-7'''), 121.0 (C-9'''), 56.5 (C-1''). MS (ESI+): m/z calcd for [$(C_{20}H_{16}ClN_2O_2S)^+$] 383.0616, found 383.0617.

***N*-Hydroxy-4-{[2-(trifluoromethyl)-10*H*-phenothiazin-10-yl]methyl}benzamide (7d).** Standard protocol 4 with 153 mg (0.306 mmol) of **6d** in 1.5 mL of CH_2Cl_2 and 400 µL (1.60 mmol, 5.2 equiv) of HCl (4 M) in 1,4-dioxane. No precipitate was obtained. Flash column chromatography of the crude residue with 100 % MeOH on RP_{18} silica gel yielded 20 mg (48 µmol, 16 %) of **7d** as a beige solid. Mp: 91 – 93 °C. ^{1}H NMR (400 MHz, DMSO-d_6): δ (ppm) =

11.16 (s, 1H, NHOH), 8.99 (s, 1H, NHOH), 7.75 – 7.65 (m, 2H, 2'-H, 6'-H), 7.48 – 7.39 (m, 2H, 3'-H, 5'-H), 7.37 (d, J = 8.0 Hz, 1H, 4'''-H), 7.24 (d, J = 8.1 Hz, 1H, 3'''-H), 7.19 (d, J = 7.5 Hz, 1H, 6'''-H), 7.12 (t, J = 7.7 Hz, 1H, 8'''-H), 7.01 (s, 1H, 1'''-H), 6.97 (t, J = 7.5 Hz, 1H, 7'''-H), 6.85 (d, J = 8.2 Hz, 1H, 9'''-H), 5.26 (s, 2H, 1''-H). ^{13}C NMR (126 MHz, DMSO-d_6): δ (ppm) = 163.9 (C-1), 144.8 (C-10a'''), 143.5 (C-9a'''), 139.9 (C-4'), 131.6 (C-1'), 128.6 (C-4a'''), 128.1 (q, ^2J = 31.9 Hz, C-2'''), 128.0 (C-8'''), 127.5 (C-4'''), 127.2 (C-2', C-6'), 127.1 (C-6'''), 126.8 (C-3', C-5'), 123.4 (C-7'''), 122.9 (q, ^1J = 272.2 Hz, CF_3), 121.8 (C-5a'''), 119.2 (q, ^3J = 3.9 Hz, C-3'''), 116.4 (C-9'''), 112.0 (q, ^3J = 3.8 Hz, C-1'''), 50.7 (C-1''). MS (ESI−): m/z calcd for $[(C_{21}H_{14}F_3N_2O_2S)^-]$ 415.0734, found 415.0736.

***N*-Hydroxy-4-[(5-oxido-10*H*-phenothiazin-10-yl)methyl]benzamide (7e).** Standard protocol 5 with 198 mg (0.567 mmol) of **5e** in 1.9 mL of anhydrous DMF, 190 µL (1.12 mmol, 2.0 equiv) of DIPEA, 369 mg (0.862 mmol, 1.5 equiv) of COMU in 0.6 mL of anhydrous DMF, and 119 mg (1.71 mmol. 3.0 equiv) of hydroxylamine hydrochloride in 0.6 mL of anhydrous DMF. The reaction mixture was stirred for 17 hours. Flash column chromatography (work-up B) with CH_2Cl_2 with 6 % MeOH and 0.1 % HOAc (R_f 0.2) was performed. After evaporation of the collected fractions the residue was washed with water, filtered off and dried at 50 °C in a drying oven to yield 104 mg (0.285 mmol, 50 %) of **7e** as a white solid. Mp: 212 - 213 °C. ^{1}H NMR (500 MHz, DMSO-d_6): δ (ppm) = 11.16 (s, 1H, NHOH), 9.02 (s, 1H, NHOH), 8.02 (dd, J = 7.7, 1.6 Hz, 2H, 4'''-H, 6'''-H), 7.74 – 7.63 (m, 2H, 2'-H, 6'-H), 7.60 (ddd, J = 8.7, 7.1, 1.6 Hz, 2H, 2'''-H, 8'''-H), 7.34 (d, J = 8.6 Hz, 2H, 1'''-H, 9'''-H), 7.30 (t, J = 7.4 Hz, 2H, 3'''-H, 7'''-H), 7.23 – 7.16 (m, 2H, 3'-H, 5'-H), 5.72 (s, 2H, 1''-H). ^{13}C NMR (126 MHz, DMSO-d_6): δ (ppm) = 163.9 (C-1), 139.4 (C-4'), 138.3 (C-9a''', C-10a'''), 133.0 (C-2''', C-8'''), 131.8 (C-1'), 131.1 (C-4''', C-6'''),

127.4 (C-2', C-6'), 126.1 (C-3', C-5'), 124.3 (C-4a''', C-5a'''), 122.1 (C-3''', C-7'''), 116.7 (C-1''', C-9'''), 50.5 (C-1''). MS (ESI−): m/z calcd for $[(C_{20}H_{15}N_2O_3S)^-]$ 363.0809, found 363.0808.

4-[(2-Chloro-10*H*-phenothiazin-10-yl)methyl]-*N*-hydroxybenzamide (7f). Standard protocol 5 with 202 mg (0.549 mmol) of **5f** in 0.5 mL of anhydrous DMF, 190 µL (1.12 mmol, 2.0 equiv) of DIPEA, 355 mg (0.829 mmol, 1.5 equiv) of COMU in 0.5 mL of anhydrous DMF, and 115 mg (1.65 mmol, 3.0 equiv) of hydroxylamine hydrochloride in 1.0 mL of anhydrous DMF. The reaction mixture was stirred for 42 hours. Following work-up A the reaction mixture was extracted with EtOAc (3 x 50 mL) prior to flash column chromatography with CH_2Cl_2 with 1 % MeOH and 0.1 % HOAc (R_f 0.2). The collected fractions were evaporated and the residue was dissolved in CH_2Cl_2 and washed with water. Evaporation of CH_2Cl_2 yielded 93 mg (0.24 mmol, 44 %) of **7f** as a beige solid. Mp: 168 – 169 °C. ^{1}H NMR (400 MHz, DMSO-d_6): δ (ppm) = 11.15 (s, 1H, NHO<u>H</u>), 9.00 (s, 1H, N<u>H</u>OH), 7.79 – 7.63 (m, 2H, 2'-H, 6'-H), 7.48 – 7.31 (m, 2H, 3'-H, 5'-H), 7.17 (d, J = 8.1 Hz, 1H, 4'''-H), 7.16 (d, J = 7.7 Hz, 1H, 6'''-H), 7.09 (td, J = 7.8, 1.5 Hz, 1H, 8'''-H), 6.97 (dd, J = 8.2, 1.8 Hz, 1H, 3'''-H), 6.93 (td, J = 7.4, 1.0 Hz, 1H, 7'''-H), 6.81 (d, J = 2.1 Hz, 1H, 1'''-H), 6.80 (dd, J = 7.8, 1.0 Hz, 1H, 9'''-H), 5.20 (s, 2H, 1''-H). ^{13}C NMR (126 MHz, DMSO-d_6): δ (ppm) = 164.0 (C-1), 145.6 (C-10a'''), 143.5 (C-9a'''), 139.9 (C-4'), 132.2 (C-2'''), 131.7 (C-1'), 127.9 (C-4'''), 127.7 (C-8'''), 127.3 (C-2', C-6'), 127.0 (C-6'''), 126.7 (C-3', C-5'), 123.2 (C-7'''), 122.4 (C-5a'''), 122.3 (C-3'''), 121.8 (C-4a'''), 116.3 (C-9'''), 115.8 (C-1'''), 50.7 (C-1''). MS (ESI−): m/z calcd for $[(C_{20}H_{14}ClN_2O_2S)^-]$ 381.0470, found 381.0474.

***N*-Hydroxy-4-[(2-methoxy-10*H*-phenothiazin-10-yl)methyl]benzamide (7g).** Standard protocol 5 with 175 mg (0.482 mmol) of **5g** in 0.5 mL of anhydrous DMF, 160 µL (0.941 mmol, 2.0 equiv) of DIPEA, 302 mg (0.705 mmol, 1.5 equiv) of COMU in 0.5 mL of anhydrous DMF, and 101 mg (1.45 mmol, 3.0 equiv) of hydroxylamine hydrochloride in 0.5 mL of anhydrous

DMF. The reaction mixture was stirred for 3 hours. Following work-up A the reaction mixture was extracted with water (3 x 50 mL) prior to flash column chromatography with CH_2Cl_2 with 1 % MeOH and 0.1 % HOAc (R_f 0.1). The collected fractions were evaporated and the residue was dissolved in CH_2Cl_2 and precipitated with *n*-pentane. Filtration yielded 87 mg (0.23 mmol, 48 %) of **7g** as a grey solid. Mp: 150 - 151 °C. ^{1}H NMR (400 MHz, DMSO-d_6): δ (ppm) = 11.14 (bs, 1H, NHOH), 9.00 (bs, 1H, NHOH), 7.76 – 7.62 (m, 2H, 2'-H, 6'-H), 7.47 – 7.33 (m, 2H, 3'-H, 5'-H), 7.15 (dd, J = 7.5, 1.1 Hz, 1H, 6'''-H), 7.07 (td, J = 7.8, 1.1 Hz, 1H, 8'''-H), 7.05 (d, J = 8.4 Hz, 1H, 4'''-H), 6.91 (t, J = 7.4 Hz, 1H, 7'''-H), 6.80 (d, J = 8.1 Hz, 1H, 9'''-H), 6.53 (dd, J = 8.4, 2.3 Hz, 1H, 3'''-H), 6.36 (d, J = 2.4 Hz, 1H, 1'''-H), 5.18 (s, 2H, 1''-H), 3.61 (s, 3H, OCH_3). ^{13}C NMR (101 MHz, DMSO-d_6): δ (ppm) = 164.0 (C-1), 159.3 (C-2'''), 145.5 (C-10a'''), 144.0 (C-9a'''), 140.4 (C-4'), 131.6 (C-1'), 127.4 (C-8'''), 127.2 (C-4'''), 127.2 (C-2', C-6'), 126.8 (C-6'''), 126.7 (C-3', C-5'), 123.4 (C-5a'''), 122.7 (C-7'''), 115.9 (C-9'''), 113.4 (C-4a'''), 107.3 (C-3'''), 103.6 (C-1'''), 55.1 (OCH_3), 50.7 (C-1''). MS (ESI−): m/z calcd for [$(C_{21}H_{17}N_2O_3S)^-$] 377.0965, found 377.0969.

4-{[2-(Ethylthio)-10*H*-phenothiazin-10-yl]methyl}-*N*-hydroxybenzamide (7h). Standard protocol 5 with 202 mg (0.513 mmol) of **5h** in 0.5 mL of anhydrous DMF, 170 µL (1.00 mmol, 1.9 equiv) of DIPEA, 336 mg (0.785 mmol, 1.5 equiv) of COMU in 0.5 mL of anhydrous DMF, and 108 mg (1.55 mmol, 3.0 equiv) of hydroxylamine hydrochloride in 0.5 mL of anhydrous DMF. The reaction mixture was stirred for 34 hours. Following work-up A the reaction mixture was extracted with EtOAc (3 x 50 mL) prior to flash column chromatography with CH_2Cl_2 with 2 % MeOH and 0.1 % HOAc (R_f 0.3). The collected fractions were evaporated and the residue was dissolved in CH_2Cl_2 and washed with water. Evaporation of CH_2Cl_2 gave 114 mg (0.279 mmol, 54 %) of **7h** as a beige solid foam. Mp: 78 °C. ^{1}H NMR (500 MHz, DMSO-d_6): δ (ppm) =

11.15 (s, 1H, NHOH), 9.00 (s, 1H, NHOH), 7.73 – 7.68 (m, 2H, 2'-H, 6'-H), 7.42 – 7.37 (m, 2H, 3'-H, 5'-H), 7.16 (dd, J = 7.6, 1.5 Hz, 1H, 6'''-H), 7.10 (td, J = 7.8, 1.5 Hz, 1H, 8'''-H), 7.08 (d, J = 7.8 Hz, 1H, 4'''-H), 6.93 (td, J = 7.5, 1.0 Hz, 1H, 7'''-H), 6.85 (dd, J = 8.0, 1.8 Hz, 1H, 3'''-H), 6.83 (dd, J = 8.1, 1.0 Hz, 1H, 9'''-H), 6.65 (d, J = 1.8 Hz, 1H, 1'''-H), 5.20 (s, 2H, 1''-H), 2.74 (q, J = 7.3 Hz, 2H, SCH_2CH_3), 0.99 (t, J = 7.3 Hz, 3H, SCH_2CH_3). ^{13}C NMR (126 MHz, DMSO-d_6): δ (ppm) = 163.9 (C-1), 144.5 (C-10a'''), 144.1 (C-9a'''), 140.3 (C-4'), 135.4 (C-2'''), 131.5 (C-1'), 127.6 (C-8'''), 127.2 (C-2', C-6'), 127.1 (C-4'''), 126.9 (C-6'''), 126.7 (C-3', C-5'), 122.9 (C-7'''), 122.8 (C-5a'''), 122.5 (C-3'''), 120.0 (C-4a'''), 116.0 (C-9'''), 115.6 (C-1'''), 50.7 (C-1''), 26.3 (SCH_2CH_3), 14.1 (SCH_2CH_3). MS (ESI−): m/z calcd for [$(C_{22}H_{19}N_2O_2S_2)^-$] 407,0893 found 407.0896.

4-[(10*H*-Benzo[*b*]pyrido[2,3-*e*][1,4]thiazin-10-yl)methyl]-*N*-hydroxybenzamide (7i). Standard protocol 5 with 129 mg (0.386 mmol) of **5i** in 1.0 mL of anhydrous DMF, 130 µL (0.764 mmol, 2.0 equiv) of DIPEA, 252 mg (0.588 mmol, 1.5 equiv) of COMU in 0.5 mL of anhydrous DMF, and 81.0 mg (1.17 mmol, 3.0 equiv) of hydroxylamine hydrochloride in 0.5 mL of anhydrous DMF. The reaction mixture was stirred for 19 hours. Flash column chromatography (work-up B) with CH_2Cl_2 with 2 % MeOH and 0.1 % HOAc (R_f 0.2) was performed. After evaporation of the collected fractions the residue was washed with water, filtered off and dried at 50 °C in a drying oven to yield 56 mg (0.160 mmol, 41 %) of **7i** as a pale beige solid. Mp: 173 - 175 °C. ^{1}H NMR (500 MHz, DMSO-d_6): δ (ppm) = 11.12 (s, 1H, NHOH), 8.99 (s, 1H, NHOH), 7.93 (d, J = 4.7 Hz, 1H, 2'''-H), 7.74 – 7.60 (m, 2H, 2'-H, 6'-H), 7.49 (d, J = 7.4 Hz, 1H, 4'''-H), 7.40 – 7.27 (m, 2H, 3'-H, 5'-H), 7.10 (d, J = 7.5 Hz, 1H, 6'''-H), 7.01 (t, J = 7.7 Hz, 1H, 8'''-H), 6.94 – 6.85 (m, 2H, 3'''-H, 7'''-H), 6.69 (d, J = 8.2 Hz, 1H, 9'''-H), 5.35 (s, 2H, 1''-H). ^{13}C NMR (126 MHz, DMSO-d_6): δ (ppm) = 164.1 (C-1), 153.5 (C-10a'''), 145.2 (C-2'''),

141.7 (C-9a'''), 141.0 (C-4'), 134.6 (C-4'''), 131.2 (C-1'), 127.7 (C-8'''), 127.0 (C-2', C-6'), 126.7 (C-6'''), 126.4 (C-3', C-5'), 123.3 (C-7'''), 119.7 (C-5a'''), 118.6 (C-3'''), 116.1 (C-9'''), 115.6 (C-4a'''), 47.7 (C-1''). (ESI−): m/z calcd for [$(C_{19}H_{14}N_3O_2S)^-$] 348.0812, found 348.0812.

4-[(10*H*-Benzo[*b*]pyrido[3,4-*e*][1,4]thiazin-10-yl)methyl]-*N*-hydroxybenzamide (7j). Standard protocol 5 with 170 mg (0.508 mmol) of **5j** in 1.5 mL of anhydrous DMF, 170 µL (1.00 mmol, 2.0 equiv) of DIPEA, 334 mg (0.780 mmol, 1.5 equiv) of COMU in 0.3 mL of anhydrous DMF, and 105 mg (1.51 mmol, 3.0 equiv) of hydroxylamine hydrochloride in 0.3 mL of anhydrous DMF. The reaction mixture was stirred for 4 hours. Flash column chromatography (work-up B) with CH_2Cl_2 with 2 % MeOH and 0.1 % HOAc (R_f 0.1) was performed. After evaporation of the collected fractions the residue was washed with water, filtered off and dried at 50 °C in a drying oven to yield 96 mg (0.27 mmol, 54 %) of **7j** as a pale beige solid. Mp: 174 - 175 °C. ^{1}H NMR (400 MHz, DMSO-d_6): δ (ppm) = 11.17 (s, 1H, NHOH), 9.02 (s, 1H, NHOH), 8.02 (d, J = 4.8 Hz, 1H, 3'''-H), 7.88 (s, 1H, 1'''-H), 7.77 – 7.65 (m, 2H, 2'-H, 6'-H), 7.45 – 7.32 (m, 2H, 3'-H, 5'-H), 7.18 (d, J = 4.8 Hz, 1H, 4'''-H), 7.14 (d, J = 7.4 Hz, 1H, 6'''-H), 7.10 (t, J = 7.7 Hz, 1H, 8'''-H), 6.95 (t, J = 7.5 Hz, 1H, 7'''-H), 6.80 (d, J = 8.1 Hz, 1H, 9'''-H), 5.23 (s, 2H, 1''-H). ^{13}C NMR (101 MHz, DMSO-d_6): δ (ppm) = 164.0 (C-1), 143.4 (C-3'''), 143.3 (C-9a'''), 139.7 (C-4'), 139.6 (C-10a'''), 135.9 (C-1'''), 133.1 (C-4a'''), 131.7 (C-1'), 128.2 (C-8'''), 127.3 (C-2', C-6'), 127.1 (C-6'''), 126.6 (C-3', C-5'), 123.2 (C-7'''), 121.1 (C-4'''), 120.2 (C-5a'''), 116.1 (C-9'''), 50.3 (C-1''). MS (ESI+): m/z calcd for [$(C_{19}H_{16}N_3O_2S)^+$] 350.0958, found 350.0958.

4-[(10*H*-Benzo[*b*]pyrazino[2,3-*e*][1,4]thiazin-10-yl)methyl]-*N*-hydroxybenzamide (7k). Standard protocol 5 with 249 mg (0.742 mmol) of **5k** in 2.5 mL of anhydrous DMF, 250 µL (1.47 mmol, 2.0 equiv) of DIPEA, 470 mg (1.10 mmol, 1.5 equiv) of COMU in 0.5 mL of anhydrous DMF, and 153 mg (2.20 mmol, 3.0 equiv) of hydroxylamine hydrochloride in 0.5 mL

of anhydrous DMF. The reaction mixture was stirred for 13 hours. Flash column chromatography (work-up B) with CH_2Cl_2 with 2 % MeOH and 0.1 % HOAc (R_f 0.2) was performed. After evaporation of the collected fractions the residue was washed with water, filtered off and dried in high vacuum to yield 100 mg (0.285 mmol, 38 %) of **7k** as a pale yellow solid. Mp: 170 - 171 °C. ^{1}H NMR (500 MHz, DMSO-d_6): δ (ppm) = 11.14 (s, 1H, NHOH), 9.00 (s, 1H, NHOH), 7.81 (d, J = 2.2 Hz, 1H, 3'''-H), 7.78 (d, J = 2.2 Hz, 1H, 2'''-H), 7.71 – 7.65 (m, 2H, 2'-H, 6'-H), 7.36 – 7.30 (m, 2H, 3'-H, 5'-H), 7.08 (d, J = 7.3 Hz, 1H, 6'''-H), 7.01 (t, J = 7.7 Hz, 1H, 8'''-H), 6.90 (t, J = 7.4 Hz, 1H, 7'''-H), 6.63 (d, J = 8.1 Hz, 1H, 9'''-H), 5.25 (s, 2H, 1''-H). ^{13}C NMR (126 MHz, DMSO-d_6): δ (ppm) = 164.1 (C-1), 149.3 (C-10a'''), 141.2 (C-4a'''), 139.9 (C-4'), 139.4 (C-9a'''), 138.8 (C-2'''), 136.7 (C-3'''), 131.4 (C-1'), 128.1 (C-8'''), 127.1 (C-2', C-6'), 126.8 (C-6'''), 126.3 (C-3', C-5'), 123.6 (C-7'''), 118.4 (C-5a'''), 116.3 (C-9'''), 47.7 (C-1''). MS (ESI−): m/z calcd for [$(C_{18}H_{13}N_4O_2S)^-$] 349.0765, found 349.0769.

4-[(10*H*-Dipyrido[2,3-*b*:2',3'-*e*][1,4]thiazin-10-yl)methyl]-*N*-hydroxybenzamide (7l). Standard protocol 5 with 191 mg (0.570 mmol) of **5l** in 1.0 mL of anhydrous DMF, 190 µL (1.12 mmol, 2.0 equiv) of DIPEA, 375 mg (0.876 mmol, 1.5 equiv) of COMU in 0.6 mL of anhydrous DMF, and 120 mg (1.73 mmol, 3.0 equiv) of hydroxylamine hydrochloride in 0.6 mL of anhydrous DMF. The reaction mixture was stirred for 26 hours. Flash column chromatography (work-up B) with CH_2Cl_2 with 2 % MeOH and 0.1 % HOAc (R_f 0.1) was performed. After evaporation of the collected fractions the residue was washed with water, filtered off and dried at 50 °C in a drying oven to yield 116 mg (0.331 mmol, 58 %) of **7l** as a beige solid. Mp: 167 - 168 °C. ^{1}H NMR (400 MHz, DMSO-d_6): δ (ppm) = 11.13 (s, 1H, NHOH), 8.99 (s, 1H, NHOH), 7.90 (d, J = 4.5 Hz, 1H, 2'''-H), 7.88 (d, J = 4.5 Hz, 1H, 7'''-H), 7.72 – 7.65 (m, 2H, 2'-H, 6'-H), 7.48 (d, J = 7.3 Hz, 1H, 4'''-H), 7.36 – 7.28 (m, 2H, 3'-H, 5'-H), 6.97 (dd, J = 8.0, 4.6 Hz, 1H, 8'''-H),

6.89 (dd, J = 7.2, 4.9 Hz, 1H, 3'''-H), 6.85 (d, J = 8.2 Hz, 1H, 9'''-H), 5.29 (s, 2H, 1''-H). ^{13}C NMR (101 MHz, DMSO-d_6): δ (ppm) = 164.1 (C-1), 151.5 (C-10a'''), 145.3 (C-2'''), 142.9 (C-5a'''), 142.6 (C-7'''), 140.1 (C-4'), 137.6 (C-9a'''), 134.8 (C-4'''), 131.4 (C-1'), 127.1 (C-2', C-6'), 126.3 (C-3', C-5'), 122.4 (C-8'''), 121.7 (C-9'''), 118.8 (C-3'''), 115.1 (C-4a'''), 47.3 (C-1''). MS (ESI−): m/z calcd for [$(C_{18}H_{13}N_4O_2S)^-$] 349.0765, found 349.0766.

4-[(10*H*-Dipyrido[3,4-*b*:3',4'-*e*][1,4]thiazin-10-yl)methyl]-*N*-hydroxybenzamide (7m). Standard protocol 5 with 139 mg (0.414 mmol) of **5m** in 1.6 mL of anhydrous DMF, 140 µL (0.823 mmol, 2.0 eqiv) of DIPEA, 263 mg (0.614 mmol, 1.5 equiv) of COMU in 0.5 mL of anhydrous DMF, and 87.0 mg (1.25 mmol, 3.0 equiv) of hydroxylamine hydrochloride in 0.6 mL of anhydrous DMF. The reaction mixture was stirred for 69 hours. Flash column chromatography (work-up B) with CH_2Cl_2 with 3 % MeOH and 0.1 % HOAc (R_f 0.2) was performed. After evaporation of the collected fractions the residue was washed with diethyl ether, filtered off and dried at 50 °C in a drying oven to yield 87 mg (0.248 mmol, 60 %) of **7m** as a white solid. Mp: 180 - 181 °C. ^{1}H NMR (500 MHz, DMSO-d_6): δ (ppm) = 11.18 (bs, 1H, NHO<u>H</u>), 9.03 (bs, 1H, N<u>H</u>OH), 8.12 (d, J = 5.7 Hz, 1H, 8'''-H), 8.12 (s, 1H, 6'''-H), 8.05 (d, J = 4.9 Hz, 1H, 3'''-H), 7.85 (s, 1H, 1'''-H), 7.78 – 7.69 (m, 2H, 2'-H, 6'-H), 7.41 – 7.32 (m, 2H, 3'-H, 5'-H), 7.20 (d, J = 4.9 Hz, 1H, 4'''-H), 6.66 (d, J = 5.6 Hz, 1H, 9'''-H), 5.25 (s, 2H, 1''-H). ^{13}C NMR (126 MHz, DMSO-d_6): δ (ppm) = 163.9 (C-1), 149.7 (C-9a'''), 149.6 (C-8'''), 146.3 (C-6'''), 144.4 (C-3'''), 138.5 (C-4'), 137.7 (C-10a'''), 136.1 (C-1'''), 132.0 (C-4a'''), 131.9 (C-1'), 127.4 (C-2', C-6'), 126.4 (C-3', C-5'), 121.6 (C-4'''), 116.0 (C-5a'''), 110.1 (C-9'''), 49.7 (C-1''). MS (ESI+): m/z calcd for [$(C_{18}H_{15}N_4O_2S)^+$] 351.0910, found 351.0911.

4-[(5*H*-Dipyrido[2,3-*b*:4',3'-*e*][1,4]thiazin-5-yl)methyl]-*N*-hydroxybenzamide (7n). Standard protocol 5 with 206 mg (0.614 mmol) of **5n** in 1.9 mL of anhydrous DMF, 210 µL (1.23 mmol,

2.0 equiv) of DIPEA, 393 mg (0.918 mmol, 1.5 equiv) of COMU in 0.6 mL of anhydrous DMF, and 128 mg (1.84 mmol, 3.0 equiv) of hydroxylamine hydrochloride in 0.6 mL of anhydrous DMF. The reaction mixture was stirred for 70 hours. Flash column chromatography (work-up B) with CH_2Cl_2 with 8 % MeOH and 0.1 % HOAc (R_f 0.3) was performed. After evaporation of the collected fractions the residue was washed with water, filtered off and dried at 50 °C in a drying oven to yield 98 mg (0.280 mmol, 46 %) of **7n** as a pale yellow solid. Mp: 213 - 215 °C. ^{1}H NMR (400 MHz, DMSO-d_6): δ (ppm) = 11.20 (s, 1H, NHOH), 9.04 (bs, 1H, NHOH), 8.18 (bs, 1H, 4'''-H), 8.13 (bs, 1H, 2'''-H), 7.99 (dd, J = 4.7, 1.2 Hz, 1H, 7'''-H), 7.77 – 7.70 (m, 2H, 2'-H, 6'-H), 7.37 – 7.30 (m, 2H, 3'-H, 5'-H), 7.07 (dd, J = 8.3, 4.7 Hz, 1H, 8'''-H), 6.97 (dd, J = 8.3, 1.2 Hz, 1H, 9'''-H), 6.64 (d, J = 5.7 Hz, 1H, 1'''-H), 5.18 (s, 2H, 1''-H). ^{13}C NMR (101 MHz, DMSO-d_6): δ (ppm) = 163.8 (C-1), 149.6 (C-10a'''), 147.6 (C-2'''), 144.3 (C-4'''), 143.8 (C-7'''), 143.7 (C-5a'''), 138.1 (C-4'), 137.4 (C-9a'''), 131.9 (C-1'), 127.4 (C-2', C-6'), 126.3 (C-3', C-5'), 122.7 (C-8'''), 122.4 (C-9'''), 117.6 (C-4a'''), 109.8 (C-1'''), 50.1 (C-1''). MS (ESI−): m/z calcd for $[(C_{18}H_{13}N_4O_2S)^-]$ 349.0765, found 349.0763.

***N*-Hydroxy-4-[(2-methyl-4*H*-benzo[*b*]thiazolo[4,5-*e*][1,4]thiazin-4-yl)methyl]benzamide (7o).** Standard protocol 5 with 137 mg (0.387 mmol) of **5o** in 1.0 mL of anhydrous DMF and 130 µL (0.764 mmol, 2.0 equiv) of DIPEA, 245 mg (0.572 mmol, 1.5 equiv) of COMU in 0.5 mL of anhydrous DMF, and 81.0 mg (1.17 mmol, 3.0 equiv) of hydroxylamine hydrochloride in 0.5 mL of anhydrous DMF. The reaction mixture was stirred for 25 hours. Flash column chromatography (work-up B) with CH_2Cl_2 with 1 % MeOH and 0.1 % HOAc (R_f 0.1) was performed. After evaporation of the collected fractions the residue was washed with water, filtered off and dried at 50 °C in a drying oven to yield 62 mg (0.17 mmol, 43 %) of **7o** as a tan solid. Mp: 167 - 169 °C. ^{1}H NMR (400 MHz, DMSO-d_6): δ (ppm) = 11.14 (s, 1H, NHOH), 8.99

(s, 1H, NHOH), 7.73 – 7.66 (m, 2H, 2'-H, 6'-H), 7.43 – 7.37 (m, 2H, 3'-H, 5'-H), 7.02 – 6.94 (m, 2H, 6'''-H, 8'''-H), 6.82 (td, *J* = 7.5, 1.1 Hz, 1H, 7'''-H), 6.61 (dd, *J* = 8.1, 1.1 Hz, 1H, 5'''-H), 5.21 (s, 2H, 1''-H), 2.52 (s, 3H, CH_3). ^{13}C NMR (101 MHz, DMSO-d_6): δ (ppm) = 164.1 (C-1), 163.3 (C-2'''), 151.8 (C-3a'''), 143.0 (C-4a'''), 141.1 (C-4'), 131.5 (C-1'), 128.0 (C-6'''/C-8'''), 127.1 (C-2', C-6'), 127.1 (C-8'''/C-6'''), 126.4 (C-3', C-5'), 122.9 (C-7'''), 118.4 (C-8a'''), 114.9 (C-5'''), 94.7 (C-9a'''), 49.2 (C-1''), 19.3 (CH_3). MS (ESI−): m/z calcd for [$(C_{18}H_{14}N_3O_2S_2)^-$] 368.0533, found 368.0534.

4-[(10*H*-Benzo[*b*]pyridazino[3,4-*e*][1,4]thiazin-10-yl)methyl]-*N*-hydroxybenzamide (7p). Standard protocol 5 with 327 mg (0.978 mmol) of **5p** in 1.5 mL of anhydrous DMF, 330 µL (1.94 mmol, 2.0 equiv) of DIPEA, 629 mg (1.47 mmol, 1.5 equiv) of COMU in 1.0 mL of anhydrous DMF, and 207 mg (2.98 mmol, 3.0 equiv) of hydroxylamine hydrochloride in 1.0 mL of anhydrous DMF. The reaction mixture was stirred for 2 hours. Flash column chromatography (work-up B) with CH_2Cl_2 with 6 % MeOH and 0.1 % HOAc (R_f 0.3) was performed. After evaporation of the collected fractions the residue was washed with water, filtered off and dried at 40 °C in a drying oven to yield 127 mg (0.362 mmol, 37 %) of **7p** as a pale yellow solid. Mp: 165 - 166 °C. ^{1}H NMR (500 MHz, DMSO-d_6): δ (ppm) = 11.15 (s, 1H, NHOH), 8.99 (s, 1H, NHOH), 8.51 (d, *J* = 5.0 Hz, 1H, 3'''-H), 7.71 – 7.66 (m, 2H, 2'-H, 6'-H), 7.36 (d, *J* = 4.9 Hz, 1H, 4'''-H), 7.35 – 7.32 (m, 2H, 3'-H, 5'-H), 7.12 (dd, *J* = 7.7, 1.5 Hz, 1H, 6'''-H), 7.06 (ddd, *J* = 8.5, 7.6, 1.5 Hz, 1H, 8'''-H), 6.92 (td, *J* = 7.5, 1.0 Hz, 1H, 7'''-H), 6.72 (dd, *J* = 8.3, 1.1 Hz, 1H, 9'''-H), 5.41 (s, 2H, 1''-H). ^{13}C NMR (126 MHz, DMSO-d_6): δ (ppm) = 164.1 (C-1), 154.6 (C-10a'''), 147.3 (C-3'''), 140.3 (C-9a'''), 140.2 (C-4'), 131.3 (C-1'), 128.4 (C-8'''), 127.1 (C-2', C-6'), 126.8 (C-6'''), 126.4 (C-3', C-5'), 126.3 (C-4a'''), 123.7 (C-4'''), 123.6 (C-7'''), 117.4 (C-5a'''), 116.6 (C-9'''), 48.3 (C-1''). MS (ESI+): m/z calcd for [$(C_{18}H_{15}N_4O_2S)^+$] 351.0910, found 351.0910.

4-[(3-Chloro-10*H*-benzo[*b*]pyridazino[3,4-*e*][1,4]thiazin-10-yl)methyl]-*N*-hydroxybenzamide (7q). Standard protocol 5 with 199 mg (0.538 mmol) of **5q** in 2.0 mL of anhydrous DMF, 180 µL (1.06 mmol, 2.0 equiv) of DIPEA, 353 mg (0.824 mmol, 1.5 equiv) of COMU in 0.5 mL of anhydrous DMF, 114 mg (1.64 mmol, 3.0 equiv) of hydroxylamine hydrochloride in 0.5 mL of anhydrous DMF. The reaction mixture was stirred for 18 hours. Flash column chromatography (work-up B) with CH_2Cl_2 with 5 % MeOH and 0.1 % HOAc (R_f 0.3) was performed. After evaporation of the collected fractions the residue was washed with water, filtered off and dried in high vacuum to yield 87 mg (0.23 mmol, 42 %) of **7q** as a yellow solid. Mp: 180 - 182 °C. ^{1}H NMR (400 MHz, DMSO-d_6): δ (ppm) = 11.16 (s, 1H, NHO<u>H</u>), 9.00 (bs, 1H, N<u>H</u>OH), 7.73 – 7.66 (m, 2H, 2'-H, 6'-H), 7.58 (s, 1H, 4'''-H), 7.39 – 7.31 (m, 2H, 3'-H, 5'-H), 7.12 (dd, J = 7.6, 1.5 Hz, 1H, 6'''-H), 7.06 (td, J = 7.9, 1.5 Hz, 1H, 8'''-H), 6.93 (td, J = 7.5, 0.8 Hz, 1H, 7'''-H), 6.70 (dd, J = 8.2, 0.6 Hz, 1H, 9'''-H), 5.34 (s, 2H, 1''-H). ^{13}C NMR (101 MHz, DMSO-d_6): δ (ppm) = 164.1 (C-1), 154.0 (C-10a'''), 149.9 (C-3'''), 139.7 (C-4'), 139.7 (C-9a'''), 131.4 (C-1'), 130.6 (C-4a'''), 128.6 (C-8'''), 127.1 (C-2', C-6'), 126.8 (C-6'''), 126.3 (C-3', C-5'), 123.8 (C-7'''), 123.6 (C-4'''), 116.7 (C-9'''), 116.6 (C-5a'''), 48.6 (C-1''). MS (ESI−): m/z calcd for [$(C_{18}H_{12}ClN_4O_2S)^-$] 383.0375, found 383.0375.

4-[(1*H*-Benzo[*b*]pyridazino[3,4-*e*][1,4]thiazin-1-yl)methyl]benzoic acid (9p). Standard protocol 2 with 137 mg (0.392 mmol) of **8p** in 3.0 mL of 1,4-dioxane/H_2O (1:1) and 490 µL (0.980 mmol, 2.5 equiv) of NaOH (2 M). The reaction mixture was stirred for 16 hours at 50 °C. The precipitate was collected and dried at 50 °C in a drying oven to yield 126 mg (0.376 mmol, 96 %) of **9p** as an orange-red solid. Mp: 250 °C. ^{1}H NMR (500 MHz, DMSO-d_6): δ (ppm) = 12.91 (s, 1H, COOH), 7.97 – 7.90 (m, 2H, 2'-H, 6'-H), 7.52 – 7.46 (m, 2H, 3'-H, 5'-H), 7.12 (d, J = 4.4 Hz, 1H, 4'''-H), 6.85 (td, J = 7.4, 2.0 Hz, 1H, 9'''-H), 6.73 – 6.64 (m, 2H, 7'''-H, 8'''-H), 6.57

(d, J = 7.8 Hz, 1H, 10'''-H), 6.34 (d, J = 4.4 Hz, 1H, 5'''-H), 5.03 (s, 2H, 1''-H). ^{13}C NMR (126 MHz, DMSO-d_6): δ (ppm) = 167.1 (C-1), 149.5 (C-1a'''), 143.4 (C-10a'''), 141.8 (C-4'), 138.6 (C-4'''), 134.1 (C-5a'''), 129.8 (C-1'), 129.4 (C-2', C-6'), 128.1 (C-3', C-5', C-9'''), 125.8 (C-10'''), 124.7 (C-7'''), 123.8 (C-8'''), 117.2 (C-6a'''), 116.8 (C-5'''), 54.6 (C-1''). MS (ESI+): m/z calcd for [$(C_{18}H_{14}N_3O_2S)^+$] 336.0801, found 336.0803.

4-[(3-Chloro-1*H*-benzo[*b*]pyridazino[3,4-*e*][1,4]thiazin-1-yl)methyl]benzoic acid (9q). Standard protocol 2 with 118 mg (0.307 mmol) of **8q** in 2.0 mL of 1,4-dioxane/H_2O (1:1) and 380 µL (0.760 mmol, 2.5 equiv) of NaOH (2 M). The reaction mixture was stirred for 24 hours at 60 °C. The precipitate was collected and dried at 50 °C in a drying oven to yield 86 mg (0.23 mmol, 75 %) of **9q** as an orange-red solid. Mp: 276 °C. ^{1}H NMR (400 MHz, DMSO-d_6): δ (ppm) = 12.95 (bs, 1H, COOH), 7.97 – 7.90 (m, 2H, 2'-H, 6'-H), 7.52 – 7.45 (m, 2H, 3'-H, 5'-H), 6.91 (td, J = 7.6, 1.6 Hz, 1H, 9'''-H), 6.81 (dd, J = 7.8, 1.6 Hz, 1H, 7'''-H), 6.74 (td, J = 7.5, 1.3 Hz, 1H, 8'''-H), 6.64 (dd, J = 7.9, 1.3 Hz, 1H, 10'''-H), 6.59 (s, 1H, 5'''-H), 4.99 (s, 2H, 1''-H). ^{13}C NMR (126 MHz, DMSO-d_6): δ (ppm) = 167.5 (C-1), 147.9 (C-1a'''), 142.6 (C-10a'''), 140.9 (C-4'), 138.2 (C-4'''/ C-5a'''), 137.6 (C-5a'''/ C-4'''), 130.8 (C-1'), 129.5 (C-2', C-6'), 128.4 (C-9'''), 128.0 (C-3', C-5'), 126.3 (C-10'''), 124.8 (C-7'''), 124.4 (C-8'''), 116.7 (C-5'''), 116.6 (C-6a'''), 54.6 (C-1''). MS (ESI−): m/z calcd for [$(C_{18}H_{11}ClN_3O_2S)^-$] 368.0266, found 368.0268.

4-[(1*H*-Benzo[*b*]pyridazino[3,4-*e*][1,4]thiazin-1-yl)methyl]-*N*-hydroxybenzamide (10p). Standard protocol 5 with 85 mg (0.25 mmol) of **9p** in 1.0 mL of anhydrous DMF, 80 µL (0.47 mmol, 1.9 equiv) of DIPEA, 160 mg (0.374 mmol, 1.5 equiv) of COMU in 0.5 mL of anhydrous DMF, and 53 mg (0.76 mmol, 3.0 equiv) of hydroxylamine hydrochloride in 0.5 mL of anhydrous DMF. Reaction mixture was stirred for 44 hours. Flash column chromatography (work-up B) with CH_2Cl_2 with 4 % MeOH and 0.1 % HOAc (R_f 0.3) was performed. After

evaporation of the collected fractions the residue was washed with water, filtered off and dried at 50 °C in a drying oven to yield 18 mg (51 µmol, 20 %) of **10p** as an orange-red solid. Mp: 132 - 133 °C. ^{1}H NMR (500 MHz, DMSO-d_6): δ (ppm) = 11.17 (s, 1H, NHOH), 9.02 (s, 1H, NHOH), 7.77 – 7.69 (m, 2H, 2'-H, 6'-H), 7.47 – 7.42 (m, 2H, 3'-H, 5'-H), 7.12 (d, *J* = 4.3 Hz, 1H, 4'''-H), 6.86 (ddd, *J* = 7.8, 6.9, 1.9 Hz, 1H, 9'''-H), 6.71 (dd, *J* = 7.7, 2.0 Hz, 1H, 7'''-H), 6.68 (td, *J* = 7.7, 1.2 Hz, 1H, 8'''-H), 6.58 (dd, *J* = 7.9, 1.2 Hz, 1H, 10'''-H), 6.35 (d, *J* = 4.3 Hz, 1H, 5'''-H), 5.01 (s, 2H, 1''-H). ^{13}C NMR (126 MHz, DMSO-d_6): δ (ppm) = 164.1 (C-1), 149.6 (C-1a'''), 143.4 (C-10a'''), 139.9 (C-4'), 138.6 (C-4'''), 134.0 (C-5a'''), 131.9 (C-1'), 128.1 (C-9'''), 128.1 (C-3', C-5'), 127.0 (C-2', C-6'), 125.8 (C-10'''), 124.7 (C-7'''), 123.8 (C-8'''), 117.2 (C-6a'''), 116.8 (C-5'''), 54.6 (C-1''). MS (ESI−): m/z calcd for [$(C_{18}H_{13}N_4O_2S)^-$] 349.0765, found 349.0766.

4-[(3-Chloro-1*H*-benzo[*b*]pyridazino[3,4-*e*][1,4]thiazin-1-yl)methyl]-*N*-hydroxybenzamide (10q). Standard protocol 5 with 68 mg (0.18 mmol) of **9q** in 1.7 mL of anhydrous DMF, 60 µL (0.35 mmol, 1.9 equiv) of DIPEA, 117 mg (0.273 mmol, 1.5 equiv) of COMU in 0.2 mL of anhydrous DMF, and 37 mg (0.53 mmol, 2.9 equiv) of hydroxylamine hydrochloride in 0.2 mL of anhydrous DMF. The reaction mixture was stirred for 37 hours. Flash column chromatography (work-up B) with CH_2Cl_2 with 6 % MeOH and 0.1 % HOAc (R_f 0.5) was performed. After evaporation of the collected fractions the residue was washed with water, filtered off and dried at 50 °C in a drying oven to yield 29 mg (75 µmol, 42 %) of **10q** as an orange-red solid. Mp: 176 - 177 °C. ^{1}H NMR (500 MHz, DMSO-d_6): δ (ppm) = 11.19 (s, 1H, NHOH), 9.02 (s, 1H, NHOH), 7.80 – 7.67 (m, 2H, 2'-H, 6'H), 7.52 – 7.40 (m, 2H, 3'-H, 5'-H), 6.91 (t, *J* = 7.5 Hz, 1H, 9'''-H), 6.81 (d, *J* = 7.5 Hz, 1H, 7'''-H), 6.75 (t, *J* = 7.4 Hz, 1H, 8'''-H), 6.65 (d, *J* = 7.8 Hz, 1H, 10'''-H), 6.58 (s, 1H, 5'''-H), 4.97 (s, 2H, 1''-H). ^{13}C NMR (126 MHz, DMSO-d_6): δ (ppm) = 164.0 (C-1), 147.9 (C-1a'''), 142.6 (C-10a'''), 139.4 (C-4'), 138.1 (C-4'''/ C-

5a'''), 137.5 (C-5a'''/ C-4'''), 132.0 (C-1'), 128.4 (C-9'''), 128.0 (C-3', C-5'), 127.1 (C-2', C-6'), 126.3 (C-10'''), 124.8 (C-7'''), 124.3 (C-8'''), 116.7 (C-5'''), 116.6 (C-6a'''), 54.5 (C-1''). MS (ESI−): m/z calcd for [($C_{18}H_{12}ClN_4O_2S$)$^-$] 383.0375, found 383.0377.

10-[4-(Methoxycarbonyl)benzyl]-2-methyl-10*H*-benzo[*b*]pyrido[3,4-*e*][1,4]thiazin-2-ium iodide (11j). To a solution of 602 mg (1.73 mmol) of **4j** in 30 mL of a mixture of acetone and EtOH (6.5:1) was added 540 µL (8.67 mmol, 5.0 equiv) of methyl iodide. The mixture was heated at reflux for 14 hours. Evaporation of the solvent *in vacuo* yielded 838 mg (1.71 mmol, 99 %) of **11j** as fine yellow crystals. Mp: 171 °C. ^{1}H NMR (500 MHz, DMSO-d_6): δ (ppm) = 8.35 (d, J = 6.3 Hz, 1H, 3'''-H), 8.11 (s, 1H, 1'''-H), 7.98 – 7.92 (m, 2H, 2'-H, 6'-H), 7.81 (d, J = 6.3 Hz, 1H, 4'''-H), 7.57 – 7.51 (m, 2H, 3'-H, 5'-H), 7.19 (dd, J = 7.7, 1.4 Hz, 1H, 6'''-H), 7.11 (td, J = 7.8, 1.5 Hz, 1H, 8'''-H), 7.00 (td, J = 7.5, 1.0 Hz, 1H, 7'''-H), 6.77 (dd, J = 8.3, 1.0 Hz, 1H, 9'''-H), 5.25 (s, 2H, 1''-H), 4.06 (s, 3H, CH_3), 3.83 (s, 3H, $COOCH_3$). ^{13}C NMR (126 MHz, DMSO-d_6): δ (ppm) = 165.9 (C-1), 145.1 (C-4a'''), 142.9 (C-10a'''), 140.6 (C-4'), 140.4 (C-9a'''), 138.6 (C-3'''), 129.6 (C-2', C-6'), 129.3 (C-1'''), 129.1 (C-8'''), 128.8 (C-1'), 127.5 (C-6'''), 127.1 (C-3', C-5'), 124.8 (C-7'''), 123.1 (C-4'''), 118.3 (C-5a'''), 117.3 (C-9'''), 52.2 ($COO\underline{C}H_3$), 50.7 (C-1''), 47.3 (CH_3). MS (ESI+): m/z calcd for [($C_{21}H_{19}N_2O_2S$)$^+$] 363.1162, found 363.1163.

Methyl 4-[(2-methyl-1,2,3,4-tetrahydro-10*H*-benzo[*b*]pyrido[3,4-*e*][1,4]thiazin-10-yl)methyl]benzoate (12j). A suspension of 816 mg (1.66 mmol) of **11j** in 49 mL of EtOH was cooled to – 15 °C and a suspension of 196 mg (5.18 mmol, 3.1 equiv) of $NaBH_4$ in 8.0 mL of EtOH was added gradually over 1 hour. The reaction mixture was stirred for further 2 hours at – 15 °C and 22 hours at room temperature. The reaction mixture was poured onto crushed ice, and extracted with CH_2Cl_2 (3 x 50 mL). The combined organic layers were dried over $MgSO_4$ and concentrated *in vacuo*. Flash column chromatography with CH_2Cl_2 with 2 % MeOH (R_f 0.2)

yielded 450 mg (1.23 mmol, 74 %) of **12j** as a yellow oil. ^{1}H NMR (400 MHz, CD_2Cl_2): δ (ppm) = 8.01 – 7.95 (m, 2H, 2'H, 6'-H), 7.54 – 7.49 (m, 2H, 3'-H, 5'-H), 7.02 – 6.95 (m, 2H, 6'''-H, 8'''-H), 6.83 (td, *J* = 7.5, 1.1 Hz, 1H, 7'''-H), 6.65 (d, *J* = 8.1 Hz, 1H, 9'''-H), 5.33 (s, 2H, 1''-H), 3.87 (s, 3H, $COOCH_3$), 2.91 (t, *J* = 2.2 Hz, 2H, 1'''-H), 2.47 (t, *J* = 5.8 Hz, 2H, 3'''-H), 2.26 (tt, *J* = 5.7, 2.3 Hz, 2H, 4'''-H), 2.23 (s, 3H, CH_3). ^{13}C NMR (101 MHz, CD_2Cl_2): δ (ppm) = 167.2 (C-1), 146.2 (C-9a'''), 144.5 (C-4'), 135.2 (C-10a'''), 130.3 (C-2', C-6'), 129.8 (C-1'), 127.3 (C-6'''/C-8'''), 127.2 (C-3', C-5'), 127.2 (C-8'''/C-6'''), 125.9 (C-5a'''), 123.0 (C-7'''), 115.5 (C-9'''), 107.4 (C-4a'''), 56.0 (C-1'''), 52.5 (C-3'''), 50.9 ($COO\underline{C}H_3$), 45.5 (C-1''), 30.2 (CH_3), 29.6 (C-4'''). MS (ESI+): m/z calcd for [$(C_{21}H_{23}N_2O_2S)^+$] 367.1475, found 367.1481.

4-[(2-Methyl-1,2,3,4-tetrahydro-10*H*-benzo[*b*]pyrido[3,4-*e*][1,4]thiazin-10-yl)methyl]benzoic acid (13j). Standard protocol 2 with 299 mg (0.816 mmol) of **12j** in 6.0 mL of 1,4-dioxane/H_2O (1:1) and 500 µL (1.00 mmol, 1.2 equiv) of NaOH (2 M). The reaction mixture was stirred for 13 hours at room temperature and 6 hours at 60 °C. The precipitate was collected and dried at 60 °C in a drying oven to yield 210 mg (0.596 mmol, 73 %) of **13j** as a pale yellow solid. Mp: 150 - 151 °C. ^{1}H NMR (400 MHz, DMSO-d_6): δ (ppm) = 7.92 – 7.86 (m, 2H, 2'-H, 6'-H), 7.53 – 7.46 (m, 2H, 3'-H, 5'-H), 7.03 – 6.94 (m, 2H, 6'''-H, 8'''-H), 6.82 (t, *J* = 7.4 Hz, 1H, 7'''-H), 6.74 (d, *J* = 8.1 Hz, 1H, 9'''-H), 4.88 (s, 2H, 1''-H), 2.96 (s, 2H, 1'''-H), 2.44 (t, *J* = 5.7 Hz, 2H, 3'''-H), 2.18 (s, 3H, CH_3), 2.16 (t, *J* = 5.7 Hz, 2H, 4'''-H). ^{13}C NMR (101 MHz, DMSO-d_6): δ (ppm) = 167.2 (C-1), 145.1 (C-9a'''), 143.8 (C-4'), 135.0 (C-10a'''), 129.7 (C-1'), 129.5 (C-2', C-6'), 126.9 (C-6'''/ C-8'''), 126.6 (C-3', C-5'), 126.4 (C-8'''/ C-6'''), 124.0 (C-5a'''), 122.4 (C-7'''), 115.1 (C-9'''), 104.7 (C-4a'''), 54.8 (C-1'''), 51.3 (C-3'''), 48.9 (C-1''), 44.7 (CH_3), 29.1 (C-4'''). MS (ESI−): m/z calcd for [$(C_{20}H_{19}N_2O_2S)^-$] 351.1173, found 351.1173.

_N_-Hydroxy-4-[(2-methyl-1,2,3,4-tetrahydro-10_H_-benzo[_b_]pyrido[3,4-_e_][1,4]thiazin-10-yl)methyl]benzamide (14j). Standard protocol 5 with 310 mg (0.880 mmol) of **13j** in 3.0 mL of anhydrous DMF, 300 µL (1.76 mmol, 2.0 equiv) of DIPEA, 578 mg (1.35 mmol, 1.5 equiv) of COMU in 1.0 mL of anhydrous DMF, and 185 mg (2.66 mmol, 3.0 equiv) of hydroxylamine hydrochloride in 1.0 mL of anhydrous DMF. The reaction mixture was stirred for 13 hours. Flash column chromatography (work-up B) with CH_2Cl_2 with 4 % MeOH (R_f 0.2) was performed. After evaporation of the collected fractions the residue was washed with water, filtered off and dried in high vacuum to yield 119 mg (0.324 mmol, 37 %) of **14j** as a pale yellow solid. Mp: 114 - 117 °C. ^{1}H NMR (500 MHz, DMSO-d_6): δ (ppm) = 11.15 (bs, 1H, NHO<u>H</u>), 9.02 (bs, 1H, N<u>H</u>OH), 7.74 – 7.66 (m, 2H, 2'-H, 6'-H), 7.49 – 7.42 (m, 2H, 3'-H, 5'-H), 7.02 – 6.94 (m, 2H, 6'''-H, 8'''-H), 6.82 (t, J = 7.4 Hz, 1H, 7'''-H), 6.75 (d, J = 8.1 Hz, 1H, 9'''-H), 4.85 (s, 2H, 1''-H), 2.95 (s, 2H, 1'''-H), 2.42 (t, J = 5.7 Hz, 2H, 3'''-H), 2.18 (s, 3H, CH_3), 2.16 (t, J = 5.6 Hz, 2H, 4'''-H). ^{13}C NMR (126 MHz, DMSO-d_6): δ (ppm) = 164.0 (C-1), 145.1 (C-9a'''), 142.0 (C-4'), 135.2 (C-10a'''), 131.5 (C-1'), 127.1 (C-2', C-6'), 126.9 (C-6'''/C-8'''), 126.4 (C-3', C-5'), 126.4 (C-8'''/C-6'''), 124.0 (C-5a'''), 122.4 (C-7'''), 115.1 (C-9'''), 104.6 (C-4a'''), 54.9 (C-1'''), 51.4 (C-3'''), 48.7 (C-1''), 44.8 (CH_3), 29.2 (C-4'''). MS (ESI−): m/z calcd for [$(C_{20}H_{20}N_3O_2S)^-$] 366.1282, found 366.1285.

4-(10_H_-Phenothiazin-10-yl)benzonitrile (16). 602 mg (3.02 mmol) of 10_H_-phenothiazine (**2a**) was dissolved in 1.5 mL of anhydrous DMF under nitrogen atmosphere and deprotonated by adding gradually 6.00 mL (6.00 mmol, 2.0 equiv) of LiHMDS (1 M) in toluene at 0 °C. After 30 min a solution of 620 mg (5.12 mmol, 1.7 equiv) of 4-fluorobenzonitrile (**15**) in 0.5 mL of anhydrous DMF was added under nitrogen atmosphere. Then the reaction mixture was allowed to warm up to room temperature, stirred for another 17 hours and then poured into water and

extracted with CH_2Cl_2 (3 x 30 mL). The combined organic layers were washed with brine, dried over $MgSO_4$, and concentrated *in vacuo*. Flash column chromatography with hexanes and CH_2Cl_2 (6:4, R_f 0.3) gave 413 mg (1.37 mmol, 46 %) of **16** as white crystals. Mp: 157 - 158 °C. ^{1}H NMR (400 MHz, CD_2Cl_2): δ (ppm) = 7.54 – 7.46 (m, 2H, 2'-H, 6'-H), 7.44 (ddd, *J* = 7.7, 1.4, 0.5 Hz, 2H, 4"-H, 6"-H), 7.32 (ddd, *J* = 8.3, 6.9, 1.4 Hz, 2H, 2"-H, 8"-H), 7.28 (ddd, *J* = 8.0, 1.9, 0.5 Hz, 2H, 1"-H, 9"-H), 7.21 (ddd, *J* = 7.7, 6.9, 1.9 Hz, 2H, 3"-H, 7"-H), 7.12 – 7.06 (m, 2H, 3'-H, 5'-H). ^{13}C NMR (126 MHz, CD_2Cl_2): δ (ppm) = 149.4 (C-4'), 141.6 (C-9a", C-10a"), 134.1 (C-2', C-6'), 133.3 (C-4a", C-5a"), 129.3 (C-4", C-6"), 128.0 (C-2", C-8"), 126.7 (C-3", C-7"), 126.4 (C-1", C-9"), 119.8 (C-1), 117.5 (C-3', C-5'), 104.8 (C-1'). MS (ESI+): m/z calcd for [$(C_{19}H_{13}N_2S)^+$] 301.0794, found 301.0797.

4-(10*H*-Phenothiazin-10-yl)benzoic acid (17). A solution of 354 mg (1.18 mmol) of **16** and 97.0 mg (1.73 mmol, 1.5 equiv) of KOH in 2 mL of a mixture of EtOH and water (7:3) was refluxed for 41 hours, then another 192 mg (3.42 mmol, 2.9 equiv) of KOH was added and refluxing was continued for 4 hours until complete consumption of **16** (TLC control). The reaction mixture was allowed to cool to room temperature, diluted with 4 mL of water and neutralized with 2 M HCl. The obtained precipitate was collected by filtration. Flash column chromatography of the crude precipitate with CH_2Cl_2 with 4 % MeOH and 0.1 % HOAc (R_f 0.5) yielded 186 mg (0.582 mmol, 49 %) of **17** as a pale beige solid. Mp: 221 - 222 °C. Further, 99 mg (0.31 mmol, 26 %) of the corresponding primary amide were obtained. ^{1}H NMR (500 MHz, DMSO-d_6): δ (ppm) = 13.02 (bs, 1H, COOH), 8.03 – 7.98 (m, 2H, 2'-H, 6'-H), 7.33 (dd, *J* = 7.7, 1.5 Hz, 2H, 4"-H, 6"-H), 7.29 – 7.24 (m, 2H, 3'-H, 5'-H), 7.18 (td, *J* = 7.9, 1.5 Hz, 2H, 2"-H, 8"-H), 7.09 (td, *J* = 7.5, 1.2 Hz, 2H, 3"-H, 7"-H), 6.82 (d, *J* = 8.1 Hz, 2H, 1"-H, 9"-H). ^{13}C NMR (126 MHz, DMSO-d_6): δ (ppm) = 167.3 (C-1), 146.8 (C-4'), 142.5 (C-9a", C-10a"), 132.0 (C-2',

C-6'), 128.2 (C-4", C-6"), 128.1 (C-2", C-8"), 128.0 (C-1'), 126.5 (C-4a", C-5a"), 125.1 (C-3", C-7"), 123.2 (C-3', C-5'), 121.9 (C-1", C-9"). (ESI−): m/z calcd for $[(C_{19}H_{12}NO_2S)^-]$ 318.0594, found 318.0595.

***N*-Hydroxy-4-(10*H*-phenothiazin-10-yl)benzamide (18).** Standard protocol 5 with 183 mg (0.573 mmol) of **17** in 1.0 mL of anhydrous DMF, 190 µL (1.12 mmol, 2.0 equiv) of DIPEA, 365 mg (0.852 mmol, 1.5 equiv) of COMU in 0.5 mL of anhydrous DMF, and 118 mg (1.70 mmol, 3.0 equiv) of hydroxylamine hydrochloride in 0.5 mL of anhydrous DMF. The reaction mixture was stirred for 14 hours. Following work-up A the reaction mixture was extracted with EtOAc (3 x 50 mL) prior to flash column chromatography with CH_2Cl_2 with 2 % MeOH and 0.1 % HOAc (R_f 0.3). The collected fractions were evaporated and the residue was dissolved in CH_2Cl_2 and washed with water. Fine crystals precipitated in CH_2Cl_2 during washing and were collected by filtration to yield 30 mg (90 µmol, 16 %) of **18** as pale yellow crystals. Mp: 160 – 162 °C. ^{1}H NMR (400 MHz, DMSO-d_6): δ (ppm) = 11.27 (s, 1H, NHOH), 9.09 (s, 1H, NHOH), 7.96 – 7.87 (m, 2H, 2'-H, 6'-H), 7.42 – 7.32 (m, 2H, 3'-H, 5'-H), 7.21 (dd, J = 7.6, 1.6 Hz, 2H, 4"-H, 6"-H), 7.07 (td, J = 7.8, 1.6 Hz, 2H, 2"-H, 8"-H), 6.98 (td, J = 7.5, 1.3 Hz, 2H, 3"-H, 7"-H), 6.50 (dd, J = 8.2, 1.2 Hz, 2H, 1"-H, 9"-H). ^{13}C NMR (101 MHz, DMSO-d_6): δ (ppm) = 163.6 (C-1), 144.1 (C-4'), 142.7 (C-9a", C-10a"), 130.8 (C-1'), 129.3 (C-2', C-6'), 127.5 (C-2", C-8"), 127.3 (C-4", C-6"), 126.4 (C-3', C-5'), 123.8 (C-3", C-7"), 122.9 (C-4a", C-5a"), 118.9 (C-1", C-9"). MS (ESI−): m/z calcd for $[(C_{19}H_{13}N_2O_2S)^-]$ 333.0703, found 333.0704.

Methyl 4-[2-(10*H*-phenothiazin-10-yl)ethyl]benzoate (20). 501 mg (2.51 mmol) of 10*H*-phenothiazine (**2a**) and 1.44 g (7.49 mmol, 3.0 equiv) of (*E*,*Z*)-methyl 4-(2-methoxyvinyl)benzoate (**19**) were suspended in 3.8 mL of CH_2Cl_2 under nitrogen atmosphere at 0 °C. To the reaction mixture were added 1.88 mL (24.4 mmol, 9.7 equiv) of TFA and 4.00 mL

(25.0 mmol, 10.0 equiv) of Et_3SiH. After 1 hour 50 ml of NaOH (2M) was carefully added and the mixture was extracted with CH_2Cl_2 (3 x 50 mL). The combined organic layers were dried over $MgSO_4$ and concentrated *in vacuo*. Flash column chromatography with CH_2Cl_2 and hexanes (1:1 R_f 0.4) yielded 731 mg (2.02 mmol, 81 %) of **20** as pale yellow crystals. Mp: 91 – 92 °C. ^{1}H NMR (500 MHz, CD_2Cl_2): δ (ppm) = 7.96 – 7.91 (m, 2H, 2'-H, 6'-H), 7.35 – 7.30 (m, 2H, 3'-H, 5'-H), 7.19 (td, *J* = 7.9, 1.5 Hz, 2H, 2'''-H, 8'''-H), 7.15 (dd, *J* = 8.0, 1.3 Hz, 2H, 4'''-H, 6'''-H), 6.98 – 6.92 (m, 4H, 1'''-H, 3'''-H, 7'''-H, 9'''-H), 4.15 – 4.10 (m, 2H, 2''-H), 3.87 (s, 3H, $COOCH_3$), 3.17 – 3.11 (m, 2H, 1''-H). ^{13}C NMR (126 MHz, CD_2Cl_2): δ (ppm) = 167.3 (C-1), 145.6 (C-9a''', C-10a'''), 145.2 (C-4'), 130.1 (C-2', C-6'), 129.4 (C-3', C-5'), 129.0 (C-1'), 128.0 (C-4''', C-6'''), 127.9 (C-2''', C-8'''), 126.0 (C-4a''', C-5a'''), 123.2 (C-3''', C-7'''), 116.2 (C-1''', C-9'''), 52.4 ($COOCH_3$), 48.8 (C-2''), 33.8 (C-1''). MS (ESI+): m/z calcd for [$(C_{22}H_{20}NO_2S)^+$] 362.1209, found 362.1207

4-[2-(10*H*-Phenothiazin-10-yl)ethyl]benzoic acid (21). Standard protocol 2 with 318 mg (0.880 mmol) of **20** in 6.0 mL of 1,4-dioxane/H_2O (1:1) and 540 µL (1.08 mmol, 1.2 equiv) of NaOH (2 M). The reaction mixture was stirred for 3 hours at 60 °C. The precipitate was collected and dried at 60 °C in a drying oven to yield 280 mg (0.806 mmol, 92 %) of **21** as a white solid. Mp: 165 - 166 °C. ^{1}H NMR (400 MHz, DMSO-d_6): δ (ppm) = 12.83 (bs, 1H, COOH), 7.91 – 7.76 (m, 2H, 2'-H, 6'-H), 7.46 – 7.33 (m, 2H, 3'-H, 5'-H), 7.22 (td, *J* = 7.6, 1.5 Hz, 2H, 2'''-H, 8'''-H), 7.16 (dd, *J* = 7.6, 1.5 Hz, 2H, 4'''-H, 6'''-H), 7.12 (dd, *J* = 8.3, 1.1 Hz, 2H, 1'''-H, 9'''-H), 6.96 (td, *J* = 7.4, 1.1 Hz, 2H, 3'''-H, 7'''-H), 4.22 – 4.03 (m, 2H, 2''-H), 3.13 – 2.97 (m, 2H, 1''-H). ^{13}C NMR (101 MHz, DMSO-d_6): δ (ppm) = 167.2 (C-1), 144.5 (C-9a''', C-10a'''), 144.4 (C-4'), 129.3 (C-2', C-6'), 129.0 (C-3', C-5'), 128.8 (C-1'), 127.7 (C-2''', C-8'''), 127.2 (C-4''', C-6'''), 124.0 (C-4a''', C-

5a'''), 122.6 (C-3''', C-7'''), 116.1 (C-1''', C-9'''), 47.6 (C-2''), 32.5 (C-1''). MS (ESI−): m/z calcd for [($C_{21}H_{16}NO_2S$)$^-$] 346.0907, found 346.0905.

4-[2-(10*H*-Phenothiazin-10-yl)ethyl]-*N*-hydroxybenzamide (22). Standard protocol 5 with 205 mg (0.590 mmol) of **21** in 1.5 mL of anhydrous DMF, 200 µL (1.18 mmol, 2.0 equiv) of DIPEA, 379 mg (0.885 mmol, 1.5 equiv) of COMU in 0.6 mL of anhydrous DMF, and 124 mg (1.78 mmol, 3.0 equiv) of hydroxylamine hydrochloride in 0.6 mL of anhydrous DMF. The reaction mixture was stirred for 4 hours. Flash column chromatography (work-up B) with CH_2Cl_2 with 2 % MeOH and 0.1 % HOAc (R_f 0.2) was performed. The collected fractions were evaporated and the residue was dissolved in CH_2Cl_2 and extracted with water. Fine crystals precipitated in CH_2Cl_2 during washing and were collected by filtration to yield 107 mg (0.295 mmol, 50 %) of **22** as pale beige crystals. Mp: 149 - 151 °C. ^{1}H NMR (500 MHz, DMSO-d_6): δ (ppm) = 11.15 (s, 1H, NHOH), 8.97 (s, 1H, NHOH), 7.76 – 7.57 (m, 2H, 2'-H, 6'-H), 7.46 – 7.31 (m, 2H, 3'-H, 5'-H), 7.23 (t, J = 7.7 Hz, 2H, 2'''-H, 8'''-H), 7.16 (d, J = 7.4 Hz, 2H, 4'''-H, 6'''-H), 7.12 (d, J = 8.1 Hz, 2H, 1'''-H, 9'''-H), 6.96 (t, J = 7.4 Hz, 2H, 3'''-H, 7'''-H), 4.21 – 4.04 (m, 2H, 2''-H), 3.12 – 2.95 (m, 2H, 1''-H). ^{13}C NMR (126 MHz, DMSO-d_6): δ (ppm) = 164.1 (C-1), 144.6 (C-9a''', C-10a'''), 142.5 (C-4'), 130.7 (C-1'), 128.8 (C-3', C-5'), 127.7 (C-2''', C-8'''), 127.2 (C-4''', C-6'''), 126.9 (C-2', C-6'), 123.9 (C-4a''', C-5a'''), 122.6 (C-3''', C-7'''), 116.0 (C-1''', C-9'''), 47.7 (C-2''), 32.3 (C-1''). MS (ESI+): m/z calcd for [($C_{21}H_{19}N_2O_2S$)$^+$] 363.1162, found 363.1160.

4-[(10*H*-Phenothiazin-10-yl)methyl]-*N*-methoxy-*N*-methylbenzamide (23). 342 mg (1.03 mmol) of **5a** was dissolved in 7.0 mL of anhydrous DMF and was deprotonated by addition of 180 µL (1.03 mmol, 1.0 equiv) of DIPEA at 0 °C. 439 mg (1.03 mmol, 1.0 equiv) of COMU was added and the mixture was stirred for 5 minutes at this temperature. To this solution 100 mg (1.03 mmol, 1.0 equiv) of *N*,*O*-dimethylhydroxylamine hydrochloride and 180 µL (1.03 mmol,

1.0 equiv) of DIPEA was added. The reaction mixture was stirred for 1 hour at 0 °C and 23 hours at room temperature. Then the mixture was poured into water and extracted with EtOAc (4 x 50 mL). The combined organic layers were dried over Na_2SO_4 and concentrated *in vacuo*. Flash column chromatography with CH_2Cl_2 with 2 % MeOH (R_f 0.4) yielded 164 mg (0.436 mmol, 42 %) of **23** as a pink solid. Mp: 47- 50 °C. ^{1}H NMR (500 MHz, DMSO-d_6): δ (ppm) = 7.57 – 7.52 (m, 2H, 2'-H, 6'-H), 7.41 – 7.37 (m, 2H, 3'-H, 5'-H), 7.15 (dd, J = 7.6, 1.5 Hz, 2H, 4'''-H, 6'''-H), 7.07 (ddd, J = 8.1, 7.4, 1.6 Hz, 2H, 2'''-H, 8'''-H), 6.91 (td, J = 7.5, 1.1 Hz, 2H, 3'''-H, 7'''-H), 6.79 (dd, J = 8.2, 1.1 Hz, 2H, 1'''-H, 9'''-H), 5.19 (s, 2H, 1''-H), 3.53 (s, 3H, OCH_3), 3.23 (s, 3H, NCH_3). ^{13}C NMR (126 MHz, DMSO-d_6): δ (ppm) = 168.9 (C-1), 144.1 (C-9a''', C-10a'''), 139.6 (C-4'), 132.9 (C-1'), 128.0 (C-2', C-6'), 127.5 (C-2''', C-8'''), 126.8 (C-4''', C-6'''), 126.4 (C-3', C-5'), 122.7 (C-3''', C-7'''), 122.6 (C-4a''', C-5a'''), 115.8 (C-1''', C-9'''), 60.7 (OCH_3), 50.8 (C-1''), 33.3 (NCH_3). MS (ESI+): m/z calcd for [($C_{22}H_{21}N_2O_2S$)$^+$] 377.1324, found 377.1320.

Corresponding Author

Franz Bracher: franz.bracher@cup.uni-muenchen.de +49 89 218077301

ORCID

Franz Bracher: 0000-0003-0009-8629

Author Contributions

K.V., W.S., M.J. and F.B. wrote the manuscript. All authors have given approval to the final version of the manuscript. Compounds were designed and synthesized by K.V., N.O. and F.B. In vitro studies were designed and performed by J.S., D.H., K.S. and M.J., as well as C.R., M.M. and T.B.S. (on HDAC8) and M.M. and K.B. (cellular assays). Docking studies were performed by D.R. and W.S. Crystal structure analysis was performed by N.J.P. and D.W.C. The data obtained were interpreted by all authors.

Notes

The authors declare no competing financial interest.

Funding Sources

MJ and WS thank the Deutsche Forschungsgemeinschaft for funding (Ju295/13-1, Si868/13-1). The work of CR, MM and TBS was supported by institutional funds from the Centre National de la Recherche Scientifique (CNRS), the Institut National de la Santé et de la Recherche Médicale (INSERM), and the Université de Strasbourg. D.W.C. and N.J.P. thank the US National Institutes of Health for grant GM49758 and Chemistry-Biology Interface training grant T32 GM071339. This research utilized the Frontier Microfocusing Macromolecular Crystallography Beamline (FMX) of the National

Synchrotron Light Source II, a U.S. Department of Energy (DOE) Office of Science User Facility operated for the DOE Office of Science by Brookhaven National Laboratory under Contract No. DE-SC0012704.

ACKNOWLEDGMENT

The authors thank Martin Morgenstern, Karl Sauvageot-Witzku and Dr. Hanns-Jürgen Krauß for support in synthesis, and Anna Niedrig for HPLC measurements.

ABBREVIATIONS

Ac: acetyl. AMC: aminomethylcoumarin. ATCC: American Type Culture Collection. CD1, CD2: catalytic domain 1, catalytic domain 2. COMU: (1-cyano-2-ethoxy-2-oxoethylidenaminooxy)dimethylamino-morpholino-carbenium hexafluorophosphate. CYP450: cytochrome P450. DIPEA: N,N-diisopropyl ethylamine. DMF: dimethylformamid. DMSO: dimethylsulfoxide. ESI: electrospray ionization. EtOAc: ethyl acetate. EtOH: ethanol. FBS: fetal bovine serum. GAPDH: glyceraldehyde 3-phosphate dehydrogenase. H3: histone 3. HA: heavy atom. HAT: histone acetyl transferase. HDAC: histone deacetylase. HOAc: acetic acid. HRP: horseradish peroxidase. LDA: lithium diisopropylamide. LE: ligand efficiency. LiHMDS: hexamethyldisilazane lithium salt. MeOH: methanol. NES: nuclear export signal. NH_2OTHP: O-(tetrahydro-2H-pyran-2-yl)hydroxylamine. NLS: nuclear localization signal. PD-L1:

programmed death receptor ligand-1. Rmsd: root mean square deviation. SAHA: suberoylanilide hydroxamic acid. SDS-Page: sodium dodecyl sulfate-polyacrylamide gel electrophoresis. SE14: serine-glutamate tetradecapeptide repeate. SF: selectivity factor. TBS-T: Tris-buffered saline with 0.1% Tween 20. TFA: trifluoroacetic acid. THP: tetrahydropyranyl. TSA: Trichostatin A. ZBG: zinc-binding group. ZMAL: (S)-[5-acetylamino-1-(4-methyl-2-oxo-2H-chromen-7-ylcarbamoyl)pentyl]carbamic acid benzyl ester.

ANCILLARY INFORMATION

Supporting Information. X-ray results. Crystallization statistics. Docking results. Screening results on additional cancer cell lines. Additional data on metabolic stability. Combination studies with Bortezomib. NMR spectra. HPLC chromatograms.

Molecular formula strings including screening data.

Accession Codes. Atomic coordinates for the crystal structure of inhibitor **7i** with the catalytic domain 2 from *Danio rerio* HDAC6BCL6 can be accessed using PDB code 5W5K (released june 27, 2018).

REFERENCES

1. Choudhary, C.; Kumar, C.; Gnad, F.; Nielsen, M. L.; Rehman, M.; Walther, T. C.; Olsen, J. V.; Mann, M. Lysine acetylation targets protein complexes and co-regulates major cellular functions. *Science* **2009,** 325, 834-840.

2. Hubbert, C.; Guardiola, A.; Shao, R.; Kawaguchi, Y.; Ito, A.; Nixon, A.; Yoshida, M.; Wang, X.-F.; Yao, T.-P. HDAC6 is a microtubule-associated deacetylase. *Nature* **2002,** 417, 455-458.

3. Kovacs, J. J.; Murphy, P. J. M.; Gaillard, S.; Zhao, X.; Wu, J.-T.; Nicchitta, C. V.; Yoshida, M.; Toft, D. O.; Pratt, W. B.; Yao, T.-P. HDAC6 regulates Hsp90 acetylation and chaperone-dependent activation of glucocorticoid receptor. *Moll. Cell* **2005,** 18, 601-607.

4. Zhang, X.; Yuan, Z.; Zhang, Y.; Yong, S.; Salas-Burgos, A.; Koomen, J.; Olashaw, N.; Parsons, J. T.; Yang, X.-J.; Dent, S. R.; Yao, T.-P.; Lane, W. S.; Seto, E. HDAC6 modulates cell motility by altering the acetylation level of cortactin. *Moll. Cell* **2007,** 27, 197-213.

5. Miyake, Y.; Keusch, J. J.; Wang, L.; Saito, M.; Hess, D.; Wang, X.; Melancon, B. J.; Helquist, P.; Gut, H.; Matthias, P. Structural insights into HDAC6 tubulin deacetylation and its selective inhibition. *Nat. Chem. Biol.* **2016,** 12, 748-754.

6. Hai, Y.; Christianson, D. W. Histone deacetylase 6 structure and molecular basis of catalysis and inhibition. *Nat. Chem. Biol.* **2016,** 12, 741-747.

7. Ouyang, H.; Ali, Y. O.; Ravichandran, M.; Dong, A.; Qiu, W.; MacKenzie, F.; Dhe-Paganon, S.; Arrowsmith, C. H.; Zhai, R. G. Protein aggregates are recruited to aggresome by histone deacetylase 6 via unanchored ubiquitin C termini. *J. Biol. Chem.* **2012,** 287, 2317-2327.

8. Zhang, Y.; Gilquin, B.; Khochbin, S.; Matthias, P. Two catalytic domains are required for protein deacetylation. *J. Biol. Chem.* **2006,** 281, 2401-2404.

9. Kawaguchi, Y.; Kovacs, J. J.; McLaurin, A.; Vance, J. M.; Ito, A.; Yao, T.-P. The deacetylase HDAC6 regulates aggresome formation and cell viability in response to misfolded protein stress. *Cell* **2003,** 115, 727-738.

10. Bertos, N. R.; Gilquin, B.; Chan, G. K. T.; Yen, T. J.; Khochbin, S.; Yang, X.-J. Role of the tetradecapeptide repeat domain of human histone deacetylase 6 in cytoplasmic retention. *J. Biol. Chem.* **2004,** 279, 48246-48254.

11. Li, Y.; Shin, D.; Kwon, S. H. Histone deacetylase 6 plays a role as a distinct regulator of diverse cellular processes. *FEBS J.* **2013,** 280, 775-793.

12. Simões-Pires, C.; Zwick, V.; Nurisso, A.; Schenker, E.; Carrupt, P.-A.; Cuendet, M. HDAC6 as a target for neurodegenerative diseases: what makes it different from the other HDACs? *Mol. Neurodegener.* **2013,** 8, 7-7.

13. Edwin F. de Zoeten; Liqing Wang, K. B., Ulf H. Beier, Tatiana Akimova, Hong Sai, James E. Bradner, Ralph Mazitschek, Alan P. Kozikowski, Patrick Matthias, Wayne W. Hancock. Histone deacetylase 6 and heat shock protein 90 control the functions of Foxp3 T-regulatory cells. *Mol. Cell. Biol.* **2011,** 31.

14. Grace I. Aldana-Masangkay, K. M. S. The role of HDAC6 in cancer. *J. Biomed. Biotechnol.* **2011,** 2011.

15. DeAngelo, D. J.; Spencer, A.; Bhalla, K. N.; Prince, H. M.; Fischer, T.; Kindler, T.; Giles, F. J.; Scott, J. W.; Parker, K.; Liu, A.; Woo, M.; Atadja, P.; Mishra, K. K.; Ottmann,

O. G. Phase Ia/II, two-arm, open-label, dose-escalation study of oral panobinostat administered via two dosing schedules in patients with advanced hematologic malignancies. *Leukemia* **2013,** 27, 1628.

16. Li, T.; Zhang, C.; Hassan, S.; Liu, X.; Song, F.; Chen, K.; Zhang, W.; Yang, J. Histone deacetylase 6 in cancer. *J. Hematol. Oncol.* **2018,** 11, 111.

17. Zhang, Y.; Kwon, S.; Yamaguchi, T.; Cubizolles, F.; Rousseaux, S.; Kneissel, M.; Cao, C.; Li, N.; Cheng, H.-L.; Chua, K.; Lombard, D.; Mizeracki, A.; Matthias, G.; Alt, F. W.; Khochbin, S.; Matthias, P. Mice lacking histone deacetylase 6 have hyperacetylated tubulin but are viable and develop normally. *Mol. Cell. Biol.* **2008,** 28, 1688-1701.

18. Dallavalle, S.; Pisano, C.; Zunino, F. Development and therapeutic impact of HDAC6-selective inhibitors. *Biochem. Pharmacol.* **2012,** 84, 756-765.

19. Haggarty, S. J.; Koeller, K. M.; Wong, J. C.; Grozinger, C. M.; Schreiber, S. L. Domain-selective small-molecule inhibitor of histone deacetylase 6 (HDAC6)-mediated tubulin deacetylation. *Proc. Natl. Acad. Sci. U.S.A.* **2003,** 100, 4389-4394.

20. Haggarty, S. J.; Koeller, K. M.; Wong, J. C.; Butcher, R. A.; Schreiber, S. L. Multidimensional chemical genetic analysis of diversity-oriented synthesis-derived deacetylase inhibitors using cell-based assays. *Chem. Biol.* **2003,** 10, 383-396.

21. Vogl, D. T.; Raje, N.; Jagannath, S.; Richardson, P.; Hari, P.; Orlowski, R.; Supko, J. G.; Tamang, D.; Yang, M.; Jones, S. S.; Wheeler, C.; Markelewicz, R. J.; Lonial, S. Ricolinostat, the first selective histone deacetylase 6 inhibitor, in combination with bortezomib and dexamethasone for relapsed or refractory multiple myeloma. *Clin. Cancer Res.* **2017,** 23, 3307-3315.

22. Bae, J.; Hideshima, T.; Tai, Y.-T.; Song, Y.; Richardson, P.; Raje, N.; Munshi, N. C.; Anderson, K. C. Histone deacetylase (HDAC) inhibitor ACY241 enhances anti-tumor activities of antigen-specific central memory cytotoxic T lymphocytes against multiple myeloma and solid tumors. *Leukemia* **2018,** 32, 1932-1947.

23. www.clinicaltrials.gov (assessed on november 7, 2018)

24. Butler, K. V.; Kalin, J.; Brochier, C.; Vistoli, G.; Langley, B.; Kozikowski, A. P. Rational design and simple chemistry yield a superior, neuroprotective HDAC6 inhibitor, Tubastatin A. *J. Am. Chem. Soc.* **2010,** 132, 10842-10846.

25. Wang, Z.; Leng, Y.; Wang, J.; Liao, H.-M.; Bergman, J.; Leeds, P.; Kozikowski, A.; Chuang, D.-M. Tubastatin A, an HDAC6 inhibitor, alleviates stroke-induced brain infarction and functional deficits: potential roles of α-tubulin acetylation and FGF-21 up-regulation. *Sci. Rep.* **2016,** 6, 1-12.

26. Zhang, L., Liu, Cui, Wu, Jie, Tao, Jing-jing, Sui, Xiao-long, Yao, Zhi-gang, Xu, Yan-feng, Huang, Lan, Zhu, Hua, Sheng, Shu-li, Qin, Chuan. Tubastatin A/ACY-1215 improves cognition in Alzheimer's disease transgenic mice *J. Alzheimers Dis.* **2014,** 41, 1193-1205.

27. Kalin, J. H.; Butler, K. V.; Akimova, T.; Hancock, W. W.; Kozikowski, A. P. Second-generation histone deacetylase 6 inhibitors enhance the immunosuppressive effects of Foxp3+ T-regulatory cells. *J. Med. Chem.* **2012,** 55, 639-651.

28. Jochems, J.; Boulden, J.; Lee, B. G.; Blendy, J. A.; Jarpe, M.; Mazitschek, R.; Van Duzer, J. H.; Jones, S.; Berton, O. Antidepressant-like properties of novel HDAC6-selective inhibitors with improved brain bioavailability. *Neuropsychopharmacology* **2014,** 39, 389-400.

29. Sellmer, A.; Stangl, H.; Beyer, M.; Grünstein, E.; Leonhardt, M.; Pongratz, H.; Eichhorn, E.; Elz, S.; Striegl, B.; Jenei-Lanzl, Z.; Dove, S.; Straub, R. H.; Krämer, O. H.; Mahboobi, S. Marbostat 100 defines a new class of potent and selective antiinflammatory and antirheumatic histone deacetylase 6 inhibitors. *J. Med. Chem.* **2018,** 61, 3454-3477.

30. Bergman, J. A.; Woan, K.; Perez-Villarroel, P.; Villagra, A.; Sotomayor, E. M.; Kozikowski, A. P. Selective histone deacetylase 6 inhibitors bearing substituted urea linkers inhibit melanoma cell growth. *J. Med. Chem.* **2012,** 55, 9891-9899.

31. Tavares, M. T.; Shen, S.; Knox, T.; Hadley, M.; Kutil, Z.; Bařinka, C.; Villagra, A.; Kozikowski, A. P. Synthesis and pharmacological evaluation of selective histone deacetylase 6 inhibitors in melanoma models. *ACS Med. Chem. Lett.* **2017,** 8, 1031-1036.

32. Lee, J.-H.; Mahendran, A.; Yao, Y.; Ngo, L.; Venta-Perez, G.; Choy, M. L.; Kim, N.; Ham, W.-S.; Breslow, R.; Marks, P. A. Development of a histone deacetylase 6 inhibitor and its biological effects. *PNAS* **2013,** 110, 15704-15709.

33. Senger, J.; Melesina, J.; Marek, M.; Romier, C.; Oehme, I.; Witt, O.; Sippl, W.; Jung, M. Synthesis and biological investigation of oxazole hydroxamates as highly selective histone deacetylase 6 (HDAC6) inhibitors. *J. Med. Chem.* **2016,** 59, 1545-1555.

34. Pérez-Salvia, M.; Aldaba, E.; Vara, Y.; Fabre, M.; Ferrer, C.; Masdeu, C.; Zubia, A.; Sebastian, E. S.; Otaegui, D.; Llinàs-Arias, P.; Rosselló-Tortella, M.; Berdasco, M.; Moutinho, C.; Setien, F.; Villanueva, A.; González-Barca, E.; Muncunill, J.; Navarro, J.-T.; Piris, M. A.; Cossio, F. P.; Esteller, M. In vitro and in vivo activity of a new small-molecule inhibitor of HDAC6 in mantle cell lymphoma. *Haematologica* **2018,** 103, e537-e540.

35. Fan, S.-J.; Huang, F.-I.; Liou, J.-P.; Yang, C.-R. The novel histone de acetylase 6 inhibitor, MPT0G211, ameliorates tau phosphorylation and cognitive deficits in an Alzheimer's disease model. *Cell Death Dis.* **2018,** 9, 655.

36. Mackwitz, M. K. W.; Hamacher, A.; Osko, J. D.; Held, J.; Schöler, A.; Christianson, D. W.; Kassack, M. U.; Hansen, F. K. Multicomponent synthesis and

binding mode of imidazo[1,2-a]pyridine-capped selective HDAC6 inhibitors. *Org. Lett.* **2018,** 20, 3255-3258.

37. Lecointre, B.; Narozny, R.; Borrello, M. T.; Senger, J.; Chakrabarti, A.; Jung, M.; Marek, M.; Romier, C.; Melesina, J.; Sippl, W.; Bischoff, L.; Ganesan, A. Isoform-selective HDAC1/6/8 inhibitors with an imidazo-ketopiperazine cap containing stereochemical diversity. *Philos. Trans. R. Soc. Lond., B, Biol. Sci* **2018,** 373.

38. De Vreese, R.; Galle, L.; Depetter, Y.; Franceus, J.; Desmet, T.; Van Hecke, K.; Benoy, V.; Van Den Bosch, L.; D'hooghe, M. Synthesis of potent and selective HDAC6 inhibitors bearing a cyclohexane- or cycloheptane-annulated 1,5-benzothiazepine scaffold. *Chem. Eur. J.* **2017,** 23, 128-136.

39. Kozikowski, A. P.; Butler, K. V. Chemical origins of isoform selectivity in histone deacetylase inhibitors. *Curr. Pharm. Des.* **2008,** 14, 505-528.

40. Porter, N. J.; Mahendran, A.; Breslow, R.; Christianson, D. W. Unusual zinc-binding mode of HDAC6-selective hydroxamate inhibitors. *PNAS* **2017,** 114, 13459-13464.

41. Shen, S.; Benoy, V.; Bergman, J. A.; Kalin, J. H.; Frojuello, M.; Vistoli, G.; Haeck, W.; Van Den Bosch, L.; Kozikowski, A. P. Bicyclic-capped histone deacetylase 6 inhibitors with improved activity in a model of axonal Charcot–Marie–Tooth disease. *ACS Chem. Neurosc.* **2016,** 7, 240-258.

42. Panguluri, N. R.; Basavaprabhu; Sureshbabu, V. V. Facile synthesis of N α -protected amino/peptide hydroxamic acids mediated by COMU. *Int. J. Pept. Res. Ther.* **2014,** 20, 377-384.

43. Subirós-Funosas, R.; Nieto-Rodriguez, L.; Jensen, K. J.; Albericio, F. COMU: scope and limitations of the latest innovation in peptide acyl transfer reagents. *J. Pept. Sci.* **2013,** 19, 408-414.

44. Warren, B. K.; Knaus, E. E. Pyridine and reduced pyridine analogues of 10H-pyrido[3,4-b][1,4]benzothiazines with analgesic activity. *Eur. J. Med. Chem.* **1987,** 22, 411-415.

45. Park, Y. S.; Choi, J.; Kim, D.; Lee, B.; Suh, H.; Kim, J. H. Synthesis, optical, and electroluminescent properties of alternating copolymer based on phenothiazine and fluorene with oxadiazole pendant. *Mol. Cryst. Liq. Cryst* **2011,** 550, 294-303.

46. Vögerl, K.; Ong, D. N.; Bracher, F. Reductive N-arylethylation of aromatic amines and N-heterocycles with enol ethers. *Synthesis* **2018,** 50, 1323-1330.

47. Heltweg, B.; Trapp, J.; Jung, M. In vitro assays for the determination of histone deacetylase activity. *Methods* **2005,** 36, 332-337.

48. Hopkins, A. L.; Keseru, G. M.; Leeson, P. D.; Rees, D. C.; Reynolds, C. H. The role of ligand efficiency metrics in drug discovery. *Nat. Rev. Drug Discov* **2014,** 13, 105-121.

49. Yu, C.-W.; Chang, P.-T.; Hsin, L.-W.; Chern, J.-W. Quinazolin-4-one derivatives as selective histone deacetylase-6 inhibitors for the treatment of Alzheimer's disease. *J. Med. Chem.* **2013,** 56, 6775-6791.

50. Blackburn, C.; Barrett, C.; Chin, J.; Garcia, K.; Gigstad, K.; Gould, A.; Gutierrez, J.; Harrison, S.; Hoar, K.; Lynch, C.; Rowland, R. S.; Tsu, C.; Ringeling, J.; Xu, H. Potent histone deacetylase inhibitors derived from 4-(aminomethyl)-N-hydroxybenzamide with high selectivity for the HDAC6 isoform. *J. Med. Chem.* **2013,** 56, 7201-7211.

51. Tang, G.; Wong, J. C.; Zhang, W.; Wang, Z.; Zhang, N.; Peng, Z.; Zhang, Z.; Rong, Y.; Li, S.; Zhang, M.; Yu, L.; Feng, T.; Zhang, X.; Wu, X.; Wu, J. Z.; Chen, L. Identification of a novel aminotetralin class of HDAC6 and HDAC8 selective inhibitors. *J. Med. Chem.* **2014,** 57, 8026-8034.

52. Yee, A. J.; Bensinger, W. I.; Supko, J. G.; Voorhees, P. M.; Berdeja, J. G.; Richardson, P. G.; Libby, E. N.; Wallace, E. E.; Birrer, N. E.; Burke, J. N.; Tamang, D. L.; Yang, M.; Jones, S. S.; Wheeler, C. A.; Markelewicz, R. J.; Raje, N. S. Ricolinostat plus lenalidomide, and dexamethasone in relapsed or refractory multiple myeloma: a multicentre phase 1b trial. *Lancet Oncol.* **2016,** 17, 1569-1578.

53. Woan, K. V.; Lienlaf, M.; Perez-Villaroel, P.; Lee, C.; Cheng, F.; Knox, T.; Woods, D. M.; Barrios, K.; Powers, J.; Sahakian, E.; Wang, H. W.; Canales, J.; Marante, D.; Smalley, K. S. M.; Bergman, J.; Seto, E.; Kozikowski, A.; Pinilla-Ibarz, J.; Sarnaik, A.; Celis, E.; Weber, J.; Sotomayor, E. M.; Villagra, A. Targeting histone deacetylase 6 mediates a dual anti-melanoma effect: Enhanced antitumor immunity and impaired cell proliferation. *Mol. Oncol.* **2015,** 9, 1447-1457.

54. Ray, A.; Das, D. S.; Song, Y.; Hideshima, T.; Tai, Y. T.; Chauhan, D.; Anderson, K. C. Combination of a novel HDAC6 inhibitor ACY-241 and anti-PD-L1 antibody enhances anti-tumor immunity and cytotoxicity in multiple myeloma. *Leukemia* **2017,** 32, 843.

55. Bazzaro, M.; Lin, Z.; Santillan, A.; Lee, M. K.; Wang, M.-C.; Chan, K. C.; Bristow, R. E.; Mazitschek, R.; Bradner, J.; Roden, R. B. S. Ubiquitin Proteasome system stress underlies synergistic killing of ovarian cancer cells by Bortezomib and a novel HDAC6 inhibitor. *Clin. Cancer Res.* **2008,** 14, 7340-7347.

56. Amengual, J. E.; Johannet, P.; Lombardo, M.; Zullo, K.; Hoehn, D.; Bhagat, G.; Scotto, L.; Jirau-Serrano, X.; Radeski, D.; Heinen, J.; Jiang, H.; Cremers, S.; Zhang, Y.; Jones, S.; O'Connor, O. A. Dual targeting of protein degradation pathways with the selective HDAC6 inhibitor ACY-1215 and Bortezomib is synergistic in lymphoma. *Clin. Cancer Res.* **2015,** 21, 4663-4675.

57. Woods, D. M.; Sodré, A. L.; Villagra, A.; Sarnaik, A.; Sotomayor, E. M.; Weber, J. HDAC inhibition upregulates PD-1 ligands in melanoma and augments immunotherapy with PD-1 blockade. *Cancer Immunol. Res.* **2015,** 3, 1375-1385.

58. Lienlaf, M.; Perez-Villarroel, P.; Knox, T.; Pabon, M.; Sahakian, E.; Powers, J.; Woan, K. V.; Lee, C.; Cheng, F.; Deng, S.; Smalley, K. S. M.; Montecino, M.; Kozikowski, A.; Pinilla-Ibarz, J.; Sarnaik, A.; Seto, E.; Weber, J.; Sotomayor, E. M.; Villagra, A. Essential role of HDAC6 in the regulation of PD-L1 in melanoma. *Mol. Oncol.* **2016,** 10, 735-750.

59. Blankenstein, T.; Coulie, P. G.; Gilboa, E.; Jaffee, E. M. The determinants of tumour immunogenicity. *Nat. Rev. Cancer* **2012,** 12, 307-313.

60. Breyer-Pfaff, U.; Kreft, H.; Rassner, H.; Prox, A. Formation of sulfone metabolites from chlorpromazine and perazine in man. *Drug Metab. Dispos.* **1978,** 6, 114-119.

61. Wójcikowski, J.; Basińska, A.; Daniel, W. A. The cytochrome P450-catalyzed metabolism of levomepromazine: a phenothiazine neuroleptic with a wide spectrum of clinical application. *Biochem. Pharmacol.* **2014,** 90, 188-195.

62. Watson, P. J.; Millard, C. J.; Riley, A. M.; Robertson, N. S.; Wright, L. C.; Godage, H. Y.; Cowley, S. M.; Jamieson, A. G.; Potter, B. V. L.; Schwabe, J. W. R. Insights into the activation mechanism of class I HDAC complexes by inositol phosphates. *Nat. Commun.* **2016,** 7, 1-13.

63. Vannini, A.; Volpari, C.; Filocamo, G.; Casavola, E. C.; Brunetti, M.; Renzoni, D.; Chakravarty, P.; Paolini, C.; De Francesco, R.; Gallinari, P.; Steinkühler, C.; Di Marco, S. Crystal structure of a eukaryotic zinc-dependent histone deacetylase, human HDAC8, complexed with a hydroxamic acid inhibitor. *Proc. Natl. Acad. Sci. USA* **2004,** 101, 15064-15069.

64. Marek, M.; Kannan, S.; Hauser, A.-T.; Moraes Mourão, M.; Caby, S.; Cura, V.; Stolfa, D. A.; Schmidtkunz, K.; Lancelot, J.; Andrade, L.; Renaud, J.-P.; Oliveira, G.; Sippl, W.; Jung, M.; Cavarelli, J.; Pierce, R. J.; Romier, C. Structural basis for the inhibition of histone deacetylase 8 (HDAC8), a key epigenetic player in the blood fluke Schistosoma mansoni. *PLOS Pathog.* **2013,** 9, e1003645.

65. Riccardi, C.; Nicoletti, I. Analysis of apoptosis by propidium iodide staining and flow cytometry. *Nat. Protoc.* **2006,** 1, 1458.

66. Ardelt, M. A.; Fröhlich, T.; Martini, E.; Müller, M.; Kanitz, V.; Atzberger, C.; Cantonati, P.; Meßner, M.; Posselt, L.; Lehr, T.; Wojtyniak, J.-G.; Ulrich, M.; Arnold, G. J.; König, L.; Parazzoli, D.; Zahler, S.; Rothenfußer, S.; Mayr, D.; Gerbes, A.; Scita, G.; Vollmar, A. M.; Pachmayr, J. Inhibition of cyclin-dependent kinase 5 – a novel strategy

to improve Sorafenib response in HCC therapy. *Hepatology* **2018,** epub ahead of print july 23, 2018.

67. Hopkins, A. L.; Groom, C. R.; Alex, A. Ligand efficiency: a useful metric for lead selection. *Drug Discov. Today* **2004,** 9, 430-431.

68. Berman, H. M.; Westbrook, J.; Feng, Z.; Gilliland, G.; Bhat, T. N.; Weissig, H.; Shindyalow, I. N.; Bourne, P. E. *Protein Data Bank, Nucleic Acids Research* **2000,** 28, 235-242.

69. *Schrödinger Suite 2012 Protein Preparation Wizard Epik Version 2.3, Schrödinger, Llc, New York, 2014, Impact Version 5.8, Schrödinger, Llc, New York, 2014, Prime Version 3.1 Schrödinger, Llc New York 2014*.

70. *Molecular Operating Environment (Moe), 2012.10, Chemical Computing Group Inc., 1010 Sherbooke St. West, Suite #910, Montreal, Qc, Canada, H3a 2r7, 2012*.

71. Heimburg, T.; Chakrabarti, A.; Lancelot, J.; Marek, M.; Melesina, J.; Hauser, A.-T.; Shaik, T. B.; Duclaud, S.; Robaa, D.; Erdmann, F.; Schmidt, M.; Romier, C.; Pierce, R. J.; Jung, M.; Sippl, W. Structure-based design and synthesis of novel inhibitors

targeting HDAC8 from Schistosoma mansoni for the treatment of schistosomiasis. *J. Med. Chem.* **2016,** 59, 2423-2435.

72. Battye, T. G. G.; Kontogiannis, L.; Johnson, O.; Powell, H. R.; Leslie, A. G. W. iMOSFLM: a new graphical interface for diffraction-image processing with MOSFLM. *Acta Crystallogr. Sect. D. Biol. Crystallogr.* **2011,** 67, 271-281.

73. Winn, M. D.; Ballard, C. C.; Cowtan, K. D.; Dodson, E. J.; Emsley, P.; Evans, P. R.; Keegan, R. M.; Krissinel, E. B.; Leslie, A. G. W.; McCoy, A.; McNicholas, S. J.; Murshudov, G. N.; Pannu, N. S.; Potterton, E. A.; Powell, H. R.; Read, R. J.; Vagin, A.; Wilson, K. S. Overview of the CCP4 suite and current developments. *Acta Crystallogr. Sect. D. Biol. Crystallogr.* **2011,** 67, 235-242.

74. McCoy, A. J.; Grosse-Kunstleve, R. W.; Adams, P. D.; Winn, M. D.; Storoni, L. C.; Read, R. J. Phaser crystallographic software. *J. Appl. Crystallogr.* **2007,** 40, 658-674.

75. Emsley, P.; Lohkamp, B.; Scott, W. G.; Cowtan, K. Features and development of Coot. *Acta Crystallogr. Sect. D. Biol. Crystallogr.* **2010,** 66, 486-501.

76. Adams, P. D.; Afonine, P. V.; Bunkóczi, G.; Chen, V. B.; Davis, I. W.; Echols, N.; Headd, J. J.; Hung, L.-W.; Kapral, G. J.; Grosse-Kunstleve, R. W.; McCoy, A. J.; Moriarty, N. W.; Oeffner, R.; Read, R. J.; Richardson, D. C.; Richardson, J. S.; Terwilliger, T. C.; Zwart, P. H. PHENIX: a comprehensive Python-based system for macromolecular structure solution. *Acta Crystallogr. Sect. D. Biol. Crystallogr.* **2010,** 66, 213-221.

77. Chen, V. B.; Arendall, W. B.; Headd, J. J.; Keedy, D. A.; Immormino, R. M.; Kapral, G. J.; Murray, L. W.; Richardson, J. S.; Richardson, D. C. MolProbity: all-atom structure validation for macromolecular crystallography. *Acta Crystallogr. Sect. D. Biol. Crystallogr.* **2010,** 66, 12-21.

78. Laskowski, R. A.; MacArthur, M. W.; Moss, D. S.; Thornton, J. M. PROCHECK: a program to check the stereochemical quality of protein structures. *J. Appl. Crystallogr.* **1993,** 26, 283-291.

79. Sharma, N.; Gupta, R.; Kumar, M.; Gupta, R. R. Synthesis of fluorophenothiazines via Smiles rearrangement and their conversion into sulfones. *J. Fluorine Chem.* **1999,** 98, 153-157.

80. Sharma, P. R.; Gupta, V.; Gautam, D. C.; Gupta, R. R. Synthesis of phenothiazines via Smiles rearrangement. *Heterocycl. Commun.* **2002,** 8, 195-198.

81. Gilman, H.; Nelson, R. D. Oxidation of 10-acyl- and 10-alkylphenothiazines. *J. Am. Chem. Soc.* **1953,** 75, 5422-5425.

82. Kutscher, B.; Dieter, H. R.; Trömer, H.-G.; Bartz, B.; Engel, J.; Kleemann, A. Neue Synthese von 4-Azaphenothiazin. *Liebigs Ann. Chem.* **1995,** 1995, 591-592.

83. Saggiomo, A. J.; Craig, P. N.; Gordon, M. Synthesis of 2-aza- and 8-chloro-2-aza-phenothiazine. *J. Org. Chem.* **1958,** 23, 1906-1909.

84. Okafor, C. O. Studies in the heterocyclic series. XIX. Synthesis of 1,4-diazaphenothiazine and its benzo derivatives. *J. Heterocycl. Chem.* **1981,** 18, 405-407.

85. Rodig, O. R.; Collier, R. E.; Schlatzer, R. K. Pyridine chemistry. II. Further studies on the Smiles rearrangement of the 3-amino-2,2'-dipyridyl sulfide system. The synthesis of some 1,6-diazaphenothiazines. *J. Med. Chem.* **1966,** 9, 116-120.

86. Pluta, B. M.-M. a. K. Synthesis of novel dipyrido-1,4-thiazines. *Heterocycles* **2007,** 71, 1347 - 1361.

87. Cassella Farbwerke Mainkur AG. Procede de Preparation de Nouveaux Composes Hetereocycliques Contenant du Soufre et de l'Azote. *FR 1401481 A* **1965**.

88. Yoneda, F.; Ohtaka, T.; Nitta, Y. Pyridazine derivatives. X. 10H-benzo[b]pyridazino[3, 4-e][1, 4]thiazine and 5H-benzo[b]pyridazino[4, 3-e][1, 4]thiazine. *Chem. Pharm. Bull.* **1966,** 14, 698-706.

Table of Contents graphic

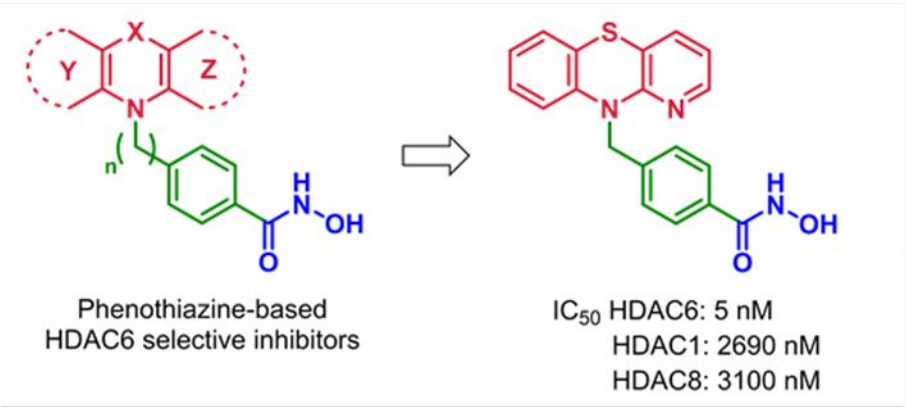
X
Y
Z
N
n
H
N
OH
O
S
N
N
H
N
OH
O
Phenothiazine-based
HDAC6 selective inhibitors
IC50 HDAC6: 5 nM
HDAC1: 2690 nM
HDAC8: 3100 nM

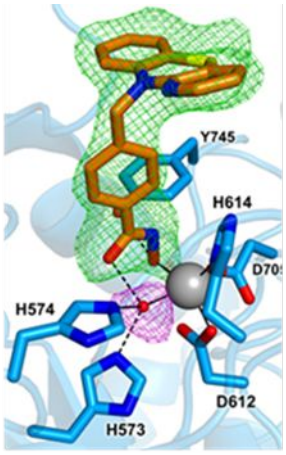
Y745
H614
H574
D612
H573

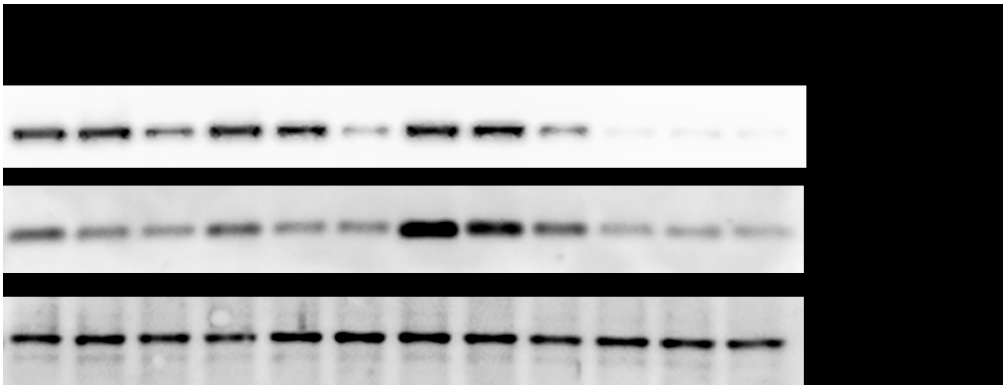

Figure 1. Western blots of acetyl-α-tubulin, acetyl-H3, and GAPDH after treatment of HL60 cells with SAHA, 7i, and 7n. GAPDH was the loading control. DMSO was the negative control.

199x76mm (150 x 150 DPI)

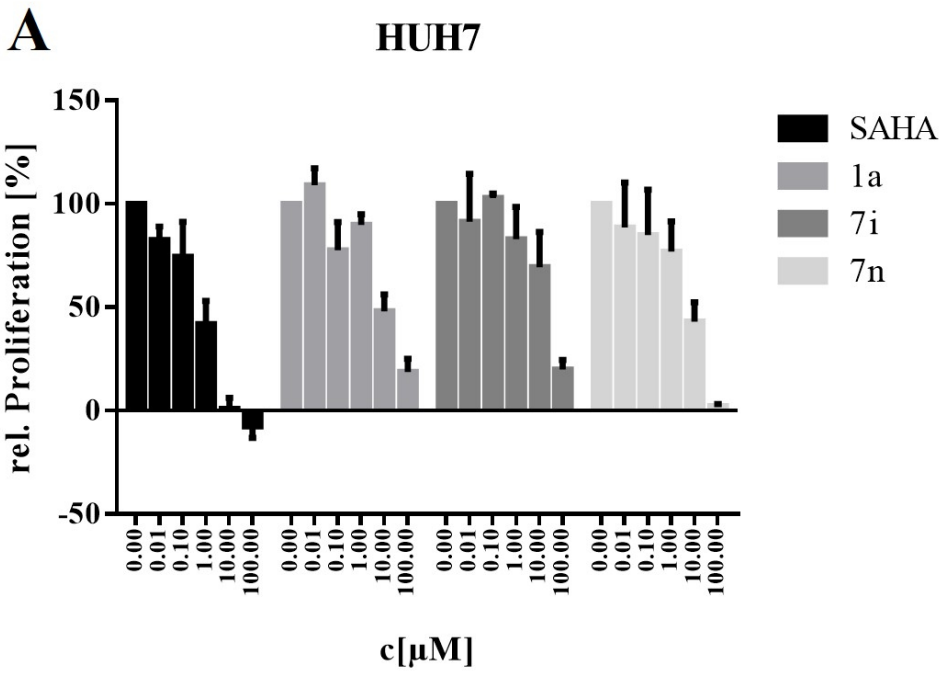

Figure 2. Biological testing of SAHA, 1a, 7i and 7n. Proliferation of (A) HUH7, (B) MDA-MB-231, and (C) T24 cells was analyzed by CellTiter-Blue® cell viability assay after treatment for 72 h. Apoptosis of (D) MDA-MB-231 and (E) T24 cells was assessed by propidium iodide staining and flow cytometry after treatment for 48 h. Expression of (F) PD-L1 and (G) GRP78 was detected by western blot analysis of T24 protein lysates upon 10 µM treatment (48 h). Protein bands were normalized to whole lane protein of the DMSO control. (H) Viability of HepaRG cells was analyzed by CellTiter-Blue® cell viability assay after treatment for 24 h. Data shown in (A)-(E) and (H) represent means ± SEM, performed in triplicates.

184x133mm (150 x 150 DPI)

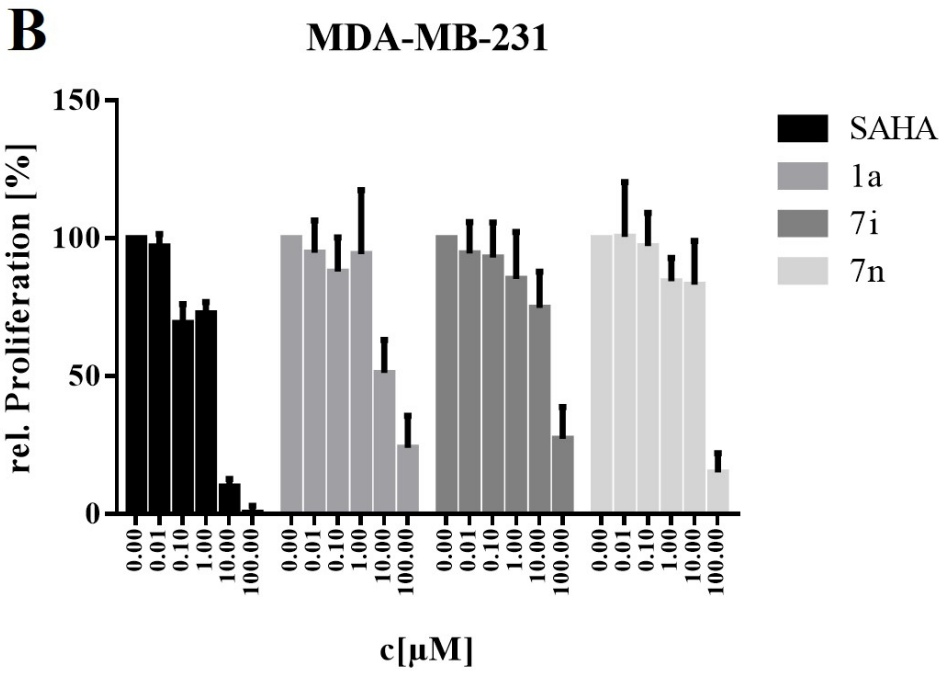

184x133mm (150 x 150 DPI)

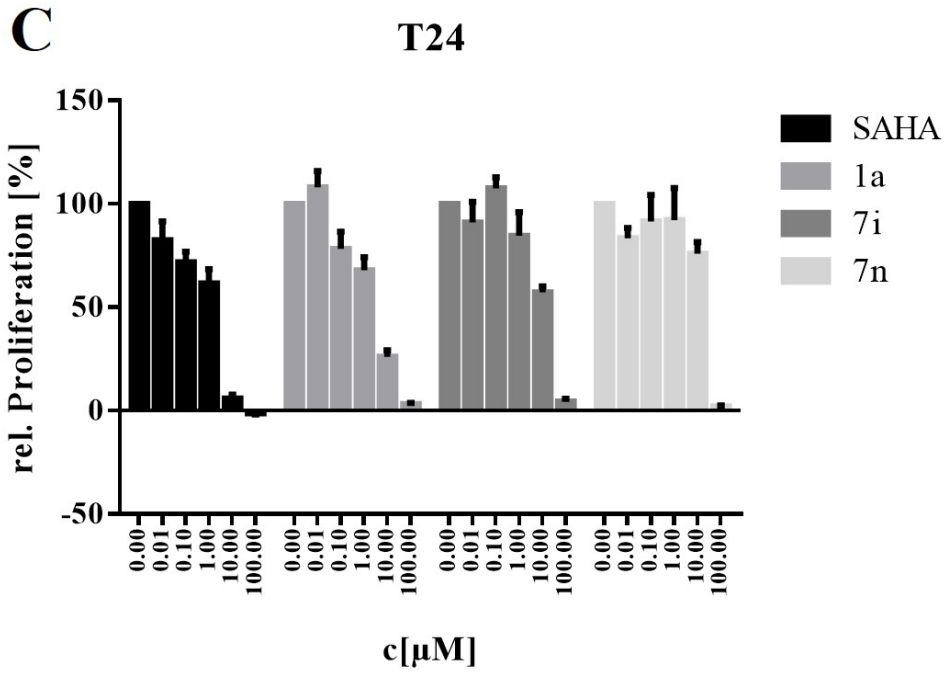

184x133mm (150 x 150 DPI)

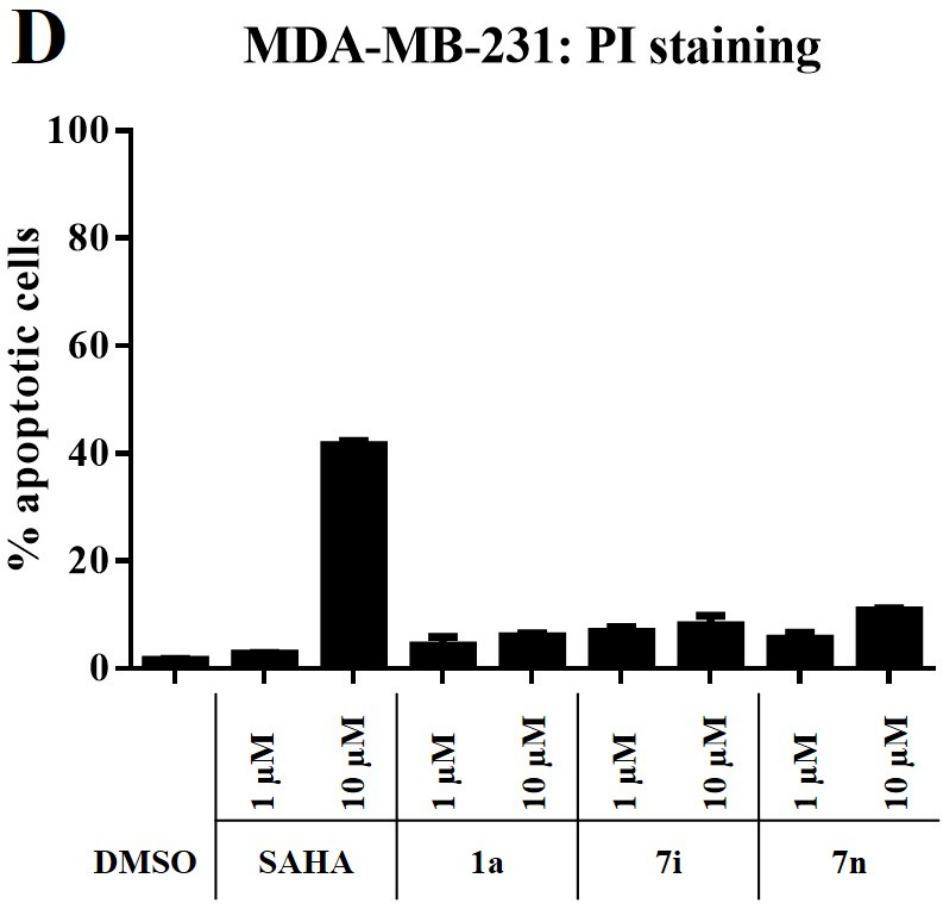

142x133mm (150 x 150 DPI)

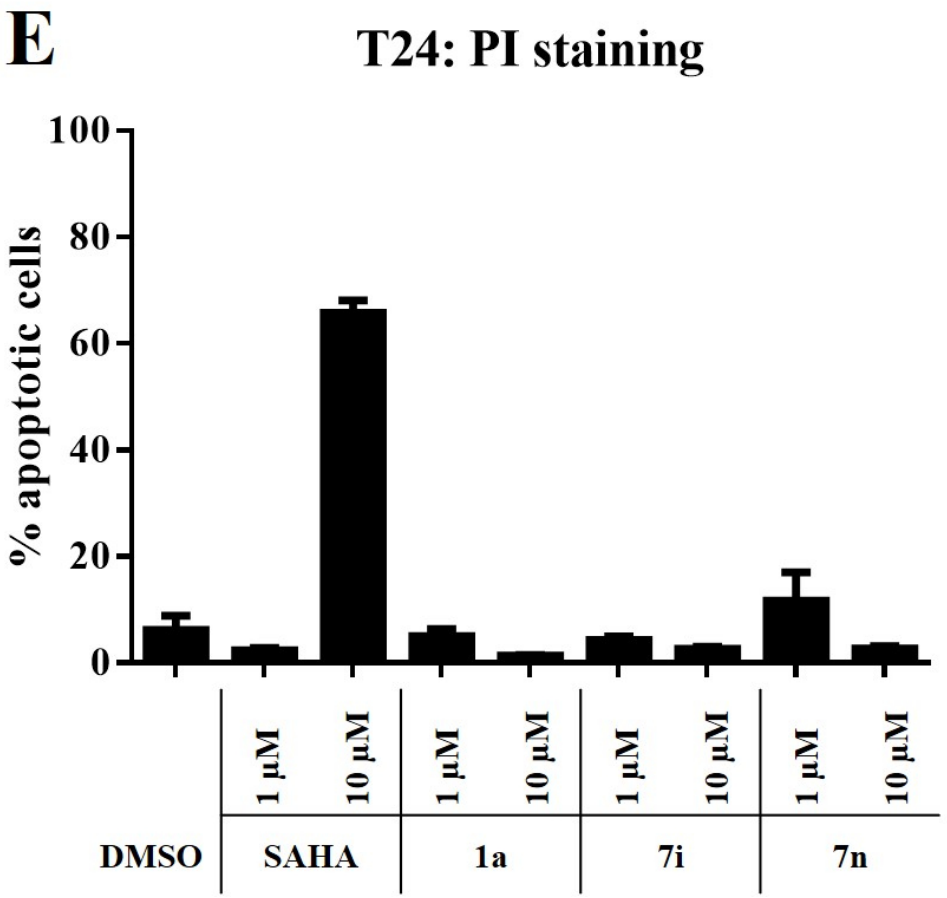

143x133mm (150 x 150 DPI)

F

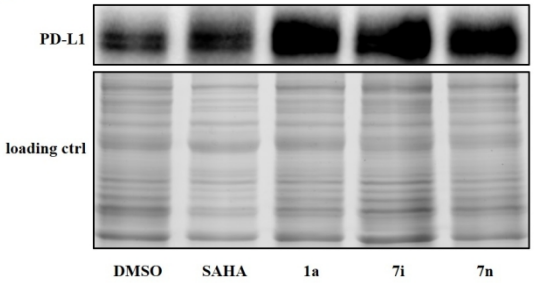

Compound	Relative normalized volume intensity
SAHA	1.94
1a	2.44
7i	1.65
7n	2.1

G

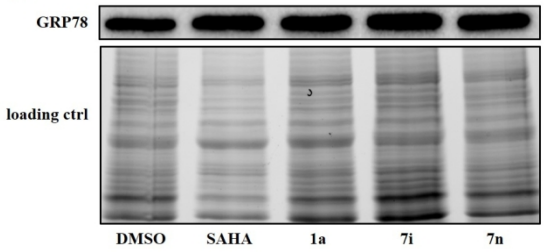

Compound	Relative normalized volume intensity
SAHA	1.90
1a	1.36
7i	1.60
7n	1.61

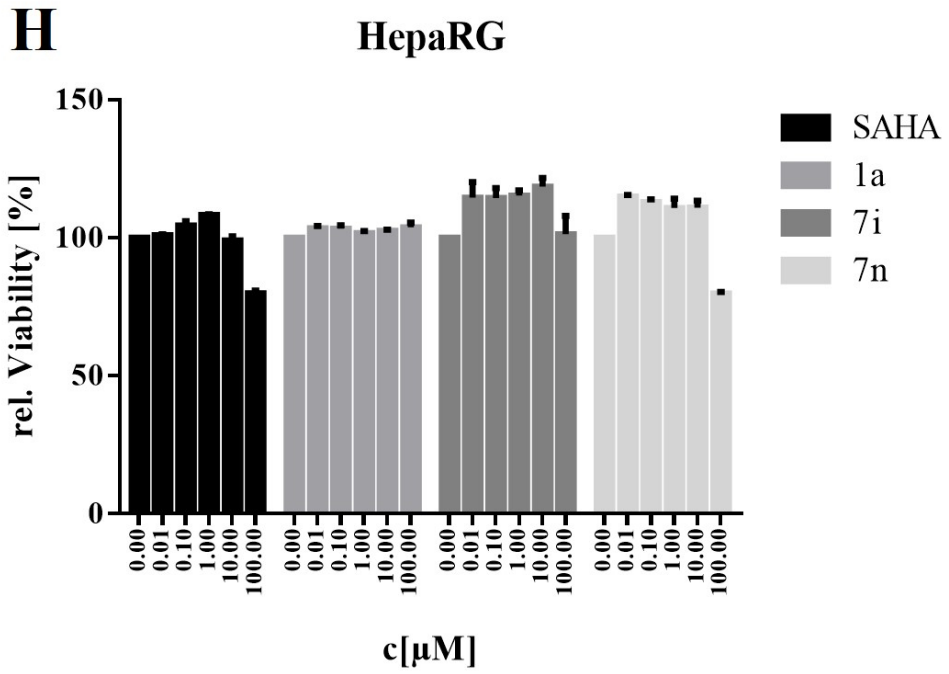

184x133mm (150 x 150 DPI)

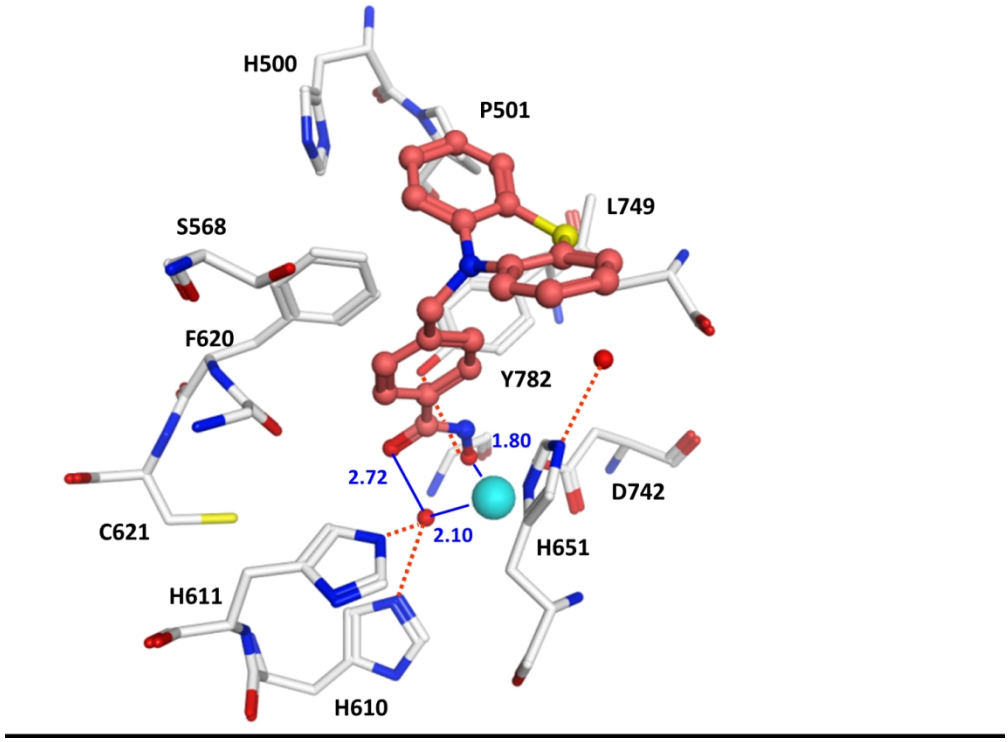

Figure 3. Docking poses calculated for inhibitor 1a (colored salmon) (A), and Tubastatin A (colored magenta) (B) at hHDAC6 (PDB ID 5EDU). Only surrounding amino acid residues are shown for clarity. Hydrogen bonds are shown as orange dashed lines. The zinc ion is shown as cyan ball and water molecules are shown as red balls. Distances between the hydroxamate and zinc ion/water are given in Å (blue colored lines).

254x191mm (150 x 150 DPI)

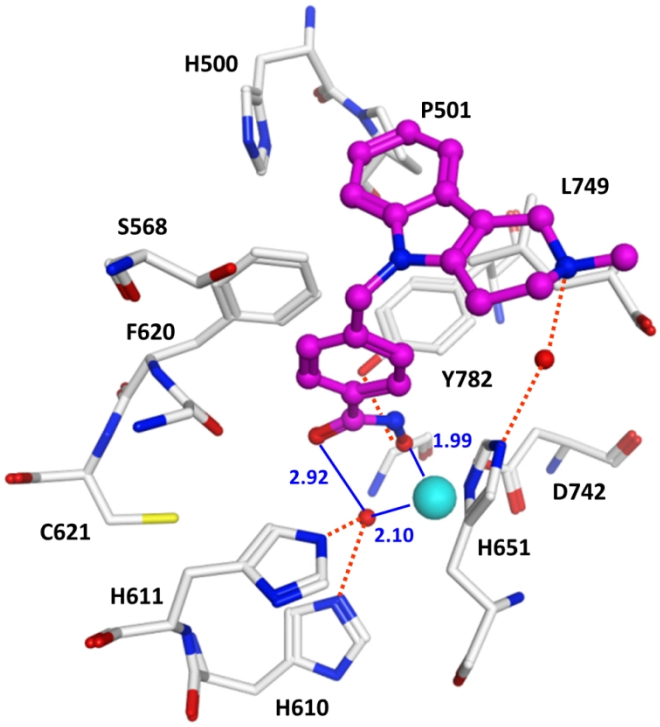

254x191mm (150 x 150 DPI)

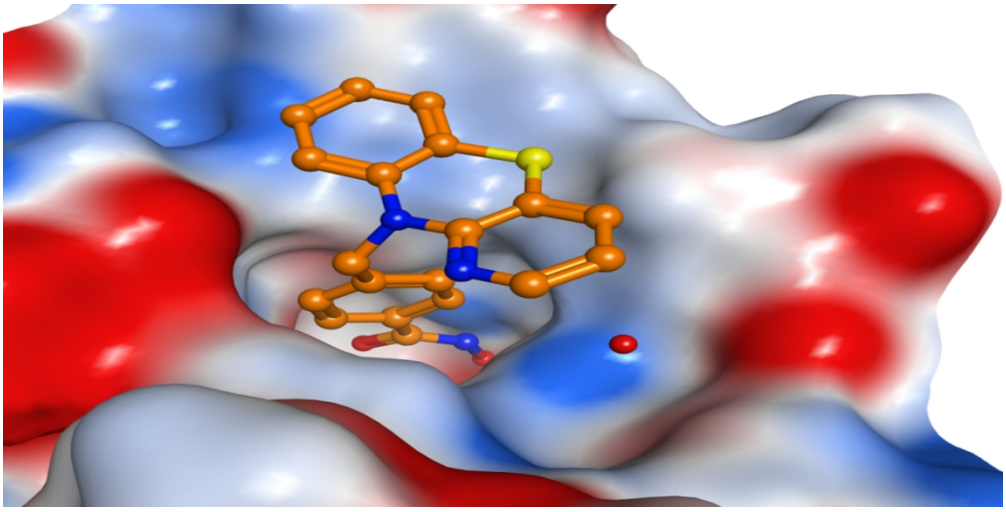

Figure 4. Docking pose calculated for inhibitor 7i (colored orange). The molecular surface of the hHDAC6 (PDB ID 5EDU) binding pocket is colored according to the electrostatic potential (blue = electropositive, red = electronegative).

254x190mm (134 x 90 DPI)

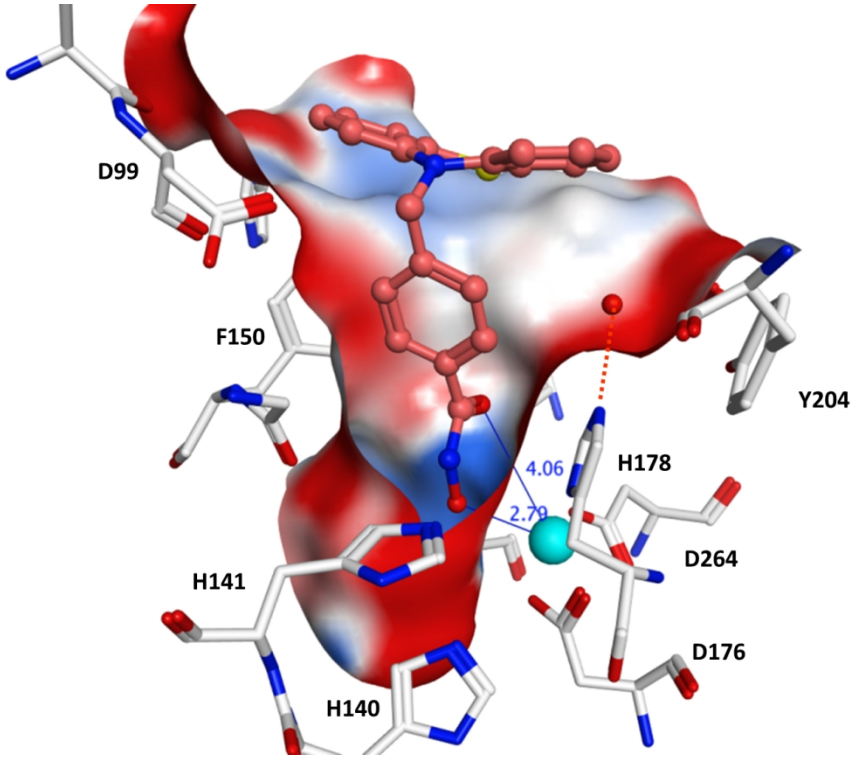

Figure 5. Molecular surface of the hHDAC1 binding pocket (PDB ID 5ICN) colored according to the electrostatic potential (blue = electropositive, red = electronegative). The docking pose of inhibitor 1a is colored salmon. Hydrogen bonds are shown as dashed orange colored lines. The distances between the hydroxamate group and the zinc ion are given in Å and are drawn as blue colored lines.

254x190mm (150 x 150 DPI)

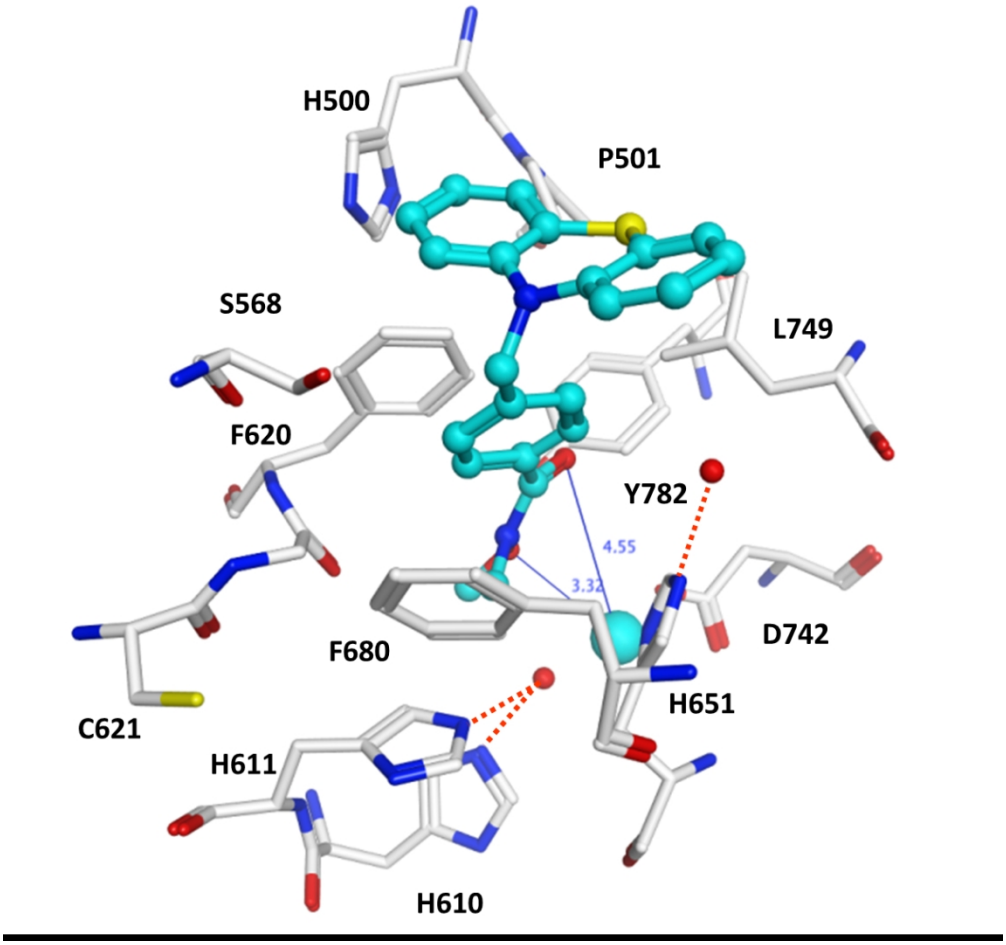

Figure 6. Docking poses of the inactive inhibitor 23 (colored cyan) at hHDAC6 (PDB ID 5EDU). Due to the full methylation of the hydroxamate group this compound is not able to coordinate to the zinc ion. Only surrounding amino acid residues are shown for clarity. Hydrogen bonds are shown as orange dashed lines. The zinc ion is shown as cyan ball. The distances between the hydroxamate group and the zinc ion are given in Å and are drawn as blue colored lines.

203x191mm (150 x 150 DPI)

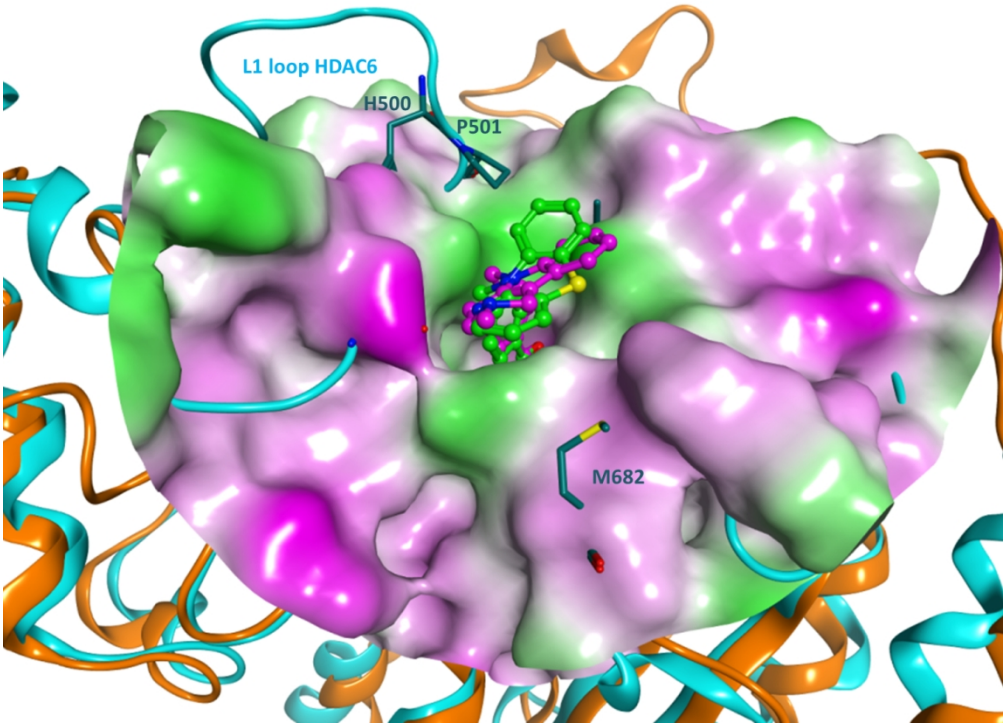

Figure 7. Comparison of the shape of the pocket rim in hHDAC8 (left side) and hHDAC6 (right side). Docking poses of Tubastatin A (magenta) and 7i (green) are shown for both HDACs. H500, P501 (Loop L1) and M682 in hHDAC6 are shown in petrol. hHDAC6 backbone is displayed as cyan colored ribbon, hHDAC8 backbone ribbon is colored orange. Molecular surface of both binding pockets is colored according to the hydrophobicity (magenta indicates polar, green hydrophobic regions).

254x190mm (150 x 150 DPI)

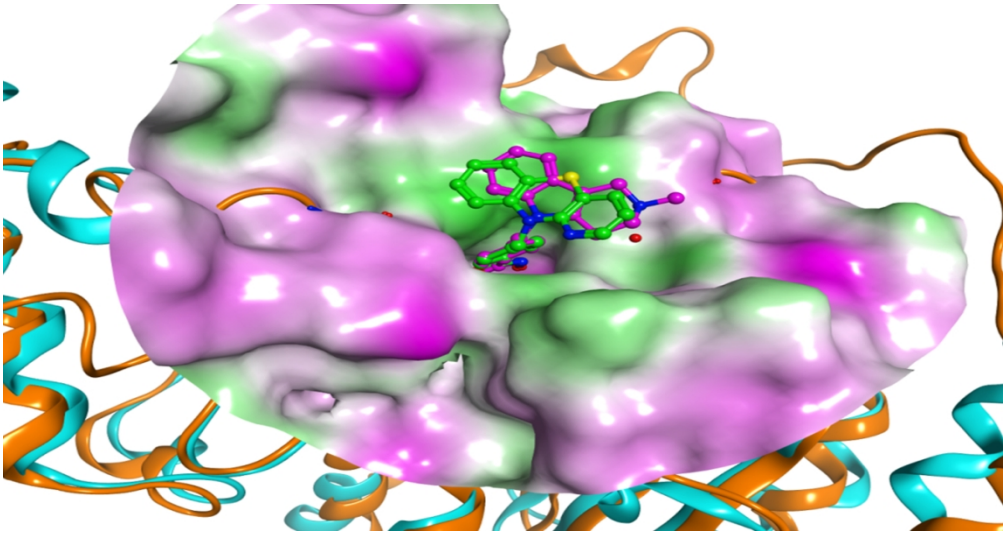

254x190mm (134 x 94 DPI)

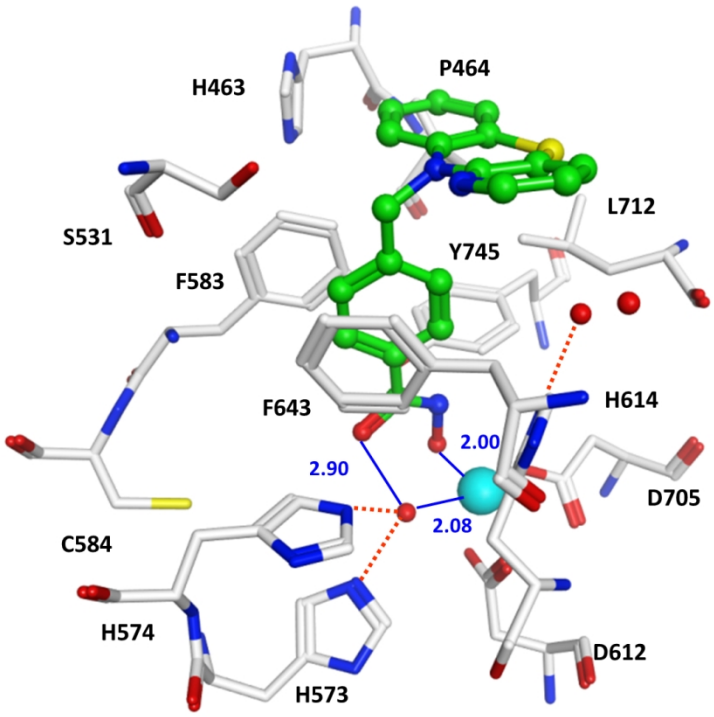

Figure 8. X-ray structure of zHDAC6 complexed with 7i (colored green) (PDB ID 5W5K). Only surrounding amino acid residues are shown for clarity. Hydrogen bonds are shown as orange dashed lines. The zinc ion is shown as cyan ball and water molecules are shown as red balls. Distances between the hydroxamate and zinc ion/water molecule are given in Å (blue colored lines).

254x190mm (150 x 150 DPI)

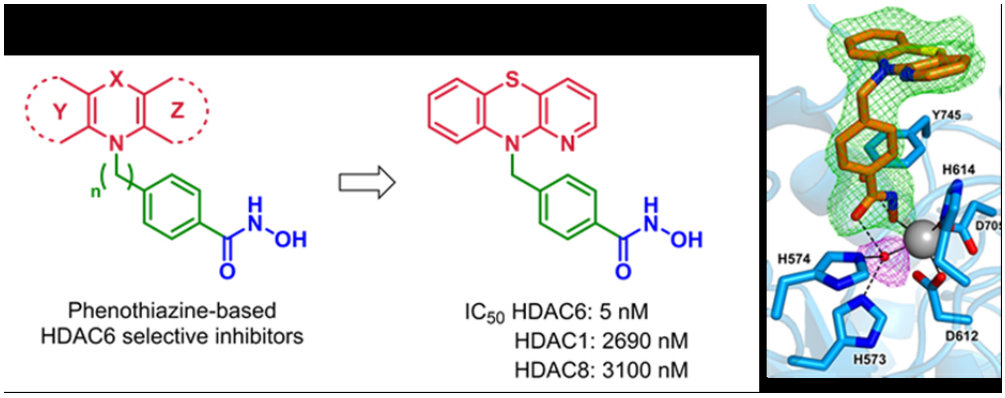

Table of contents graphic

157x61mm (150 x 150 DPI)